

DEFORMATIONS OF DIMER MODELS

AKIHIRO HIGASHITANI AND YUSUKE NAKAJIMA

ABSTRACT. The mutation of polygons, which makes a given lattice polygon another one, is an important operation to understand mirror partners for 2-dimensional Fano manifolds, and the mutation equivalent polygons give the \mathbb{Q} -Gorenstein deformation equivalent toric varieties. On the other hand, for a dimer model, which is a bipartite graph described on the real two-torus, we assign the lattice polygon called the perfect matching polygon. It is known that for each lattice polygon P there exist dimer models such that they give P as the perfect matching polygon and satisfy the consistency condition. Moreover, a dimer model has rich information regarding toric geometry associated to the perfect matching polygon. In this paper, we introduce the operations, which we call the deformations of consistent dimer models, and show that the deformations of consistent dimer models induce the mutations of the associated perfect matching polygons.

CONTENTS

1. Introduction	1
1.1. Backgrounds and Motivations	1
1.2. Our results	2
2. Dimer models and perfect matching polygons	3
2.1. What is a dimer model?	3
2.2. Perfect matchings and the perfect matching polygon	4
3. Zigzag paths and their properties	6
3.1. Consistency conditions	6
3.2. Relationships between perfect matchings and zigzag paths	8
4. Deformations of consistent dimer models	11
4.1. Definition of deformations of consistent dimer models	11
4.2. Examples of deformations of consistent dimer models	16
4.3. The proof of the non-degeneracy	17
5. Zigzag paths on deformed dimer models	20
5.1. Behaviors of zigzag paths after deformations	20
5.2. Properties of zigzag paths on deformed dimer models	24
5.3. The perfect matching polygons of deformed dimer models	26
6. Relationships with mutations of polygons	27
6.1. Preliminaries on mutations of polytopes	27
6.2. Mutations of the PM polygon are induced by deformations	30
Appendix A. Mutations of dimer models	34
Appendix B. Large examples	35
Appendix C. Remarks on deformations of hexagonal and square dimer models	38
Acknowledgement	39
References	39

1. INTRODUCTION

1.1. Backgrounds and Motivations. Fano manifolds are one of well studied classes in geometry, and the classification of Fano manifolds, which were done in low dimensions, is a fundamental problem. Here, a *Fano manifold* X is a complex projective manifold such that the anticanonical line bundle $-K_X$ is ample. Recently, the new approach which uses mirror symmetry have been proposed for classifying Fano

2010 *Mathematics Subject Classification.* Primary 52B20; Secondary 14M25, 14J33.

Key words and phrases. Dimer models, Mutation of polygons, Mirror symmetry.

manifolds as follows. First, a Fano manifold is expected to correspond to a certain Laurent polynomial via mirror symmetry (see [Coates et al.]). That is, a Laurent polynomial $f \in \mathbb{C}[x_1^\pm, \dots, x_n^\pm]$ is said to be a *mirror partner* for a n -dimensional Fano manifold X if the Taylor expansion of the *classical period* π_f of f coincides with a *generating function for Gromov-Witten invariants* of X (see the references quoted above for the details of these terminologies). Furthermore, if a Fano manifold X is a mirror partner of f , it is expected that X admits a toric degeneration X_P . Here, $P := \text{Newt}(f)$ is the Newton polytope of f , which is defined as the convex hull of exponents of monomials of f , and X_P is the toric variety defined by the *spanning fan* of P (i.e., the fan whose cones are spanned by the faces of P). Thus, Laurent polynomials having the same classical period are considered as mirror partners for the same Fano manifold X , and in general there are many Laurent polynomials that are mirror partners for X . In order to understand the relationship between such Laurent polynomials, the operation called the *mutation* of f , which is a birational transformation analogue to a cluster transformation, was introduced in [GU]. In particular, it was shown that if $f, g \in \mathbb{C}[x_1^\pm, \dots, x_n^\pm]$ are transformed into each other by mutations, then their classical periods are the same, that is, $\pi_f = \pi_g$ [ACGK, Lemma 1]. Moreover, this mutation of Laurent polynomials f and g can be defined in terms of the associated Newton polytopes $P = \text{Newt}(f)$ and $Q = \text{Newt}(g)$ as defined in [ACGK] (see also Subsection 6.1). Also, it was shown in [Itt] that if P and Q are Fano polytopes and are transformed into each other by mutations, then the associated toric varieties X_P and X_Q are related by a *Q-Gorenstein (= qG) deformation*, that is, there exists a flat family $\mathfrak{X} \rightarrow \mathbb{P}^1$ such that the relative canonical divisor is \mathbb{Q} -Cartier and $\mathfrak{X}_0 \cong X_P$, $\mathfrak{X}_\infty \cong X_Q$ where \mathfrak{X}_p is the fiber of $p \in \mathbb{P}^1$. Thus, it has been conjectured that there is a bijection between qG-deformation equivalence classes of “class TG” Fano manifolds and mutation equivalence classes of Fano polytopes. Until now, there are several affirmative results (see e.g., [Akhtar et al., KNP]).

1.2. Our results. As we mentioned, the mutations of polytopes are quite important in mirror symmetry of Fano manifolds. In this paper, we focus on the two dimensional case, and the polygons which we are interested in are not necessarily Fano. First, it is known that any lattice polygon in \mathbb{R}^2 can be realized as the *perfect matching polygon* Δ_Γ of a dimer model Γ satisfying the consistency condition (see Section 2 and 3). A *dimer model* is a bipartite graph on the real two-torus (see Section 2 for more details), which was first introduced in the field of statistical mechanics. From 2000s, string theorists have been used it for studying quiver gauge theories (see e.g., [Kenn, Keny] and references therein). Subsequently, the relationships between dimer models and many branches of mathematics have been discovered (see e.g., [Boc3] and references therein). From these backgrounds, we expect that there is a certain operation on consistent dimer models that induces the mutation of perfect matching polygons. In this paper, we introduce the concept called the *deformations of consistent dimer models*.

To explain our main theorem, we briefly recall the mutations of polygons (see Subsection 6.1 for more precise definition). Let $N \cong \mathbb{Z}^2$ be a rank two lattice and $M := \text{Hom}_{\mathbb{Z}}(N, \mathbb{Z}) \cong \mathbb{Z}^2$. First, we consider a lattice polygon P in $N_{\mathbb{R}} := N \otimes_{\mathbb{Z}} \mathbb{R}$ and choose an edge E of P . We then take a primitive inner normal vector $w \in M$ for E , and consider the linear map $\langle w, - \rangle : N_{\mathbb{R}} \rightarrow \mathbb{R}$. Using these, we determine the *height* $\langle w, u \rangle$ of each point $u \in P$. In particular, a primitive lattice element $u_E \in N$ satisfying $\langle w, u_E \rangle = 0$ plays an important role to define the mutation. Such an element u_E is determined uniquely up to sign, thus we fix one of them. Then, we define the line segment $F := \text{conv}\{\mathbf{0}, u_E\}$, which is called a *factor* of P with respect to w . Using these data, we have the lattice polygon $\text{mut}_w(P, F)$, which is called the *mutation* of P given by the vector w and the factor F , as defined in Definition 6.2. In addition, we also define another mutation $\text{mut}_w(P, -F)$ in a similar way. We note that although $\text{mut}_w(P, F)$ looks different from $\text{mut}_w(P, -F)$, they are transformed into each other by the $\text{GL}(2, \mathbb{Z})$ -transformation. Furthermore, for the given lattice polygon P there exists a consistent dimer model Γ such that $P = \Delta_\Gamma$.

Under these backgrounds, the deformation of a consistent dimer model are compatible with the above mutations in the following sense. Let Γ be the consistent dimer model as above. The deformations of Γ are defined for a certain set of “zigzag paths” $\{z_1, \dots, z_r\}$ on Γ corresponding to the vector $-w$ (see Section 3 concerning zigzag paths), and there are two kinds of deformations which we call the *deformation at zig* and the *deformation at zag*, which are respectively denoted by $\nu_{\mathcal{X}}^{\text{zig}}(\Gamma, \{z_1, \dots, z_r\})$ and $\nu_{\mathcal{Y}}^{\text{zag}}(\Gamma, \{z_1, \dots, z_r\})$, see Definition 4.3 and 4.5 for more details. Here, \mathcal{X} and \mathcal{Y} are the deformation parameters (see Definition 4.1). The deformations preserve the consistency condition on a dimer model (see Proposition 4.7), and the associated perfect matching polygons satisfy the desired property as follows.

Theorem 1.1 (see Theorem 6.10). *With the above settings, we have that*

$$\mathbf{mut}_w(\Delta_\Gamma, F) = \Delta_{\nu_{\mathcal{X}}^{\text{zig}}(\Gamma, \{z_1, \dots, z_r\})},$$

$$\mathbf{mut}_w(\Delta_\Gamma, -F) = \Delta_{\nu_{\mathcal{Y}}^{\text{zag}}(\Gamma, \{z_1, \dots, z_r\})},$$

where $\Delta_{\nu_{\mathcal{X}}^{\text{zig}}(\Gamma, \{z_1, \dots, z_r\})}$ and $\Delta_{\nu_{\mathcal{Y}}^{\text{zag}}(\Gamma, \{z_1, \dots, z_r\})}$ are the perfect matching polygons of $\nu_{\mathcal{X}}^{\text{zig}}(\Gamma, \{z_1, \dots, z_r\})$ and $\nu_{\mathcal{Y}}^{\text{zag}}(\Gamma, \{z_1, \dots, z_r\})$ respectively.

Therefore, the perfect matching polygons of the deformed dimer models satisfy the properties which are exactly the same as the mutation of a polygon (see Subsection 6.2). We remark that we have to determine the shape of the perfect matching polygon Δ_Γ in advance for defining the mutations $\mathbf{mut}_w(\Delta_\Gamma, F)$ and $\mathbf{mut}_w(\Delta_\Gamma, -F)$, whereas we can define the deformations $\nu_{\mathcal{X}}^{\text{zig}}(\Gamma, \{z_1, \dots, z_r\})$ and $\nu_{\mathcal{Y}}^{\text{zag}}(\Gamma, \{z_1, \dots, z_r\})$ even if we do not know the perfect matching polygon Δ_Γ .

Since dimer models are related with many branches of mathematics and physics, it is interesting problem to compare a certain object on a consistent dimer model Γ to that of $\nu_{\mathcal{X}}^{\text{zig}}(\Gamma, \{z_1, \dots, z_r\})$ (or $\nu_{\mathcal{Y}}^{\text{zag}}(\Gamma, \{z_1, \dots, z_r\})$).

The structure of this paper is as follows. In Section 2, we introduce a dimer model and related notions. In particular, the notion of the perfect matching polygon introduced in this section is one of main ingredients in this paper. In Section 3, we introduce the notion of zigzag paths, which is a special path on a dimer model. We define the consistency condition using zigzag paths, and we then discuss the relationships between perfect matchings and zigzag paths on a consistent dimer model. After that, we especially focus on type I zigzag paths, which are zigzag paths having typical properties. Using these type I zigzag paths, we introduce the deformations of consistent dimer models in Section 4, and show their fundamental properties. In Section 5, we observe the behavior of zigzag paths and the perfect matching polygons for the deformed dimer models. In Section 6, we first recall the definition of the mutations of polygons. Then, we show our main theorem that the deformations of consistent dimer models are compatible with the mutations of polygons, that is, the perfect matching polygon of the deformed dimer model coincides with the mutation of the perfect matching polygon of the original dimer model (see Theorem 6.10). After that we give some corollaries which are induced by the fundamental properties on the mutation of polygons. As we will mention in Remark 4.4, the deformation of a consistent dimer model is not determined uniquely, whereas the perfect matching polygon of the deformation of a consistent dimer model is determined uniquely. This ambiguity is caused by the fact that there are several consistent dimer models giving the same perfect matching polygon. However, it has been conjectured that such consistent dimer models are transformed into each other by the *mutation of dimer models*, and hence “conjecturally” our deformation of a consistent dimer model is determined uniquely up to the mutation. Thus, we introduce this mutation of dimer models in Appendix A. In Appendix B, we give an additional example of the deformation, which is enormous to write in the main body of this paper. Also, in Appendix C, we show that the definition of the deformations can be simplified for some special classes of dimer models, which we call hexagonal dimer models and square dimer models.

2. DIMER MODELS AND PERFECT MATCHING POLYGONS

2.1. What is a dimer model? A *dimer model* (or *brane tiling*) Γ is a finite bipartite graph on the real two-torus $\mathbb{T} := \mathbb{R}^2/\mathbb{Z}^2$, that is, the set Γ_0 of nodes is divided into two parts Γ_0^+, Γ_0^- , and the set Γ_1 of edges consists of the ones connecting nodes in Γ_0^+ and those in Γ_0^- . In order to make the situation clear, we color nodes in Γ_0^+ white, and color nodes in Γ_0^- black. A connected component of $\mathbb{T} \setminus \Gamma_1$ is called a *face* of Γ , and we denote by Γ_2 the set of faces. We also obtain the bipartite graph $\tilde{\Gamma}$ on \mathbb{R}^2 induced via the universal cover $\mathbb{R}^2 \rightarrow \mathbb{T}$. We call $\tilde{\Gamma}$ the universal cover of a dimer model Γ . For example, the bipartite graph shown in the left side of Figure 1 is a dimer model where the outer frame is the fundamental domain of \mathbb{T} .

As the dual of a dimer model Γ , we define the quiver Q_Γ associated with Γ . Namely, we assign a vertex dual to each face in Γ_2 , an arrow dual to each edge in Γ_1 . The orientation of arrows is determined so that the white node is on the right of the arrow. For example, the right side of Figure 1 is the quiver associated with the dimer model on the left. Sometimes we simply denote the quiver Q_Γ by Q .

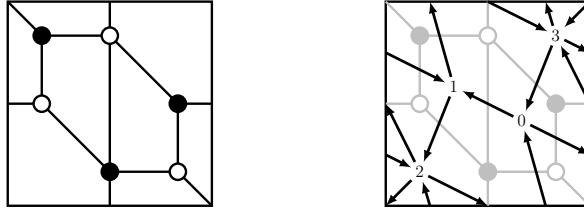


FIGURE 1. A dimer model and the associated quiver

The *valency* of a node is the number of edges incident to that node. We say that a node on a dimer model is n -*valent* if its valency is n . We then define several operations on a dimer model. The *join move* is the operation removing a 2-valent node and joining two distinct nodes connected to it as shown in Figure 2. Thus, using join moves we obtain a dimer model having no 2-valent nodes. We say that a dimer model is *reduced* if it has no 2-valent nodes. Thus, the quiver associated with a reduced dimer model contains no 2-cycles. On the other hand, there is the operation called the *split move*, which inserts a 2-valent node (see Figure 2).

We say that reduced dimer models Γ, Γ' are *isomorphic*, which is denoted by $\Gamma \cong \Gamma'$, if their underlying cell decompositions of \mathbb{T} are homotopy equivalent.

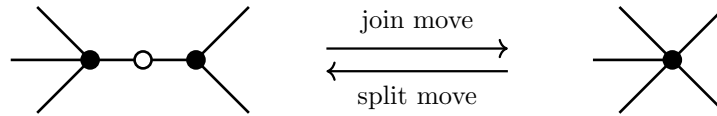


FIGURE 2. An example of the join and split move

2.2. Perfect matchings and the perfect matching polygon. Next, we assign a lattice polygon to each dimer model. For this purpose, we will introduce the notion of perfect matchings, and we construct the polygon called the *perfect matching polygon*.

Definition 2.1. A *perfect matching* (or *dimer configuration*) on a dimer model Γ is a subset P of Γ_1 such that each node is the end point of precisely one edge in P .

In general, every dimer model does not necessarily have a perfect matching. In this paper, we will mainly discuss consistent dimer models, and such a dimer model has a perfect matching. Moreover, we can extend this perfect matching P to the one on $\tilde{\Gamma}$ via the universal cover $\mathbb{R}^2 \rightarrow \mathbb{T}$. We call this a *perfect matching* on $\tilde{\Gamma}$, and use the same notion P . For example, some perfect matchings on the dimer model given in Figure 1 are shown in Figure 3. (This dimer model has eight perfect matchings in total.)

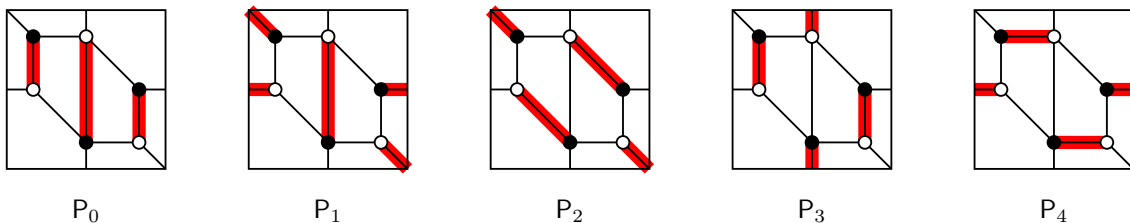


FIGURE 3. Some perfect matchings on the dimer model given in Figure 1

We say that a dimer model is *non-degenerate* if every edge is contained in some perfect matchings. It is known that this non-degeneracy condition is equivalent to the *strong marriage condition*, that is, the dimer model has an equal numbers of black and white nodes and every proper subset of the black nodes of size n is connected to at least $n + 1$ white nodes (see e.g., [Bro, Remark 2.12]).

Following [IU2, Section 5], we next define the perfect matching polygon. We first fix a perfect matching P_0 , and call this the *reference perfect matching*. For any perfect matching P , we consider the connected

components of \mathbb{R}^2 divided by $P \cup P_0$. Then, we define the *height function* h_{P, P_0} which is a locally constant function on $\mathbb{R}^2 \setminus (P \cup P_0)$ defined as follows. First, we choose a connected component of \mathbb{R}^2 , and define the value of h_{P, P_0} as 0. Then, this function increases by 1 when we crosses

- an edge $e \in P$ with the black node on the right, or
- an edge $e \in P_0$ with the white node on the right,

and decreases by 1 when we crosses

- an edge $e \in P$ with the white node on the right, or
- an edge $e \in P_0$ with the black node on the right.

This function is determined up to an addition of constant (i.e., up to a choice of a component valued at 0). For example, Figure 4 is the height function h_{P_2, P_3} on the dimer model given in Figure 1, where the red square stands for the fundamental domain of \mathbb{T} , edges in P_2 (resp. P_3) are colored by blue (resp. green), and the number filled in each component is the value of h_{P_2, P_3} .

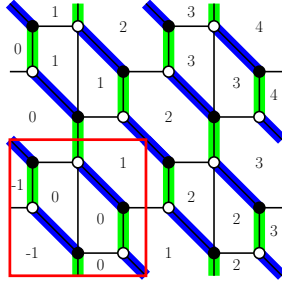


FIGURE 4. The height function h_{P_2, P_3}

We then take a point $\mathbf{pt} \in \mathbb{R}^2 \setminus (P \cup P_0)$, and define the *height change*

$$h(P, P_0) = (h_x(P, P_0), h_y(P, P_0)) \in \mathbb{Z}^2$$

of P with respect to P_0 as the differences of the height function:

$$h_x(P, P_0) = h_{P, P_0}(\mathbf{pt} + (1, 0)) - h_{P, P_0}(\mathbf{pt}),$$

$$h_y(P, P_0) = h_{P, P_0}(\mathbf{pt} + (0, 1)) - h_{P, P_0}(\mathbf{pt}).$$

We remark that this does not depend on a choice of $\mathbf{pt} \in \mathbb{R}^2 \setminus (P \cup P_0)$. We then consider the height change $h(P, P')$ for any pair of perfect matchings P, P' , but since we have

$$h(P, P') = h(P, P_0) - h(P', P_0), \quad (2.1)$$

we may consider only height changes with the form $h(P, P_0)$ for the reference perfect matching P_0 . Then, the *perfect matching (= PM) polygon* (or *characteristic polygon*) $\Delta_\Gamma \subset \mathbb{R}^2$ of a dimer model Γ is defined as the convex hull of $\{h(P, P_0) \in \mathbb{Z}^2 \mid P \in \text{PM}(\Gamma)\}$ where $\text{PM}(\Gamma)$ is the set of perfect matchings on Γ .

Remark 2.2. The description of height changes depends on a choice of the coordinate system fixed in \mathbb{T} (i.e., a choice of the fundamental domain). A change of a coordinate system induces $GL(2, \mathbb{Z})$ action on the PM polygon, and this action does not affect our problem. In the following, we say that two polygons P and Q are $GL(2, \mathbb{Z})$ -equivalent if they are transformed into each other by $GL(2, \mathbb{Z})$ -transformations, in which case we denote $P \cong Q$. Thus, we may fix the fundamental domain of \mathbb{T} . Also, we remark that the description of this polygon Δ_Γ depends on a choice of the reference perfect matching, but it is determined up to translations.

Definition 2.3. Fix a perfect matching P_0 . We say that a perfect matching P is

- a *corner* (or *extremal*) *perfect matching* if $h(P, P_0)$ is a vertex of Δ_Γ ,
- a *boundary* (or *external*) *perfect matching* if $h(P, P_0)$ is a lattice point on an edge of Δ_Γ (especially a corner perfect matching is a boundary one),
- an *internal perfect matching* if $h(P, P_0)$ is an interior lattice point of Δ_Γ .

In the next subsection, we will introduce consistent dimer models (see Definition 3.2), which have several nice properties. If a dimer model is consistent, then there exists a unique corner perfect matching corresponding to each vertex of Δ_Γ (see e.g., [Bro, Corollary 4.27], [IU2, Proposition 9.2]). Thus, we can

give a cyclic order to corner perfect matchings along the corresponding vertices of Δ_Γ in the anti-clockwise direction. We say that two corner perfect matchings are *adjacent* if they are adjacent with respect to the given cyclic order.

Example 2.4. We consider the dimer model given in Figure 1, and fix the perfect matching P_0 shown in Figure 3 as the reference one. Then, we see that the perfect matchings P_1, \dots, P_4 correspond to lattice points $(1, 0), (1, 1), (-1, 0), (0, -1)$ respectively. Also, we see that P_0 and the other perfect matchings that are not listed in Figure 3 correspond to $(0, 0)$. Thus, the PM polygon takes the form as shown in Figure 5, and hence P_1, \dots, P_4 are corner perfect matchings ordered with this order.

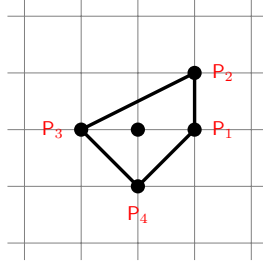


FIGURE 5. The PM polygon of the dimer model given in Figure 1

In this way, we can obtain the PM polygon from a dimer model. On the other hand, it is known that any lattice polygon can be obtained as the PM polygon of a certain dimer model.

Theorem 2.5 ([Gul, IU2]). *For any lattice polygon Δ in \mathbb{R}^2 , there exists a dimer model Γ giving Δ as the PM polygon Δ_Γ . Furthermore, we can take this Γ as it satisfies the consistency condition (see Definition 3.2).*

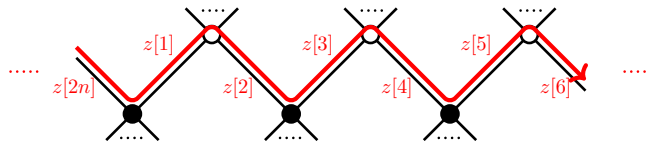
Thus, for a given lattice polygon Δ , we say that Γ is a *dimer model associated with Δ* if the PM polygon of Γ coincides with Δ . We remark that for a given polygon Δ , the associated consistent dimer model is not unique in general.

3. ZIGZAG PATHS AND THEIR PROPERTIES

3.1. Consistency conditions. In this subsection, we introduce the consistency condition. In order to define this condition, we first introduce the notion of zigzag paths, and such paths are also main ingredients for introducing deformations of dimer models.

Definition 3.1. We say that a path on a dimer model is a *zigzag path* if it makes a maximum turn to the right on a white node and a maximum turn to the left on a black node. Also, we say that a zigzag path is *reduced* if it does not factor through 2-valent nodes. (We remark that we can make a zigzag path reduced using the join moves. In particular, any zigzag path on a reduced dimer model is reduced.)

Since a dimer model has only finitely many edges, we see that all zigzag paths are periodic. For a zigzag path z on Γ , we define the length of z , which is denoted by $\ell(z)$, as the number of edges of Γ constituting z . In particular, we see that $\ell(z)$ is even integer. Thus, edges on a zigzag path are indexed by elements in $\mathbb{Z}/(2n)\mathbb{Z}$ for some integer $\ell(z)/2 = n \geq 1$. Fix a black node on a zigzag path z as the starting point of z , and we denote z as a sequence of edges starting from the fixed black node: $z = z[1]z[2] \cdots z[2n-1]z[2n]$.



An edge in a zigzag path z is called a *zig* (resp. *zag*) of z if it is indexed by an odd (resp. even) integer. We denote by $\text{Zig}(z)$ (resp. $\text{Zag}(z)$) the set of zigs (resp. zags) appearing in a zigzag path z , which is a finite set. We note that if z does not have a self-intersection, $\text{Zig}(z)$ and $\text{Zag}(z)$ are disjoint sets. For any edge e of a dimer model, we can uniquely determine the zigzag path containing e as a zig and the zigzag path containing e as a zag respectively. Thus, any edge e is contained in at most two zigzag paths. If

such zigzag paths do not have a self-intersection, e is contained in exactly two zigzag paths. For example, zigzag paths on the dimer model given in the left of Figure 1 are shown in Figure 6.

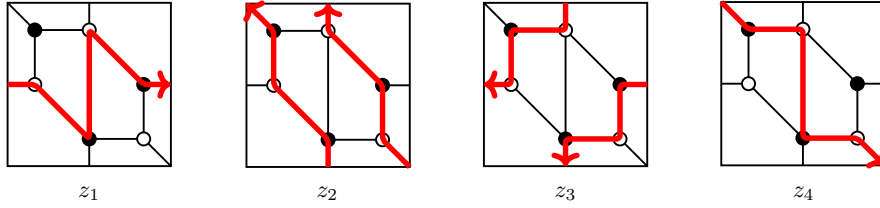


FIGURE 6. Zigzag paths on the dimer model given in Figure 1

For a zigzag path z on a dimer model Γ , we also consider the lift of z to the universal cover $\tilde{\Gamma}$, especially $\tilde{z}(\alpha)$ denotes a zigzag path on $\tilde{\Gamma}$ whose projection on Γ is z where $\alpha \in \mathbb{Z}$. When we do not need to specify these, we simply denote each of them by \tilde{z} . Then, we see that a zigzag path on $\tilde{\Gamma}$ is either periodic or infinite in both directions. Using these notions, we introduce the consistency condition.

Definition 3.2 (see [IU1, Definition 3.5]). We say that a dimer model is (*zigzag*) *consistent* if it satisfies the following conditions:

- (1) there is no homologically trivial zigzag path,
- (2) no zigzag path on the universal cover has a self-intersection,
- (3) no pair of zigzag paths on the universal cover intersect each other in the same direction more than once. That is, if a pair of zigzag paths (\tilde{z}, \tilde{w}) on the universal cover has two intersections a_1, a_2 and \tilde{z} points from a_1 to a_2 , then \tilde{w} points from a_2 to a_1 .

Here, we remark that two zigzag paths are said to *intersect* if they share an edge (not a node).

In the literature, there are several conditions that are equivalent to Definition 3.2 (for more details, see [Boc1, IU1]), and it is known that a consistent dimer model is non-degenerate (see e.g., [IU2, Proposition 8.1]). For example, we see that the dimer model given in Figure 1 is consistent by checking zigzag paths shown in Figure 6. We also remark that this dimer model satisfies the stronger condition called *isoradial* (see Definition 3.4).

In this paper, we also use another condition called *properly ordered*. To explain the properly ordering, we prepare several notations. First, considering a zigzag path z as a 1-cycle on \mathbb{T} , we have the homology class $[z] \in H_1(\mathbb{T}) \cong \mathbb{Z}^2$. We call this element $[z] \in \mathbb{Z}^2$ the *slope* of z . We remark that even if we apply the join and split moves to nodes contained in a zigzag path, such operations do not change the slope. If a zigzag path does not have a self-intersection, the slope of each zigzag path is primitive. Now, we consider slopes $(a, b) \in \mathbb{Z}^2$ of zigzag paths that are not homologically trivial. The set of such slopes has a natural cyclic order by considering (a, b) as the element of the unit circle:

$$\frac{(a, b)}{\sqrt{a^2 + b^2}} \in S^1.$$

Thus, we say that two zigzag paths are *adjacent* if their slopes are adjacent with respect to the above cyclic order. Using this cyclic order, we define a properly ordered dimer model as follows. In particular, it is known that a dimer model is consistent in the sense of Definition 3.2 if and only if it is properly ordered (see [IU1, Proposition 4.4]).

Definition 3.3 (see [Gul, Section 3.1]). A dimer model is said to be *properly ordered* if

- (1) there is no homologically trivial zigzag path,
- (2) no zigzag path on the universal cover has a self-intersection,
- (3) no pair of zigzag paths with the same slope have a common node,
- (4) for any node on the dimer model, the natural cyclic order on the set of zigzag paths incident to that node coincides with the cyclic order determined by their slopes.

We also introduce isoradial dimer models which are stronger than consistent ones.

Definition 3.4 ([KS, Theorem 5.1], see also [Duf, Mer]). We say that a dimer model Γ is *isoradial* (or *geometrically consistent*) if

- (1) every zigzag path is a simple closed curve,
- (2) any pair of zigzag paths on the universal cover share at most one edge.

3.2. Relationships between perfect matchings and zigzag paths. We then discuss the relationship between perfect matchings and zigzag paths. The following proposition is essential throughout this paper.

Proposition 3.5 (see [Gul, Theorem 3.3],[IU2, Section 9]). *There exists a one-to-one correspondence between the set of slopes of zigzag paths on a consistent dimer model Γ and the set of primitive side segments of the PM polygon Δ_Γ . Precisely, each slope of a zigzag path is the primitive outer normal vector for each primitive side segment of Δ_Γ .*

Moreover, zigzag paths having the same slope arise as the difference of two adjacent corner perfect matchings P, P' (i.e., edges in $P \cup P' \setminus P \cap P'$ forms zigzag paths). Thus, any corner perfect matching intersects with half of the edges constituting a certain zigzag path.

For example, the zigzag path z_1 shown in Figure 6 is obtained from the pair of adjacent corner perfect matchings (P_1, P_2) given in Figure 3. Also, the zigzag paths z_2, z_3, z_4 are obtained by pairs $(P_2, P_3), (P_3, P_4), (P_4, P_1)$ respectively.

By Proposition 3.5, we can assign the edge of the PM polygon to each zigzag path z , thus we will call this the edge corresponding to z . In particular, the edges corresponding to zigzag paths having the same slope are all the same.

Let P, P' be adjacent corner perfect matchings on a consistent dimer model, and z_1, \dots, z_r be the zigzag paths arising from P and P' as in Proposition 3.5. In particular, these zigzag paths have the same slope. In this case, we see that $P \cap z_i = \text{Zig}(z_i)$ and $P' \cap z_i = \text{Zag}(z_i)$ (or $P \cap z_i = \text{Zag}(z_i)$ and $P' \cap z_i = \text{Zig}(z_i)$) for any $i = 1, \dots, r$. Here, $P \cap z_i$ denotes the subset of edges in P contained in z_i . Then, we have the description of boundary perfect matchings using the corner ones.

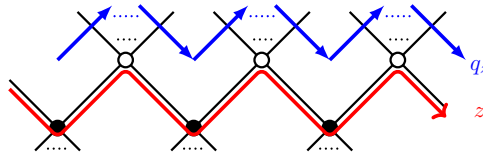
Proposition 3.6 (see e.g., [Bro, Proposition 4.35], [Gul, Corollary 3.8]). *Let P, P' and z_1, \dots, z_r be the same as above. Let E be the edge of the PM polygon of Γ corresponding to z_1, \dots, z_r . We assume that $P \cap z_i = \text{Zig}(z_i)$ and $P' \cap z_i = \text{Zag}(z_i)$. Then, any boundary perfect matching corresponding to a lattice point on E can be described as*

$$(P \setminus \bigcup_{i \in I} \text{Zig}(z_i)) \cup \bigcup_{i \in I} \text{Zag}(z_i) \quad \text{or} \quad (P' \setminus \bigcup_{i \in I} \text{Zag}(z_i)) \cup \bigcup_{i \in I} \text{Zig}(z_i),$$

where I is a subset of $\{1, \dots, r\}$. In particular, the number of perfect matchings corresponding to a lattice point \mathfrak{q} on E is $\binom{r}{m}$, where m is the number of primitive side segments of E between \mathfrak{q} and one of the endpoint of E .

We then observe the relationship between zigzag paths and height changes of perfect matchings. Some of them are well-known for experts, but we note the details because these statements are quite important when we define the deformation of consistent dimer models in Section 4, and also for the self-containedness.

Observation 3.7 (cf. [IU2, subsection 5.3]). Let Γ be a consistent dimer model. For a zigzag path z , the slope $[z]$ is an element in $H_1(\mathbb{T})$. On the other hand, we can consider height changes as elements in the cohomology group $H^1(\mathbb{T}) \cong \mathbb{Z}^2$, and hence we have a pairing $\langle -, - \rangle : H^1(\mathbb{T}) \times H_1(\mathbb{T}) \rightarrow \mathbb{Z}$. By Proposition 3.5 and 3.6, there is a perfect matching P' that intersects half of the edges constituting z . Then, for any perfect matching P , we have that $\langle h(P, P'), [z] \rangle \leq 0$. In fact, we first replace z by the path p_z on the quiver Q_Γ going along the left side of z (see the figure below).



Then, considering this path p_z as the element $[p_z] \in H_1(\mathbb{T})$, we have that $[z] = [p_z]$. By a choice of P' , this p_z does not cross any edge in P' , and if p_z crosses an edge in P , we can see the white node on the right by the definition of Q_Γ . Thus, we have the desired inequality.

For a perfect matching P and a zigzag path z on a dimer model Γ , we denote by $|P \cap z|$ the number of edges in $P \cap z$. Since the number of perfect matchings is finite, the maximum (resp. minimum) number $\omega_{\max}(z)$ (resp. $\omega_{\min}(z)$) of $|P \cap z|$ exists for each zigzag path z . For a consistent dimer model, z can be

obtained as the difference of adjacent perfect matchings (see Proposition 3.6), thus we clearly have that $\ell(z)/2 = \omega_{\max}(z)$. We set

$$\begin{aligned} \text{PM}_{\max}(z) &= \{P \in \text{PM}(\Gamma) \mid |P \cap z| = \omega_{\max}(z)\}, \\ \text{PM}_{\min}(z) &= \{P \in \text{PM}(\Gamma) \mid |P \cap z| = \omega_{\min}(z)\}. \end{aligned}$$

In particular, if P, P' are adjacent corner perfect matchings on a consistent dimer model Γ , and z is one of the zigzag paths obtained by P, P' , then we have that $P \cap z = \text{Zig}(z)$ and $P' \cap z = \text{Zag}(z)$ (or $P \cap z = \text{Zag}(z)$ and $P' \cap z = \text{Zig}(z)$), and hence the next lemma easily follows from Proposition 3.5 and 3.6.

Lemma 3.8. *Let z be a zigzag path on a consistent dimer model Γ , and E be the edge of the PM polygon of Γ corresponding to z . If P_1, \dots, P_s are boundary perfect matchings corresponding to lattice points on E , then we have that $\{P_1, \dots, P_s\} = \text{PM}_{\max}(z)$, and $\omega_{\max}(z) = |P_i \cap z| = \ell(z)/2$ for any $i = 1, \dots, s$.*

Next, we prepare several lemmas, which play crucial roles to define the deformations of consistent dimer models.

Lemma 3.9. *Let the notation be the same as Lemma 3.8. For any perfect matching P , we have that*

$$|P \cap z| = \ell(z)/2 - \langle h(P, P_i), -[z] \rangle.$$

In particular, we have that

$$\langle h(P, P_i), -[z] \rangle \leq \omega_{\max}(z) - \omega_{\min}(z),$$

and the equality holds for $P \in \text{PM}_{\min}(z)$.

Proof. First, the maximum number of $|P \cap z|$ is $\ell(z)/2$, in which case $P = P_i$ by Lemma 3.8. If the path p_z as in Observation 3.7 crosses an edge e in P , it means that e is not an edge constituting z , and thus any edge sharing the same white node as e is not contained in P . By Observation 3.7, we see that for any perfect matching P the number of edges in P intersecting with p_z coincides with $-\langle h(P, P_i), [z] \rangle$, thus we have the first equation.

The second assertion follows from the first equation and Lemma 3.8. \square

By this lemma, we see that $P \in \text{PM}_{\min}(z)$ if and only if $\langle h(P, P_i), [z] \rangle \leq \langle h(P', P_i), [z] \rangle$ for any $P' \in \text{PM}(\Gamma)$. Thus, we see that $P \in \text{PM}_{\min}(z)$ lies on either a vertex of the PM polygon Δ_Γ or an edge of Δ_Γ . Also, even if zigzag paths z_j and z_k have the same slope, $\ell(z_j) \neq \ell(z_k)$ and $|P \cap z_j| \neq |P \cap z_k|$ in general, but their difference is the same as follows.

Lemma 3.10. *Let Γ be a consistent dimer model, and z, z' be zigzag paths on Γ having the same slope. Then, for any perfect matching P , we have that*

$$\ell(z)/2 - |P \cap z| = \ell(z')/2 - |P \cap z'|.$$

In particular, we have that

$$\ell(z)/2 - \omega_{\min}(z) = \ell(z')/2 - \omega_{\min}(z').$$

Proof. Since $[z] = [z']$, the first equation follows from Lemma 3.9. Considering a perfect matching P such that the value of $\langle h(P, P_i), -[z] \rangle = \langle h(P, P_i), -[z'] \rangle$ is maximal, we have the second equation. \square

We then divide zigzag paths on a consistent dimer model into the following two types. In particular, type I zigzag paths are used to define the deformation of consistent dimer models.

Definition 3.11. Let Γ be a dimer model, and z be a zigzag path on Γ .

- (1) We say that z is *type I* if z is reduced and \tilde{z} intersects with any other zigzag paths on the universal cover $\tilde{\Gamma}$ at most once.
- (2) We say that z is *type II* if z is reduced and there exists a zigzag path \tilde{w} on the universal cover $\tilde{\Gamma}$ such that \tilde{w} intersects with \tilde{z} in the opposite direction more than once.

We note that any zigzag path on a reduced consistent dimer model is either type I or II. In particular, if Γ is isoradial, then any zigzag path is type I (see Definition 3.4).

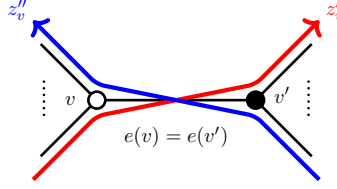
As the following lemmas show, type I zigzag paths are particularly nice.

Lemma 3.12. *Let z be a type I zigzag path on a consistent dimer model Γ . Then, there exists a perfect matching P on Γ satisfying $|P \cap z| = 0$, in which case P is in $\text{PM}_{\min}(z)$.*

Proof. In order to find a perfect matching \mathbf{P} , we will use the method discussed in [Gul, Section 3], [Bro, Section 4]. Thus, we first prepare some notation.

We consider the sequence $[z_1], \dots, [z_n]$ of slopes of zigzag paths on Γ . Since Γ is consistent, it is properly ordered, thus we assume that they are ordered cyclically with this order. We note that some of the slopes may coincide. Then, we define the normal fan in $H_1(\mathbb{T}) \otimes_{\mathbb{Z}} \mathbb{R}$ whose rays are slopes $[z_1], \dots, [z_n]$. In particular, each two dimensional cone σ is generated by adjacent different slopes. We denote by θ_i the angle formed by $[z_i]$. Here, we suppose that $z = z_k$. Let \mathcal{R} be a ray whose angle is $\theta_k + \pi + \epsilon$ where $\epsilon > 0$ is a sufficiently small angle satisfying the condition that $\theta_k + \pi + \epsilon$ does not coincides with any θ_i .

Then, for each node $v \in \Gamma_0$ we define the fan $\xi(v)$ generated by the slopes of zigzag paths factoring through v . In this fan $\xi(v)$, we can find the zigzag path z'_v whose slope makes the smallest clockwise angle with \mathcal{R} , and z''_v whose slope make the smallest anti-clockwise angle with \mathcal{R} . Since Γ is properly ordered, these zigzag paths are consecutive around v . Then, as the intersection of z'_v and z''_v , we have the edge $e(v)$ which has v as an endpoint.



We then apply the same argument to the node v' which is the other endpoint of $e(v)$. Then, the properly ordering on Γ induces the conclusion that $e(v) = e(v')$ (see the above figure). We repeat these arguments for any node, but clearly we only consider $e(v)$'s for any $v \in \Gamma_0^+$ (or $v \in \Gamma_0^-$). By [Gul, Subsection 3.2] or [Bro, Lemma 4.19], we see that the subset of edges $e(v)$ for all $v \in \Gamma_0^+$ forms a perfect matching. Furthermore, since $z = z_k$ is type I, there exists a zigzag path whose slope is located at an angle less than π in an anti-clockwise (resp. clockwise) direction from $[z]$ in $\xi(v)$ by [Bro, Lemma 4.11 and its proof], in which case such a slope is located between $[z]$ and $[z'_v]$ (resp. $[z''_v]$) or coincides with $[z'_v]$ (resp. $[z''_v]$). Thus, we especially have that $z \neq z'_v$ and $z \neq z''_v$ by the definition of the ray \mathcal{R} . Therefore, in this case $e(v)$ is not contained in z by the above construction. Also, we clearly see that if a node v does not lie on z , $e(v)$ is not contained in z . Thus, the perfect matching constructed by the above fashion satisfies the desired condition. \square

Lemma 3.13. *Let z be a type I zigzag path on a consistent dimer model. Then, we have that $\omega_{\min}(z) = 0$, and hence $\ell(z)$ is the same for all type I zigzag paths having the same slope.*

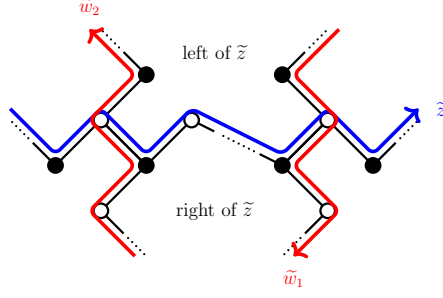
Proof. This follows from Lemma 3.10 and 3.12. \square

For a zigzag paths z, w on a dimer model Γ , we denote by $z \cap w$ the subset of edges that are intersections of z and w on Γ . We remark that if z is type I then the number of intersections of \tilde{z} and \tilde{w} on $\tilde{\Gamma}$ is less than or equal to one, but there are more intersections of z and w if we consider them on Γ .

Lemma 3.14. *Let z be a type I zigzag path on a reduced consistent dimer model Γ . We suppose that a zigzag path w has intersections with z on Γ . Then, we see that $z \cap w \subset \mathbf{Zig}(z)$ or $z \cap w \subset \mathbf{Zag}(z)$.*

Proof. Let e_1, e_2 be edges of Γ , and we assume that w intersects with z at e_1 and e_2 . If e_i is a zig of z , then it is a zag of w , and vice versa. Then, we assume that e_1 is a zig of z and e_2 is a zag of z .

We then lift these on the universal cover $\tilde{\Gamma}$. Let \tilde{e}_1, \tilde{e}_2 be edges of $\tilde{\Gamma}$ whose restrictions on Γ are e_1, e_2 respectively. In particular, \tilde{e}_1 is a zig of \tilde{z} and \tilde{e}_2 is a zag of \tilde{z} . Then, there exist zigzag paths \tilde{w}_1, \tilde{w}_2 on $\tilde{\Gamma}$ whose restriction on Γ is just w , and \tilde{w}_1 (resp. \tilde{w}_2) intersects with \tilde{z} at \tilde{e}_1 (resp. \tilde{e}_2). The zigzag path \tilde{z} splits \mathbb{R}^2 into two pieces, and \tilde{w}_1 (resp. \tilde{w}_2) intersects with \tilde{z} from left to right (resp. right to left) by the definition of zigzag paths (see the figure below).



Since z is type I, there is no intersections of \tilde{z} and \tilde{w}_i except \tilde{e}_i where $i = 1, 2$. Thus, we can not superimpose \tilde{w}_1 and \tilde{w}_2 using translations. This contradicts a choice of \tilde{w}_1, \tilde{w}_2 . \square

The following lemma follows from the argument in the proof of [Bro, Proposition 3.12].

Lemma 3.15. *Let z, w be zigzag paths on a consistent dimer model Γ . We assume that \tilde{z} intersects with \tilde{w} on the universal cover $\tilde{\Gamma}$ at most once. Then, the slopes $[z], [w]$ are linearly independent if and only if \tilde{z} and \tilde{w} intersect in precisely one edge.*

Lemma 3.16. *Let z_1, \dots, z_r be type I zigzag paths on a reduced consistent dimer model Γ having the same slope. We suppose that a zigzag path w has intersections with z_j for some j . Then, we have that w intersects with any z_i ($i = 1, \dots, r$), and the intersections $w \cap z_1, \dots, w \cap z_r$ are all in $\text{Zig}(w)$ or $\text{Zag}(w)$. Moreover, we have that $|w \cap z_1| = \dots = |w \cap z_r|$.*

Proof. Since z_1, \dots, z_r are type I, \tilde{w} intersects with each \tilde{z}_i at most once. Thus, each pair of zigzag paths (\tilde{w}, \tilde{z}_i) for $i = 1, \dots, r$ satisfies the assumption in Lemma 3.15. Since w has intersections with z_j , \tilde{w} intersects with \tilde{z}_j precisely once on the universal cover. By Lemma 3.15, we see that $[w]$ and $[z_j]$ are linearly independent, and hence $[w]$ and $[z_i]$ are linearly independent for any i . Thus, \tilde{w} intersects with \tilde{z}_i precisely once for any $i = 1, \dots, r$.

The latter assertion follows from a similar argument as in the proof of Lemma 3.14. More precisely, since \tilde{w} intersects with \tilde{z}_i precisely once for any $i = 1, \dots, r$, if \tilde{w} intersects with \tilde{z}_i from right to left (resp. left to right), then so do zigzag paths having the same slope. This means that intersections are in $\text{Zig}(w)$ (resp. $\text{Zag}(w)$).

Also, let \tilde{z}_1 and \tilde{z}'_1 be zigzag paths on $\tilde{\Gamma}$ that are projected onto the zigzag path z_1 on Γ . We assume that there is no zigzag path projected onto z_1 between \tilde{z}_1 and \tilde{z}'_1 . Also, we assume that \tilde{w} first intersects with \tilde{z}_1 , then intersects with \tilde{z}'_1 . Then, for all $i = 2, \dots, r$ we can find a unique zigzag paths \tilde{z}_i on $\tilde{\Gamma}$ such that it is projected onto z_i and is located between \tilde{z}_1 and \tilde{z}'_1 . Thus, after \tilde{w} intersects with \tilde{z}_1 , it intersects with $\tilde{z}_2, \dots, \tilde{z}_r$ precisely once and then arrives at \tilde{z}'_1 . We can do the same arguments for any pair $(\tilde{z}_1, \tilde{z}'_1)$ of zigzag paths on $\tilde{\Gamma}$ satisfying the above properties, thus projecting onto Γ we have that $|w \cap z_1| = \dots = |w \cap z_r|$. \square

4. DEFORMATIONS OF CONSISTENT DIMER MODELS

In this section, we will introduce the concept of the deformation of consistent dimer models. This operation is defined for type I zigzag paths on a consistent dimer model, and there are two kinds of deformations, which we call the deformation at zig (see Definition 4.3) and the deformation at zag (see Definition 4.5). These deformations preserve the consistency condition, but they change the associated PM polygon. Whereas the PM polygon of the deformed dimer model is exactly the mutation of a polygon (see Section 6).

4.1. Definition of deformations of consistent dimer models. Let Γ be a reduced consistent dimer model, and hence any slope of a zigzag path on Γ is primitive. Let $\mathcal{Z}_v(\Gamma)$ be the subset of zigzag paths on Γ whose slopes are the same primitive vector $v \in \mathbb{Z}^2$, and $\mathcal{Z}_v^I(\Gamma)$ be the subset of $\mathcal{Z}_v(\Gamma)$ consisting of type I zigzag paths. We first prepare the *deformation data*.

Definition 4.1 (Deformation data). Let Γ be a reduced consistent dimer model. In order to define the deformation of Γ , we fix the following data.

- (1) We choose a type I zigzag path z , and let $2n := \ell(z)$ and $v := [z]$.
- (2) We then fix positive integers r, h such that $r \leq |\mathcal{Z}_v^I(\Gamma)|$ and $n = r + h$.

- (3) We take a subset $\{z_1, \dots, z_r\} \subset \mathcal{Z}_v^I(\Gamma)$ of type I zigzag paths, in which case we have that $2n = \ell(z_1) = \dots = \ell(z_r)$ by Lemma 3.13. Therefore, each z_i can be described as

$$z_i = z_i[1]z_i[2] \cdots z_i[2n-1]z_i[2n].$$

- (4) We consider all zigzag paths x_1, \dots, x_s (resp. y_1, \dots, y_t) intersected with z at some zags (resp. zigs) of z . In this case, each of x_1, \dots, x_s (resp. y_1, \dots, y_t) intersects with any z_i at some zags (resp. zigs) of z_i for all $i = 1, \dots, r$ by Lemma 3.16. We may assume that z_1, \dots, z_r are ordered cyclically in the sense that if x_j (resp. y_k) intersects with z_i , then it intersects with z_{i-1} (resp. z_{i+1}).
- (5) We recall that $|x_j \cap z_i|$ (resp. $|y_k \cap z_i|$) is the same number for all z_1, \dots, z_r by Lemma 3.16. Thus, for some z_i , let $m_j := |x_j \cap z_i|$ be the number of intersections between x_j and z_i on Γ for $j = 1, \dots, s$. Similarly, let $m'_k := |y_k \cap z_i|$ for $k = 1, \dots, t$. We note that $n = m_1 + \dots + m_s = m'_1 + \dots + m'_t$.
- (6) Then, we divide each zigzag path x_j into m_j parts $x_j^{(1)}, \dots, x_j^{(m_j)}$ as follows. We first fix one of the intersections of z_r and x_j as the starting edge of $x_j^{(1)}$, and tracing along x_j we will arrive at another intersection of z_r and x_j . We consider the edge of x_j just before this intersection as the ending edge of $x_j^{(1)}$, and hence such an intersection is considered as the starting edge of $x_j^{(2)}$. Repeating these procedures, we have $x_j^{(1)}, \dots, x_j^{(m_j)}$. Thus, we have the set of sub-zigzag paths:

$$\{x_1^{(1)}, \dots, x_1^{(m_1)}, x_2^{(1)}, \dots, x_2^{(m_2)}, \dots, x_s^{(1)}, \dots, x_s^{(m_s)}\}. \quad (4.1)$$

Similarly, we also divide each zigzag path y_k into m'_k parts $y_k^{(1)}, \dots, y_k^{(m'_k)}$ by considering one of the intersections of z_1 and y_k as the starting edge of $y_k^{(1)}$, and have the set of sub-zigzag paths:

$$\{y_1^{(1)}, \dots, y_1^{(m'_1)}, y_2^{(1)}, \dots, y_2^{(m'_2)}, \dots, y_t^{(1)}, \dots, y_t^{(m'_t)}\}. \quad (4.2)$$

- (7) We then assign one of $\{z_1, \dots, z_r\}$ to $x_j^{(a_j)}$ for $j = 1, \dots, s$ and $a_j = 1, \dots, m_j$. Then, we define the set X_i of edges consisting of the intersections between z_i and the sub-zigzag paths in (4.1) that are assigned with z_i . We assume that $|X_i| \geq 1$ and set $p_i := |X_i| - 1$ for $i = 1, \dots, r$. We call $\mathcal{X} := \{X_1, \dots, X_r\}$ the *zig deformation parameter* with respect to z_1, \dots, z_r and call non-negative integers $\mathbf{p} = (p_1, \dots, p_r) \in \mathbb{Z}_{\geq 0}^r$ the *weight* of \mathcal{X} . Similarly, we assign one of $\{z_1, \dots, z_r\}$ to $y_k^{(b_k)}$ for $k = 1, \dots, t$ and $b_k = 1, \dots, m'_k$. Then, we define the set Y_i of edges consisting of the intersections between z_i and the sub-zigzag paths in (4.2) that are assigned with z_i . We assume that $|Y_i| \geq 1$ and set $q_i := |Y_i| - 1$ for $i = 1, \dots, r$. We call $\mathcal{Y} := \{Y_1, \dots, Y_r\}$ the *zag deformation parameter* with respect to z_1, \dots, z_r and call non-negative integers $\mathbf{q} = (q_1, \dots, q_r) \in \mathbb{Z}_{\geq 0}^r$ the *weight* of \mathcal{Y} . We remark that $p_1 + \dots + p_r = m_1 + \dots + m_s - r = n - r = h$, and also $q_1 + \dots + q_r = h$.

Remark 4.2. We note several remarks concerning the deformation data.

- (1) To define the deformation data, we need a type I zigzag path. If a dimer model is isoradial then any zigzag path is type I (see Definition 3.4), and hence $|\mathcal{Z}_v^I(\Gamma)| = |\mathcal{Z}_v(\Gamma)|$. Also, even if Γ contains no type I zigzag paths, we sometimes make a type II zigzag path type I by using the *mutations of dimer models* (see Appendix A, especially Example A.4).
- (2) When we choose $r = 1$ in Definition 4.1, we have the zig (resp. zag) deformation parameter $\mathcal{X} = \{X_1\}$ (resp. $\mathcal{Y} = \{Y_1\}$) with respect to z_1 , and the weights of \mathcal{X} and \mathcal{Y} are both $h = \ell(z_1)/2 - 1$. In this case, we only need these data to define the deformations (see Definition 4.8).

Definition 4.3 (Deformation at zig). Let the notation be the same as Definition 4.1. For the zig deformation parameter $\mathcal{X} = \{X_1, \dots, X_r\}$ of the weight $\mathbf{p} = (p_1, \dots, p_r)$, we consider the following procedures:

- (zig-1) Using split moves, we insert p_i white nodes and p_i black nodes in each zig of z_i .

[Notation]

- For a zig $z_i[2m-1]$ of z_i where $m = 1, \dots, n$ and $i = 1, \dots, r$, we denote by $b_i[2m-1]$ (resp. $w_i[2m-1]$) the black (resp. white) node that is the endpoint of $z_i[2m-1]$.
- We denote the white nodes added in the zig $z_i[2m-1]$ by $w_{i,1}[2m-1], \dots, w_{i,p_i}[2m-1]$, and denote the black ones by $b_{i,1}[2m-1], \dots, b_{i,p_i}[2m-1]$. Here, the subscripts increase in the direction from $b_i[2m-1]$ to $w_i[2m-1]$.

- (zig-2) We remove all zag of z_i for all $i = 1, \dots, r$.

- (zig-3) If $p_i \neq 0$, then we connect the white node $w_{i,j}[2m-1]$ to the black node $b_{i,j}[2m+1]$ where $j = 1, \dots, p_i$ and $m = 1, \dots, n$. (Note that $w_{i,j}[2n-1]$ is connected to $b_{i,j}[2n+1] := b_{i,j}[1]$.) We denote by $z_{i,j}$ the new 1-cycle, which will be a zigzag path on the deformed dimer model, obtained by connecting

$$w_{i,j}[2n-1], b_{i,j}[2n-1], w_{i,j}[2n-3], b_{i,j}[2n_i-3], \dots, w_{i,j}[1], b_{i,j}[1]$$

cyclically ($i = 1, \dots, r$ and $j = 1, \dots, p_i$).

- (zig-4) For $m = 1, \dots, n$ and $i = 1, \dots, r$, if the zag $z_i[2m]$ of the original zigzag path z_i on Γ is not contained in X_i , then we add edges, which we call *bypasses*, connecting the following pairs of black and white nodes:

$$(w_{i,1}[2m-1], b_i[2m+1]), (w_{i,2}[2m-1], b_{i,1}[2m+1]), \\ \dots, (w_{i,p_i}[2m-1], b_{i,p_i-1}[2m+1]), (w_i[2m-1], b_{i,p_i}[2m+1]).$$

We denote the resulting dimer model by $\bar{\nu}_{\mathcal{X}}^{\text{zig}}(\Gamma, \{z_1, \dots, z_r\})$. We note that $\bar{\nu}_{\mathcal{X}}^{\text{zig}}(\Gamma, \{z_1, \dots, z_r\})$ is non-degenerate by Proposition 4.12.

- (zig-5) Then, we make the dimer model $\bar{\nu}_{\mathcal{X}}^{\text{zig}}(\Gamma, \{z_1, \dots, z_r\})$ consistent using the method given in the proof of [BIU, Theorem 1.1] (see Operation 4.6 and Proposition 4.7).
- (zig-6) If there exist 2-valent nodes, then we apply the join moves to the dimer model obtained by the above procedures and make it reduced.

We denote the resulting dimer model by $\nu_{\mathcal{X}}^{\text{zig}}(\Gamma, \{z_1, \dots, z_r\})$, and call it the *deformation of Γ at zig of $\{z_1, \dots, z_r\}$ with respect to the zig deformation parameter \mathcal{X}* . If a situation is clear, we simply denote this by $\nu_{\mathcal{X}}^{\text{zig}}(\Gamma)$.

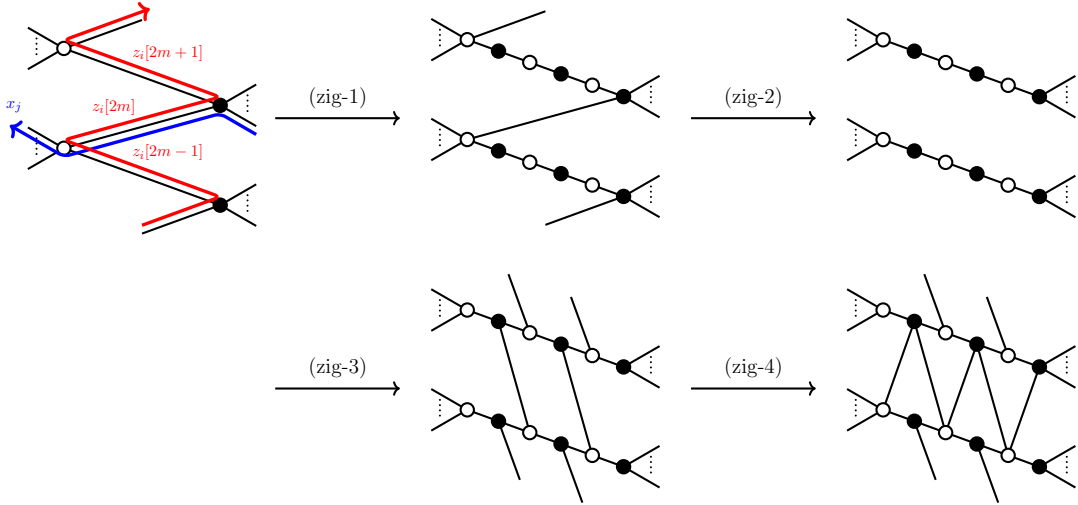


FIGURE 7. The deformation at zig of z_i with $p_i = 2$. (We assume that $z_i[2m]$ is not contained in X_i .)

Remark 4.4. The non-degenerate dimer model $\bar{\nu}_{\mathcal{X}}^{\text{zig}}(\Gamma, \{z_1, \dots, z_r\})$ is determined uniquely for a given deformation data, but in the operation (zig-5), the way to remove edges is not unique. Therefore, the resulting consistent dimer model is not unique, whereas since the set of slopes of zigzag paths is the same for all possible consistent dimer models (see Proposition 4.7(2)), the associated PM polygon is the same by Proposition 3.6. In addition, it has been believed that all consistent dimer models associated with the same lattice polygon are transformed into each other by the *mutations of dimer models* (see Appendix A). Thus, we expect that the deformation of a consistent dimer model is determined uniquely up to “*mutation equivalence*”. (We encounter the same situation for the deformation at zag given in Definition 4.5 below.)

Similarly, we can define the “zag version” of this deformation as follows.

Definition 4.5 (Deformation at zag). Let the notation be the same as Definition 4.1. For the zag deformation parameter $\mathcal{Y} = \{Y_1, \dots, Y_r\}$ of the weight $\mathbf{q} = (q_1, \dots, q_r)$, we consider the following procedures:

(zag-1) Using split moves, we insert q_i white nodes and q_i black nodes in each zag of z_i .

[Notation]

- For a zag $z_i[2m]$ of z_i where $m = 1, \dots, n$ and $i = 1, \dots, r$, we denote by $w_i[2m]$ (resp. $b_i[2m]$) the white (resp. black) node that is the endpoint of $z_i[2m]$.
- We denote the white nodes added in the zag $z_i[2m]$ by $w_{i,1}[2m], \dots, w_{i,q_i}[2m]$, and denote the black ones by $b_{i,1}[2m], \dots, b_{i,q_i}[2m]$. Here, the subscripts increase in the direction from $w_i[2m]$ to $b_i[2m]$.

(zag-2) We remove all zig of z_i for all $i = 1, \dots, r$.

(zag-3) If $q_i \neq 0$, then we connect the black node $b_{i,j}[2m]$ to the white node $w_{i,j}[2m+2]$ where $j = 1, \dots, q_i$ and $m = 1, \dots, n$. (Note that $b_{i,j}[2n]$ is connected to $w_{i,j}[2n+2] := w_{i,j}[2]$.) We denote by $z_{i,j}$ the new 1-cycle, which will be a zigzag path on the deformed dimer model, obtained by connecting

$$b_{i,j}[2n], w_{i,j}[2n], b_{i,j}[2n-2], w_{i,j}[2n-2], \dots, b_{i,j}[2], w_{i,j}[2]$$

cyclically ($i = 1, \dots, r$ and $j = 1, \dots, q_i$).

(zag-4) For $m = 1, \dots, n$ and $i = 1, \dots, r$, if the zig $z_i[2m-1]$ of the original zigzag path z_i on Γ is not contained in Y_i , then we add edges, which we call *bypasses*, connecting the following pairs of black and white nodes:

$$(b_{i,1}[2m], w_{i,1}[2m+2]), (b_{i,2}[2m], w_{i,1}[2m+2]), \\ \dots, (b_{i,q_i}[2m], w_{i,q_i-1}[2m+2]), (b_i[2m], w_{i,q_i}[2m+2]).$$

We denote the resulting dimer model by $\overline{\nu}_{\mathcal{Y}}^{\text{zag}}(\Gamma, \{z_1, \dots, z_r\})$. We note that $\overline{\nu}_{\mathcal{Y}}^{\text{zag}}(\Gamma, \{z_1, \dots, z_r\})$ is non-degenerate by Proposition 4.12.

(zag-5) Then, we make the dimer model $\overline{\nu}_{\mathcal{Y}}^{\text{zag}}(\Gamma, \{z_1, \dots, z_r\})$ consistent using the method given in the proof of [BIU, Theorem 1.1] (see Operation 4.6 and Proposition 4.7).

(zag-6) If there exist 2-valent nodes, then we apply the join moves to the dimer model obtained by the above procedures and make it reduced.

We denote the resulting dimer model by $\nu_{\mathcal{Y}}^{\text{zag}}(\Gamma, \{z_1, \dots, z_r\})$, and call it the *deformation of Γ at zag of $\{z_1, \dots, z_r\}$ with respect to the zag deformation parameter \mathcal{Y}* (see also Remark 4.4). If a situation is clear, we simply denote this by $\nu_{\mathcal{Y}}^{\text{zag}}(\Gamma)$.

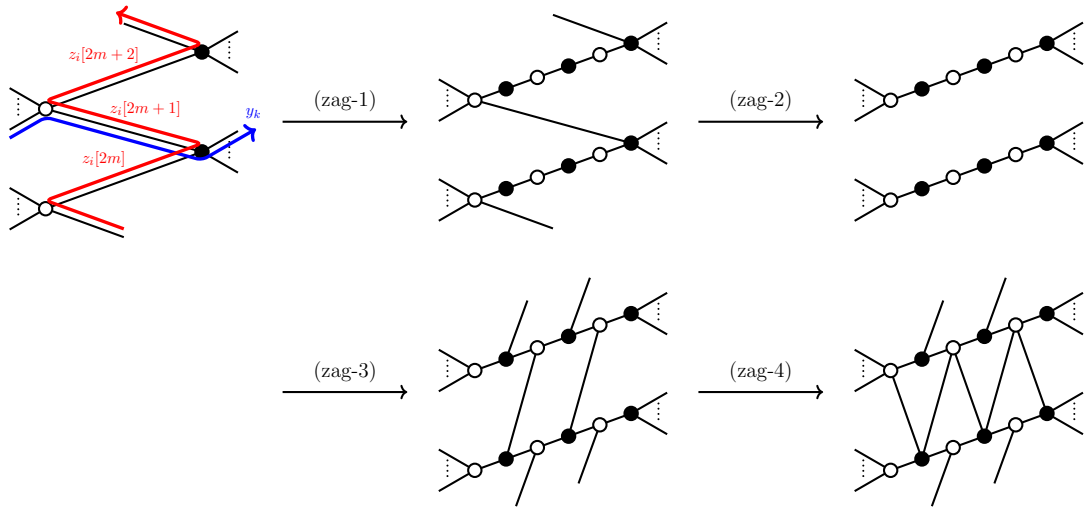


FIGURE 8. The deformation at zag of z_i with $q_i = 2$. (We assume that $z_i[2m+1]$ is not contained in Y_i .)

Operation 4.6. We note the operation given in the proof of [BIU, Theorem 1.1], which is used in (zig-5) and (zag-5).

- (a) The dimer model $\bar{\nu}_\lambda^{\text{zig}}(\Gamma, \{z_1, \dots, z_r\})$ (resp. $\bar{\nu}_y^{\text{zag}}(\Gamma, \{z_1, \dots, z_r\})$), which is obtained by applying the operations (zig-1)–(zig-4) (resp. (zag-1)–(zag-4)) to the reduced consistent dimer model Γ , sometimes contains zigzag paths having a self-intersection on the universal cover. In this case, we use the operation given in the proof of [BIU, Theorem 1.1], that is, we remove all the edges at the self-intersection (see Figure 9). We note that this operation does not change the slope of the argued zigzag path.

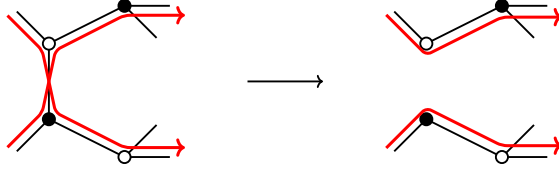


FIGURE 9. An example of removing a self-intersection of a zigzag path

After these processes, there might be a connected component of the resulting bipartite graph that is contained in a simply-connected domain in \mathbb{T} . In that case, we remove such a connected component. We note that this removal does not affect our purpose, because our main concern is the PM polygon which is recovered from the slopes of zigzag paths, and the slope of the zigzag path corresponding to the argued connected component is trivial.

- (b) On the other hand, the dimer model $\bar{\nu}_\lambda^{\text{zig}}(\Gamma, \{z_1, \dots, z_r\})$ (resp. $\bar{\nu}_y^{\text{zag}}(\Gamma, \{z_1, \dots, z_r\})$) might have a pair of zigzag paths on the universal cover that intersect with each other in the same direction more than once. In this case, we use another operation given in the proof of [BIU, Theorem 1.1], that is, we choose any such pair of zigzag paths and remove a pair of consecutive intersections of this pair of zigzag paths (see Figure 10). We note that this operation does not change the slopes of zigzag paths and the resulting bipartite graph is also a dimer model because $\bar{\nu}_\lambda^{\text{zig}}(\Gamma, \{z_1, \dots, z_r\})$ (resp. $\bar{\nu}_y^{\text{zag}}(\Gamma, \{z_1, \dots, z_r\})$) satisfies the strong marriage condition as we will see in Proposition 4.12.

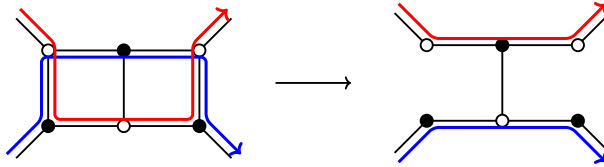


FIGURE 10. An example of removing a pair of consecutive intersections of zigzag paths

Since the dimer model $\bar{\nu}_\lambda^{\text{zig}}(\Gamma, \{z_1, \dots, z_r\})$ (resp. $\bar{\nu}_y^{\text{zag}}(\Gamma, \{z_1, \dots, z_r\})$) is non-degenerate by Proposition 4.12 and it does not contain a homologically trivial zigzag path (see the proofs of Proposition 5.4, 5.5 and 5.8), we can make $\bar{\nu}_\lambda^{\text{zig}}(\Gamma, \{z_1, \dots, z_r\})$ (resp. $\bar{\nu}_y^{\text{zag}}(\Gamma, \{z_1, \dots, z_r\})$) another dimer model satisfying conditions in Definition 3.2 by iterating the operations given in Operation 4.6. Thus, it is consistent, but it is not necessarily isoradial even if Γ is isoradial (see Example 4.11). Furthermore, since these operations and (zig-6) (resp. (zag-6)) do not change the slopes of the operated zigzag paths, we have the following proposition.

Proposition 4.7. *Let the notation be the same as Definition 4.1, 4.3 and 4.5. Then, we have the followings.*

- (1) *The dimer models $\bar{\nu}_\lambda^{\text{zig}}(\Gamma, \{z_1, \dots, z_r\})$ and $\bar{\nu}_y^{\text{zag}}(\Gamma, \{z_1, \dots, z_r\})$ are consistent.*
- (2) *The set of slopes of zigzag paths on $\bar{\nu}_\lambda^{\text{zig}}(\Gamma, \{z_1, \dots, z_r\})$ (resp. $\bar{\nu}_y^{\text{zag}}(\Gamma, \{z_1, \dots, z_r\})$) is the same as that of $\bar{\nu}_\lambda^{\text{zig}}(\Gamma, \{z_1, \dots, z_r\})$ (resp. $\bar{\nu}_y^{\text{zag}}(\Gamma, \{z_1, \dots, z_r\})$).*

The operations (zig-4) and (zig-5) (resp. (zag-4) and (zag-5)) would be complicated if a given dimer model is large. However, if we choose $r = 1$ as the deformation data, then $\mathcal{X} = \{X_1\}$ and $\mathcal{Y} = \{Y_1\}$ where X_1 (resp. Y_1) is the set of intersections between a chosen type I zigzag path z and x_1, \dots, x_s (resp. y_1, \dots, y_t). In particular, X_1 (resp. Y_1) coincides with the set of zags (resp. zigs) of z , and hence they are determined uniquely. Thus, in this case we may skip the operations (zig-4) (resp. (zag-4)), in which case we may also skip (zig-5) (resp. (zag-5)) since there are no bypasses (see Observation 5.2, 5.3 and Lemma 5.6). Thus, we only need the weight p (resp. q) of \mathcal{X} (resp. \mathcal{Y}) to define the deformation at zig (resp. zag). We call p (resp. q) the *zig* (resp. *zag*) *deformation weight* with respect to z , and we sometimes denote the deformed dimer models as $\nu_{\mathcal{X}}^{\text{zig}}(\Gamma, z) = \nu_p^{\text{zig}}(\Gamma, z)$ and $\nu_{\mathcal{Y}}^{\text{zag}}(\Gamma, z) = \nu_q^{\text{zag}}(\Gamma, z)$. We here note the simplified definition of the deformations for the case of $r = 1$.

Definition 4.8 (Deformations for the case of $r = 1$). Let the notation be the same as Definition 4.1 with $r = 1$ (see also Remark 4.2(2)). In particular, for a chosen type I zigzag path z , we have the zig (resp. zag) deformation parameter $\mathcal{X} = \{X_1\}$ (resp. $\mathcal{Y} = \{Y_1\}$) of the weight $p = h$ (resp. $q = h$) where $h = \ell(z)/2 - 1$.

Then, the *deformation of a consistent dimer model Γ at zig of z with the weight p* is defined by the operations (zig-1)–(zig-3) and (zig-6), and the resulting consistent dimer model is denoted by $\nu_p^{\text{zig}}(\Gamma, z)$. Similarly, the *deformation of Γ at zag of z with the weight q* is defined by the operations (zag-1)–(zag-3) and (zag-6), and the resulting consistent dimer model is denoted by $\nu_q^{\text{zag}}(\Gamma, z)$.

We remark that $\nu_p^{\text{zig}}(\Gamma, z)$ (resp. $\nu_q^{\text{zag}}(\Gamma, z)$) is determined uniquely by definition.

Remark 4.9. We note additional remarks concerning the definition of the deformations.

- (1) We can skip the operations (zig-4) and (zig-5) (resp. (zag-4) and (zag-5)) for some classes of dimer models even if $r \neq 1$. For example, if a given dimer model is a hexagonal dimer model or a square dimer model, in which case the associated PM polygon is a triangle or parallelogram, then we can skip these operations (see Appendix C for more details).
- (2) The join move does not change slopes of zigzag paths, and hence it does not affect the associated PM polygon. Thus, when we are interested in only the PM polygon, we may skip (zig-6) and (zag-6).
- (3) Even if we choose the other sets of intersections X'_1, \dots, X'_r (resp. Y'_1, \dots, Y'_r) in Definition 4.1(7), the PM polygon of the deformed dimer model is the same as that of $\nu_{\mathcal{X}}^{\text{zig}}(\Gamma)$ (resp. $\nu_{\mathcal{Y}}^{\text{zag}}(\Gamma)$) as we will show in Proposition 5.10.

4.2. Examples of deformations of consistent dimer models. In this subsection we give several examples. In these examples, we do not need the operations (zig-4) and (zig-5) (resp. (zag-4) and (zag-5)) because $r = 1$. We will give a large example which requires these operations in Appendix B.

Example 4.10. Let Γ be the dimer model given in Figure 1. We recall that zigzag paths on Γ are Figure 6, and we use the same notations given in these figures.

We first collect the deformation data (see Definition 4.1). Let us choose the zigzag path z_3 , and we will denote this by z . We see that $\ell(z) = 6$, $v := [z] = (-1, -1)$, and $|\mathcal{Z}_v^1(\Gamma)| = 1$. Since $|\mathcal{Z}_v^1(\Gamma)| = 1$, we can take only $r = 1$, in which case $h = \ell(z)/2 - r = 2$. Thus, we have that the zig (resp. zag) deformation weight is $p = h = 2$ (resp. $q = h = 2$). More precisely, we see that z_2 intersects with z at zig of z , and z_1, z_4 intersect with z at zag of z . Thus, $\mathcal{X} = \{X_1\}$ (resp. $\mathcal{Y} = \{Y_1\}$) consists of the intersections between z and z_2 (resp. z and z_1 or z_4). Since $|z_1 \cap z| = 1$, $|z_2 \cap z| = 3$, and $|z_4 \cap z| = 2$, we have the weights $p = q = 2$.

Then, we apply the deformation of Γ at zig of z with $p = 2$ as shown in Figure 11.

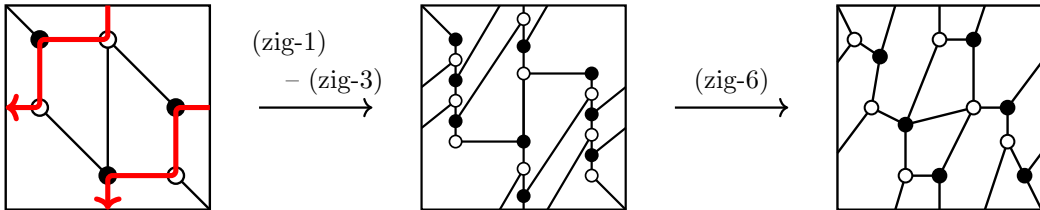


FIGURE 11. The deformation of Γ at zig of z

We also apply the deformation of Γ at zag of z with $q = 2$ as shown in Figure 12.

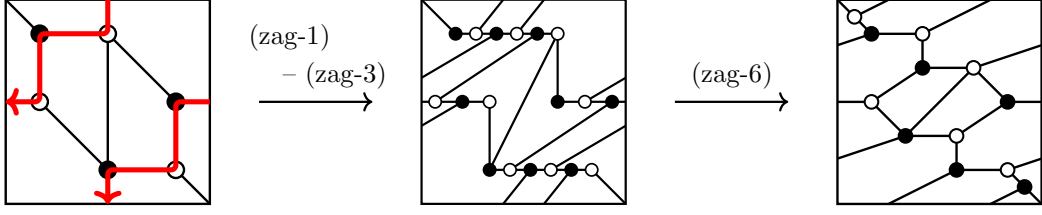


FIGURE 12. The deformation of Γ at zag of z

Example 4.11. We remark that even if Γ is an isoradial dimer model, the deformed ones are not necessarily isoradial.

For example, the leftmost dimer model Γ in Figure 13 is isoradial. We choose a type I zigzag path z whose slope is $v = (-1, 0)$, in which case $|\mathcal{Z}_v^I(\Gamma)| = 2$ and $\ell(z) = 4$. We fix $r = 1$, and hence $h = \ell(z)/2 - r = 1$. Applying the deformation of Γ at zig of z with the zig deformation weight $p = 1$, we have the rightmost one in Figure 13, and easily check that this deformed dimer model is consistent but not isoradial.

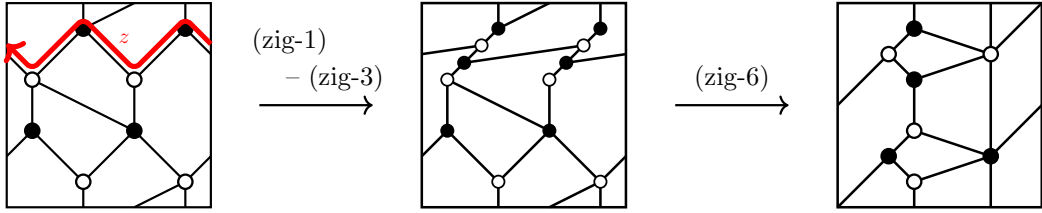


FIGURE 13. An example of the deformed dimer model that is not isoradial

4.3. The proof of the non-degeneracy. In this subsection, we show the non-degeneracy of the dimer models $\overline{\mathcal{V}}_{\mathcal{X}}^{\text{zig}}(\Gamma, \{z_1, \dots, z_r\})$ and $\overline{\mathcal{V}}_{\mathcal{Y}}^{\text{zag}}(\Gamma, \{z_1, \dots, z_r\})$.

Proposition 4.12. *Let the notation be the same as Definition 4.1, 4.3 and 4.5. Then, we have that the dimer models $\overline{\mathcal{V}}_{\mathcal{X}}^{\text{zig}}(\Gamma, \{z_1, \dots, z_r\})$ and $\overline{\mathcal{V}}_{\mathcal{Y}}^{\text{zag}}(\Gamma, \{z_1, \dots, z_r\})$ are non-degenerate.*

Proof. We prove the case of $\overline{\mathcal{V}}_{\mathcal{X}}^{\text{zig}}(\Gamma) = \overline{\mathcal{V}}_{\mathcal{X}}^{\text{zig}}(\Gamma, \{z_1, \dots, z_r\})$, and the other case is similar.

Let Γ' be the dimer model obtained by applying the operations (zig-1)–(zig-3) to Γ .

(The first step): Here, we recall that the non-degeneracy condition is equivalent to the strong marriage condition, that is, a dimer model has equal numbers of black and white nodes and every proper subset S of the black nodes satisfies the condition that S is connected to at least $|S| + 1$ white nodes.

Suppose that Γ' is non-degenerate. Then Γ' satisfies the strong marriage condition. By applying the operation (zig-4), we obtain the dimer model $\overline{\mathcal{V}}_{\mathcal{X}}^{\text{zig}}(\Gamma, \{z_1, \dots, z_r\})$. Since (zig-4) is the operation that adds new edges, it also satisfies the strong marriage condition, and hence it is non-degenerate. Therefore, it is enough to show that Γ' is non-degenerate.

(The second step): We next consider a sub-dimer model Γ'' of Γ satisfying the condition (*) below, where we mean that Γ'' is a *sub-dimer model* of Γ if the set of the nodes coincide and the set of edges in Γ'' is the subset of edges in Γ .

Condition (*): For any given edge e in Γ'' , let z' and z'' be the different zigzag paths on Γ'' each of which contains e . Then either (*1) or (*2) holds:

- (*1) either $[z'] \in \{[z_i], -[z_i]\}$ or $[z''] \in \{[z_i], -[z_i]\}$ holds;
- (*2) If z' intersects with z_i in $\text{Zig}(z_i)$ (resp. $\text{Zag}(z_i)$), then z'' intersects with z_i in $\text{Zag}(z_i)$ (resp. $\text{Zig}(z_i)$) for any i .

A desired sub-dimer model Γ'' of Γ satisfying $(*)$ can be constructed as follows. Here, to obtain such a sub-dimer model, we employ the algorithm developed in [Gul, IU2] for showing Theorem 2.5, and we modify it to our situation.

First, let us consider the original dimer model Γ and let E_1, E_2, \dots, E_m be all edges of Δ_Γ , where the primitive outer normal vector for E_1 is the slope $[z_1] = \dots = [z_r]$. We assume that these edges are ordered cyclically in the anti-clockwise direction (see Figure 26 as reference). Also, let v_j be the primitive outer normal vector corresponding to E_j for each $1 \leq j \leq m$. Let a be the index such that $v_a = -v_1$ if there exists such an edge among E_2, \dots, E_m , that is, E_a is parallel to E_1 . If there is no such edge, then let $E_a = \emptyset$ for simplicity of notation. We recall that by Proposition 3.5, for each $E_j \neq \emptyset$ there exist zigzag paths on Γ such that the associated slopes coincide with v_j , and the set of such zigzag paths is denoted by $\mathcal{Z}_{v_j} = \mathcal{Z}_{v_j}(\Gamma)$. By our assumption, each slope of the zigzag paths in $\mathcal{Z}_1 := \mathcal{Z}_{v_2} \cup \dots \cup \mathcal{Z}_{v_{a-1}}$ and v_1 are linearly independent. Thus, the zigzag paths in \mathcal{Z}_1 intersect with a type I zigzag path z_i precisely once in the universal cover (see Lemma 3.15). By definition of E_2, \dots, E_{a-1} , such an intersection is given from the right of z_i to the left of z_i , and hence zigzag paths in \mathcal{Z}_1 intersect with z_i in $\mathbf{Zag}(z_i)$. Similarly, we have that the zigzag paths in $\mathcal{Z}_2 := \mathcal{Z}_{v_{a+1}} \cup \dots \cup \mathcal{Z}_{v_m}$ intersect with z_i precisely once in the universal cover, and especially they intersect with z_i in $\mathbf{Zig}(z_i)$.

We assume that there are at least two edges between E_2 and E_{a-1} (i.e., $a \geq 4$). Then, we take adjacent two edges, say, E_2 and E_3 . Since v_2 and v_3 are linearly independent, the zigzag paths $z'_2 \in \mathcal{Z}_{v_2}$ and $z'_3 \in \mathcal{Z}_{v_3}$ intersect at some edge of Γ . Clearly, such an intersection $z'_2 \cap z'_3$ is neither any edge constituting any zigzag path whose slope is $[z_i]$ nor $-[z_i]$. Now, remove an edge in $z'_2 \cap z'_3$. This operation merges z'_2 and z'_3 , in which case the resulting dimer model stays consistent and the associated PM polygon becomes “small” (see [Gul, Section 5, 6] for more details). Furthermore, since $z'_2 \cap z_i \subset \mathbf{Zag}(z_i)$ and $z'_3 \cap z_i \subset \mathbf{Zag}(z_i)$ for each i , edges in $z'_2 \cap z'_3$ do not share a node with z_i for any i . Thus, z_i is still type I even if we apply this operation and the merged zigzag path intersects with z_i in $\mathbf{Zag}(z_i)$. We repeat this procedure until there are no two edges between E_2 and E_{a-1} . Similarly, if there are at least two edges between E_{a+1} and E_m (i.e., $m - a \geq 2$), then we do the same procedures as above until there are no two edges between E_{a+1} and E_m . After removing all suitable edges from Γ , we get a consistent dimer model, which is clearly a sub-dimer model of Γ , and we will denote this by Γ_{sub} . Since we do not remove edges contained in a zigzag path whose slope is $\pm[z_i]$ in the above arguments, the edges E_1 and E_a (if this is not empty) of Δ_Γ are preserved on $\Delta_{\Gamma_{\text{sub}}}$ (and hence we will use the same notation). Also, the edges E_2, \dots, E_{a-1} (resp. E_{a+1}, \dots, E_m) of Δ_Γ are substituted by the single edge in $\Delta_{\Gamma_{\text{sub}}}$, thus we denote such an edge by E'_2 (resp. E'_m). We note that zigzag paths corresponding to E'_2 (resp. E'_m) are obtained by merging the ones corresponding to E_2, \dots, E_{a-1} (resp. E_{a+1}, \dots, E_m). In particular, the PM polygon $\Delta_{\Gamma_{\text{sub}}}$ is constituted by E_1, E'_2, E_a, E'_m , in which case $\Delta_{\Gamma_{\text{sub}}}$ is a triangle or a trapezoid. Then, it follows from the construction of Γ_{sub} that

- The zigzag paths z_1, \dots, z_r on Γ are preserved on Γ_{sub} and they are type I;
- The zigzag paths on Γ corresponding to E_a (if this is not empty) are preserved on Γ_{sub} ;
- The zigzag paths corresponding to E'_2 (resp. E'_m) are intersected with z_i in $\mathbf{Zag}(z_i)$ (resp. $\mathbf{Zig}(z_i)$) (see also the argument in the proof of Lemma 3.14).

From these facts, it is easy to verify that Γ_{sub} is our desired sub-dimer model Γ'' of Γ that satisfies the condition $(*)$.

(The third step): Now, we apply the operations (zig-1)–(zig-3) in Definition 4.3 to Γ_{sub} , which is possible since z_1, \dots, z_r are preserved on Γ_{sub} . Then, we denote the resulting dimer model by Γ'_{sub} . By the construction, Γ' can be obtained by adding some edges to Γ'_{sub} . Thus, similar to the discussion in the first step, it is enough to show that Γ'_{sub} is non-degenerate for proving the non-degeneracy of Γ' .

Then, we finally show that Γ'_{sub} is non-degenerate. To do this, we prove the existence of a perfect matching that contains a given edge e of Γ'_{sub} . We divide the set of edges into four cases (i)–(iv):

- (i) e is of the form $(b_{i,j-1}[2m-1], w_{i,j}[2m-1])$ for some $1 \leq i \leq r, 1 \leq j \leq p_i + 1$ and $1 \leq m \leq n$, where we let $b_{i,0}[2m-1] = b_i[2m-1]$ and $w_{i,p_i+1}[2m-1] = w_i[2m-1]$;
- (ii) e is of the form $(w_{i,j}[2m-1], b_{i,j}[2m-1])$ for some $1 \leq i \leq r, 1 \leq j \leq p_i$ and $1 \leq m \leq n$;
- (iii) e is of the form $(b_{i,j}[2m-1], w_{i,j}[2m-3])$ for some $1 \leq i \leq r, 1 \leq j \leq p_i$ and $1 \leq m \leq n$;
- (iv) e is of the form except for (i)–(iii).

Namely, (i) and (ii) are the edges emanated in the process (zig-1), (iii) is one added in the process (zig-3), and (iv) is one which is invariant between Γ'_{sub} and Γ_{sub} .

Since Γ_{sub} is consistent and contains the type I zigzag paths z_1, \dots, z_r , there exist corner perfect matchings P and P' on Γ_{sub} that are adjacent and satisfy $P \cap z_i = \mathbf{Zig}(z_i)$ and $P' \cap z_i = \mathbf{Zag}(z_i)$ for

$1 \leq i \leq r$ (see subsection 3.2). Similarly, let Q be a corner perfect matching on Γ_{sub} with $Q \cap z_i = \emptyset$ for $1 \leq i \leq r$. The existence of such Q is guaranteed by Lemma 3.12. We will use these P, P' and Q in order to find a suitable perfect matching on Γ'_{sub} containing a given edge e . We divide our discussions into the following cases (i)–(iv) that correspond to the above division of edges respectively.

Case (i): Let

$$P'' = (P \setminus \bigcup_{i=1}^r \text{Zig}(z_i)) \cup \left(\bigcup_{i=1}^r \bigcup_{j=1}^{p_i+1} \bigcup_{m=1}^n (b_{i,j-1}[2m-1], w_{i,j}[2m-1]) \right), \quad (4.3)$$

see Figure 14. It is easy to see that P'' is a perfect matching on Γ'_{sub} containing e in the case (i).

Case (ii): Let

$$P'' = Q \cup \left(\bigcup_{i=1}^r \bigcup_{j=1}^{p_i} \bigcup_{m=1}^n (w_{i,j}[2m-1], b_{i,j}[2m-1]) \right),$$

see Figure 15. Then, we see that P'' is a perfect matching on Γ'_{sub} containing e in the case (ii).

Case (iii): Let

$$P'' = Q \cup \left(\bigcup_{i=1}^r \bigcup_{j=1}^{p_i} \bigcup_{m=1}^n (b_{i,j}[2m-1], w_{i,j}[2m-3]) \right),$$

see Figure 16. Then, we see that P'' is a perfect matching on Γ'_{sub} containing e in the case (iii).

Case (iv): We note that an edge e in the case (iv) also appears in Γ_{sub} since e is unchanged even if we apply (zig-1)–(zig-3). Thus, we can regard e as an edge of Γ_{sub} . Since Γ_{sub} satisfies the condition (*), the zigzag paths z', z'' on Γ_{sub} that contain e satisfy either (*1) or (*2).

- We assume that z' and z'' satisfy (*1).
 - Let, say, $[z'] = [z_i]$. Since zigzag paths having the same slopes are obtained as the difference of adjacent corner perfect matchings, either P or P' contains e . If $e \in P$, then we let P'' be the same as (4.3). Then, P'' is a perfect matching on Γ'_{sub} containing e . Even if $e \in P'$, we have the same conclusion by letting

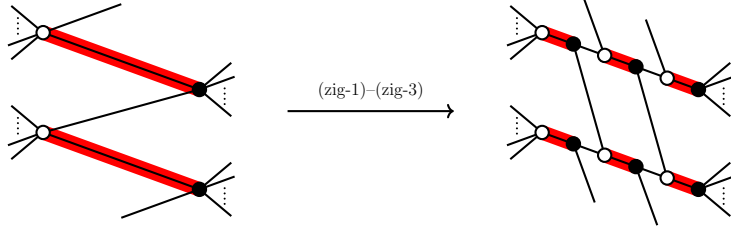
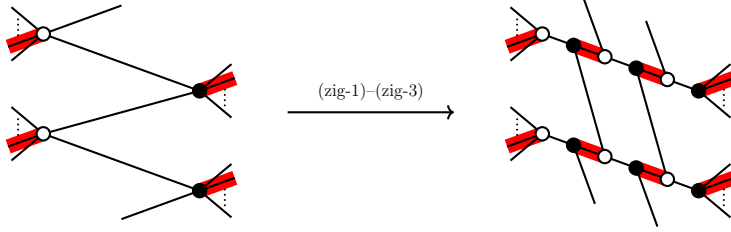
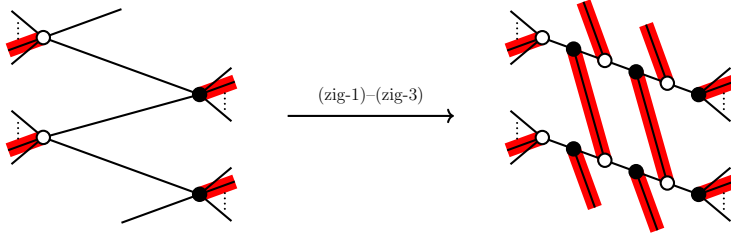
$$P'' = (P' \setminus \bigcup_{i=1}^r \text{Zag}(z_i)) \cup \left(\bigcup_{i=1}^r \bigcup_{j=1}^{p_i+1} \bigcup_{m=1}^n (b_{i,j-1}[2m-1], w_{i,j}[2m-1]) \right).$$

- Let, say, $[z'] = -[z_i]$, in which case $E_a \neq \emptyset$ and z' corresponds to E_a . Let Q' and Q'' be the corner perfect matchings on Γ_{sub} whose difference forms z' . Let $e \in Q'$. Since $h(Q', P_0)$ lies on E_a where P_0 is the reference perfect matching, we have that $Q' \cap z_i = \emptyset$ for any i by Lemma 3.9. Thus, we let

$$P'' = Q' \cup \left(\bigcup_{i=1}^r \bigcup_{j=1}^{p_i} \bigcup_{m=1}^n (w_{i,j}[2m-1], b_{i,j}[2m-1]) \right),$$

and see that P'' is a perfect matching on Γ'_{sub} containing e .

- We assume that z' and z'' satisfy (*2).
 - Let, say, z' intersects with each z_i in $\text{Zig}(z_i)$. Let Q' and Q'' be the corner perfect matchings on Γ_{sub} whose difference forms z' . Let $e \in Q'$. As noted above, we see that all zigzag paths in Γ_{sub} intersecting with z_i at some zig of z_i have the same slopes. This implies that Q' contains all zigs of z_i , i.e., $Q' \cap z_i = \text{Zig}(z_i)$. This also means that $Q' = P$. Hence, we let P'' be the same as (4.3) and see that P'' is a perfect matching containing e .


 FIGURE 14. The perfect matchings P on Γ_{sub} (left) and P'' on Γ'_{sub} (right) for the case (i)

 FIGURE 15. The perfect matchings Q on Γ_{sub} (left) and P'' on Γ'_{sub} (right) for the case (ii)

 FIGURE 16. The perfect matchings Q on Γ_{sub} (left) and P'' on Γ'_{sub} (right) for the case (iii)

□

5. ZIGZAG PATHS ON DEFORMED DIMER MODELS

In this section, we observe zigzag paths of the deformed dimer models and their slopes. We mainly discuss the deformation at zig, but the same assertions hold for the deformation at zag by a similar argument. Thus, we will work with the setting in Definition 4.1, and consider the deformation $\nu_{\mathcal{X}}^{\text{zig}}(\Gamma, \{z_1, \dots, z_r\})$ of Γ (see Definition 4.3).

5.1. Behaviors of zigzag paths after deformations. First, we give the following observation and fix the notations which we will use throughout this sections.

Observation 5.1. Let Γ and z_1, \dots, z_r be the same as in Definition 4.1, especially z_1, \dots, z_r are type I and $[z_1] = \dots = [z_r]$. These zigzag paths are ordered along the subscript $i = 1, \dots, r$ cyclically. For any $\alpha \in \mathbb{Z}$ and $i = 1, \dots, r$, let $\tilde{z}_i(\alpha)$ be a zigzag path on the universal cover $\tilde{\Gamma}$ whose projection on Γ is z_i . Each $\tilde{z}_i(\alpha)$ divides \mathbb{R}^2 into two parts, thus it makes sense to consider the left of $\tilde{z}_i(\alpha)$ and the right of $\tilde{z}_i(\alpha)$. Then, we can write a straight line $\ell_{i,\alpha}^L$ (resp. $\ell_{i,\alpha}^R$) on the left (resp. right) of $\tilde{z}_i(\alpha)$ such that the gradient of $\ell_{i,\alpha}^L$ (resp. $\ell_{i,\alpha}^R$) is $v = [z_i]$ and nodes contained in the region obtained as the intersection of

the right of $\ell_{i,\alpha}^L$ and the left of $\ell_{i,\alpha}^R$ are precisely the ones located on $\tilde{z}_i(\alpha)$. We will call such a region the (i, α) -th deformed part (see Figure 17).

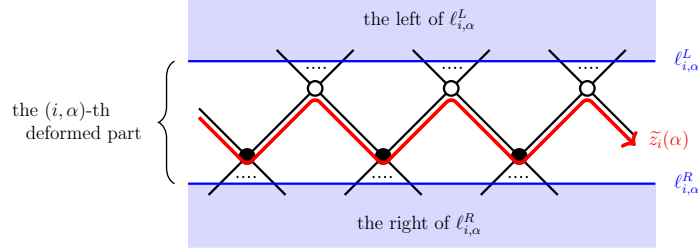


FIGURE 17.

Also, we call the region obtained as the intersection of the right of $\ell_{i-1,\alpha}^R$ and the left of $\ell_{i,\alpha}^L$ the (i, α) -th irrelevant part. Here, we say that the intersection of the right of $\ell_{r,\alpha}^R$ and the left of $\ell_{1,\alpha+1}^L$ is the $(1, \alpha + 1)$ -th irrelevant part. We remark that sometimes there are no nodes in an irrelevant part. We sometimes omit $\alpha \in \mathbb{Z}$ from these notations unless it causes confusion. We also use these terminologies for Γ . That is, a part of Γ obtained by projecting a deformed (resp. irrelevant) part of $\tilde{\Gamma}$ onto Γ is said to be a deformed (resp. irrelevant) part of Γ .

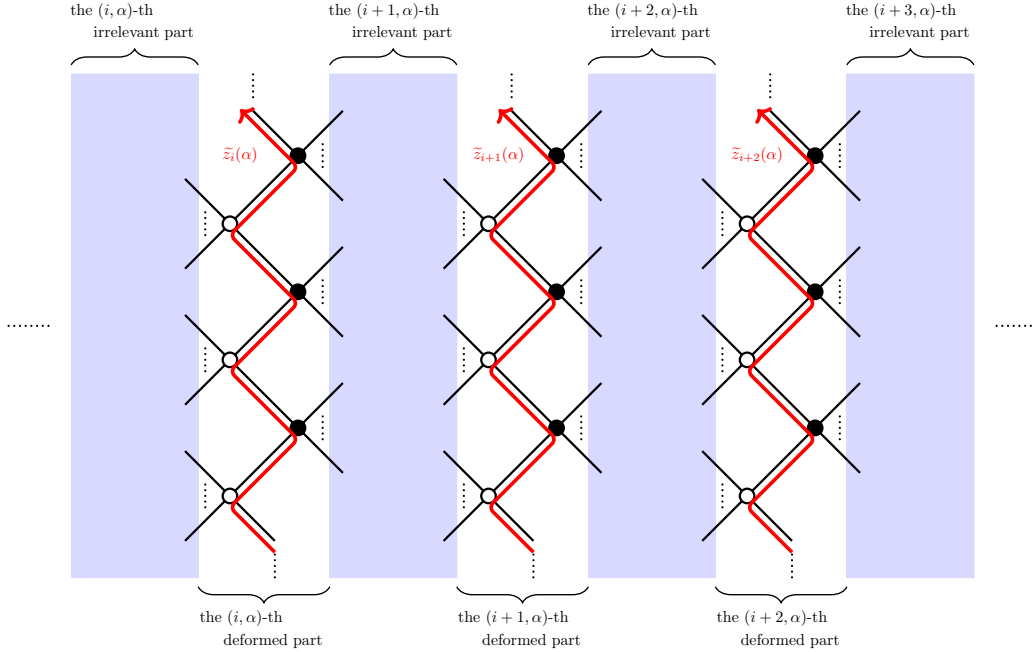


FIGURE 18.

By the condition of Definition 3.3(3), z_1, \dots, z_r do not have a common node, thus the irrelevant parts do not overlap each other. Since the operations (zig-1)–(zig-4) (or (zag-1)–(zag-4)) are local operations on each deformed part, any irrelevant part will be unchanged even if we apply these operations. Thus, we hand over these terminologies “deformed parts” and “irrelevant parts”. We then consider a zigzag path w satisfying the following properties:

- (a) If $[z_i]$ and $[w]$ are linearly independent, then by Lemma 3.15 \tilde{w} intersects with $\tilde{z}_i(\alpha)$ precisely once, and so does any $\tilde{z}_i(\alpha)$ with $i = 1, \dots, r$ and $\alpha \in \mathbb{Z}$. In particular, all intersections are zigs of w or zags of w by Lemma 3.16. If \tilde{w} intersects with $\tilde{z}_i(\alpha)$ at a zig (resp. zag) of $\tilde{z}_i(\alpha)$, then we easily see that \tilde{w} crosses the (i, α) -th deformed part in the direction from the (i, α) -th (resp. $(i + 1, \alpha)$ -th) irrelevant part to the $(i + 1, \alpha)$ -th (resp. (i, α) -th) irrelevant part.

- (b) If $[z_i]$ and $[w]$ are linearly dependent, then by Lemma 3.15 \tilde{w} and $\tilde{z}_i(\alpha)$ do not intersect for any $i = 1, \dots, r$ and $\alpha \in \mathbb{Z}$. This is equivalent to the condition that \tilde{w} is contained in some irrelevant part. In this case, w is unchanged even if we apply the deformations because (zig-1)–(zig-4) (or (zag-1)–(zag-4)) are operations on the deformed parts and (zig-5) (or (zag-5)) does not affect w by Lemma 5.6 below.

In the rest, we discuss the behavior of zigzag paths after applying the operations (zig-1)–(zig-3) given in Definition 4.3. (We can do the same arguments below for the case of (zag-1)–(zag-3) given in Definition 4.5.)

Observation 5.2. We consider a zigzag path y_k on a consistent dimer model Γ intersecting with z_i at a zig of z_i . Let \tilde{z}_i and \tilde{y}_k be zigzag paths on $\tilde{\Gamma}$ projecting onto z_i and y_k respectively. By Observation 5.1(a), \tilde{y}_k crosses the i -th deformed part in the direction from the i -th irrelevant part to the $(i+1)$ -th irrelevant part, and \tilde{y}_k intersects with \tilde{z}_i precisely once. We suppose that the zig $\tilde{z}_i[2m-1]$ of \tilde{z}_i is such an intersection. In this case, $\tilde{z}_i[2m-1]$ is also a zag of \tilde{y}_k , thus we may write it as $\tilde{y}_k[2m]$.

Now, we apply the operations (zig-1)–(zig-3) to Γ , and we denote the resulting dimer model by Γ' and its universal cover by $\tilde{\Gamma}'$. Then, some new nodes are inserted in $\tilde{z}_i[2m-1] = \tilde{y}_k[2m]$ and zigzag paths $\tilde{z}_{i,1}, \dots, \tilde{z}_{i,p_i}$ on $\tilde{\Gamma}'$, which project onto zigzag paths $z_{i,1}, \dots, z_{i,p_i}$ on Γ' respectively, appear in the i -th deformed part.

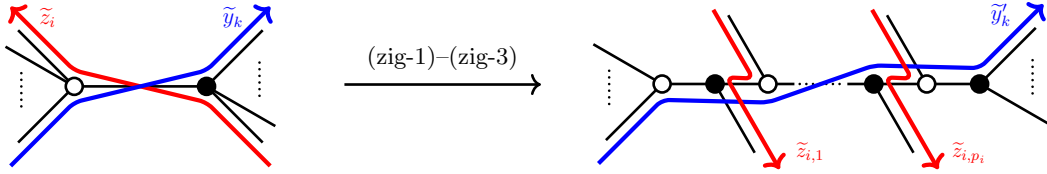
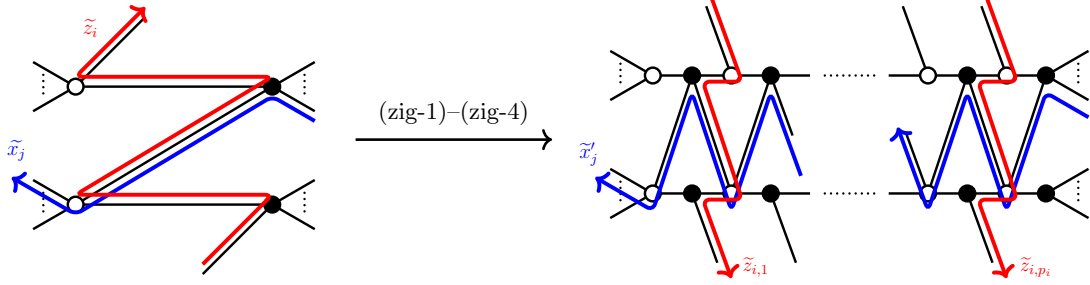
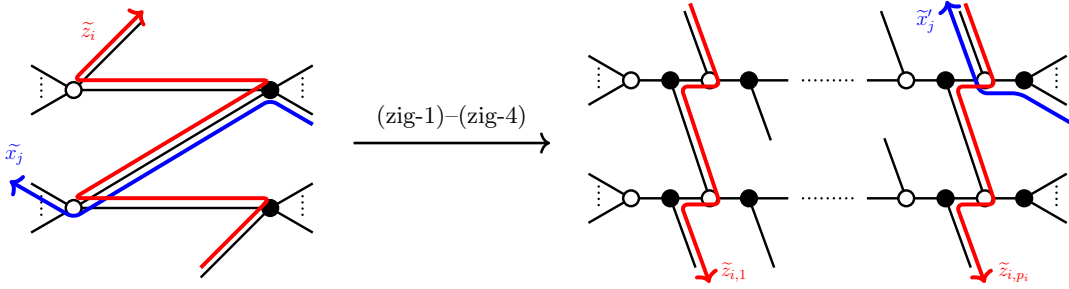


FIGURE 19.

We consider the zigzag path \tilde{y}'_k on $\tilde{\Gamma}'$ passing through $\tilde{y}_k[2m-1]$ as a zig. That is, \tilde{y}'_k starts from $\tilde{y}_k[2m-1]$, crosses through zigzag paths $\tilde{z}_{i,1}, \dots, \tilde{z}_{i,p_i}$ in the i -th deformed part, and arrives at $\tilde{y}_k[2m+1]$ (see the right of Figure 19). In particular, it crosses the i -th deformed part in the direction from the i -th irrelevant part to the $(i+1)$ -th irrelevant part. Although \tilde{y}'_k looks different from \tilde{y}_k in the deformed parts, it connects the zigs $\tilde{y}_k[2m-1]$ and $\tilde{y}_k[2m+1]$ of \tilde{y}_k in the i -th deformed part for all i , thus \tilde{y}'_k shares the same nodes and edges as \tilde{y}_k in any irrelevant part. As a conclusion, \tilde{y}'_k coincides with \tilde{y}_k in all irrelevant parts, and behaves as the right of Figure 19 in each deformed part. Also, we see that bypasses inserted in the operation (zig-4) do not affect the behavior of \tilde{y}'_k , because \tilde{y}'_k never passes through bypasses.

Observation 5.3. We consider a zigzag path x_j on Γ intersecting with z_i at a zag of z_i . Let \tilde{x}_j be a zigzag path on $\tilde{\Gamma}$ projecting onto x_j . By Observation 5.1(a), \tilde{x}_j crosses the i -th deformed part in the direction from the $(i+1)$ -th irrelevant part to the i -th irrelevant part, and \tilde{x}_j intersects with \tilde{z}_i precisely once. We suppose that the zag $\tilde{z}_i[2m]$ of \tilde{z}_i is such an intersection. In this case, $\tilde{z}_i[2m]$ is also a zig of \tilde{x}_j , thus we may write it as $\tilde{x}_j[2m+1]$. We then apply the operations (zig-1)–(zig-4) to Γ , and we have the dimer model $\tilde{\nu}_{\mathcal{X}}^{\text{zig}}(\Gamma) = \tilde{\nu}_{\mathcal{X}}^{\text{zig}}(\Gamma, \{z_1, \dots, z_r\})$.

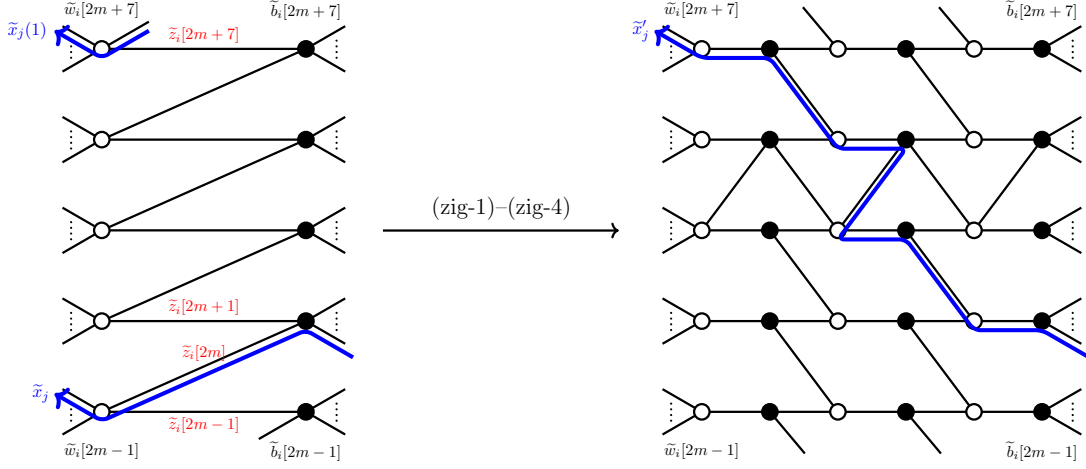
Now, we assume that $z_i[2m]$ which is the projection of $\tilde{z}_i[2m] = \tilde{x}_j[2m+1]$ on Γ is not contained in X_i , in which case bypasses are inserted. We consider the zigzag path \tilde{x}'_j on the universal cover of $\tilde{\nu}_{\mathcal{X}}^{\text{zig}}(\Gamma)$ passing through $\tilde{x}_j[2m]$ as a zag of \tilde{x}'_j . That is, \tilde{x}'_j starts from $\tilde{x}_j[2m]$, behaves as in the right of Figure 20, and arrives at $\tilde{x}_j[2m+2]$. In particular, \tilde{x}'_j crosses the i -th deformed part in the direction from the $(i+1)$ -th irrelevant part to the i -th irrelevant part, and behaves as the same as \tilde{x}_j in each irrelevant part.


 FIGURE 20. The case where the projection of $\tilde{z}_i[2m] = \tilde{x}_j[2m+1]$ on Γ is not contained in X_i

 FIGURE 21. The case where the projection of $\tilde{z}_i[2m] = \tilde{x}_j[2m+1]$ on Γ is contained in X_i

We then assume that $z_i[2m]$ is contained in X_i , in which case bypasses are not inserted. We again consider the zigzag path \tilde{x}'_j on the universal cover of $\bar{\nu}_{\mathcal{X}}^{\text{zig}}(\Gamma)$ passing through $\tilde{x}_j[2m]$ as a zag of \tilde{x}'_j (see e.g., Figure 21). Unlike the previous case, after passing through $\tilde{x}_j[2m]$, \tilde{x}'_j goes to the edge $\{\tilde{b}_i[2m+1], \tilde{w}_{i,1}[2m+1]\}$. (Here, we denote the edge whose endpoints are a black node b and a white node w by $\{b, w\}$.) If $z_i[2m+2] \in X_i$, in which case bypasses are not inserted, then \tilde{x}'_j goes to the edge $\{\tilde{w}_{i,1}[2m+1], \tilde{b}_{i,1}[2m+3]\}$. On the other hand, if $z_i[2m+2] \notin X_i$, in which case we insert bypasses, then \tilde{x}'_j goes to the edge $\{\tilde{w}_{i,1}[2m+1], \tilde{b}_i[2m+3]\}$. In such a way, \tilde{x}'_j crosses the i -th deformed part in the direction from the $(i+1)$ -th irrelevant part to the i -th irrelevant part. More precisely, if we assume that \tilde{x}'_j goes through the edge $\{\tilde{b}_{i,s}[2m-1], \tilde{w}_{i,s+1}[2m-1]\}$ in the i -th deformed part, then \tilde{x}'_j behaves as follows:

- (1) if $z_i[2m] \in X_i$, in which case bypasses are not inserted, then \tilde{x}'_j goes through the edge $\{\tilde{w}_{i,s+1}[2m-1], \tilde{b}_{i,s+1}[2m+1]\}$ and then $\{\tilde{b}_{i,s+1}[2m+1], \tilde{w}_{i,s+2}[2m+1]\}$,
- (2) if $z_i[2m] \notin X_i$, in which case we insert bypasses, then \tilde{x}'_j goes through the edge $\{\tilde{w}_{i,s+1}[2m-1], \tilde{b}_{i,s}[2m+1]\}$ and then $\{\tilde{b}_{i,s}[2m+1], \tilde{w}_{i,s+1}[2m+1]\}$,

where $m = 1, \dots, n$ and $s = 0, \dots, p_i - 1$ with $\tilde{b}_{i,0}[-] = \tilde{b}_i[-]$ and $\tilde{w}_{i,p_i+1}[-] = \tilde{w}_i[-]$. When we consider \tilde{x}'_j in the i -th deformed part, we encounter the case of (1) $|X_i|$ times and the case of (2) $\ell(z_i)/2 - |X_i|$ times. Since $p_i = |X_i| - 1$, we see that \tilde{x}'_j goes out the i -th deformed part from $\tilde{w}_i[2m-1+2n] = \tilde{w}_i[2m-1+\ell(z_i)]$, and then it goes into the i -th irrelevant part. Thus, \tilde{x}'_j behaves as the same as the shift of \tilde{x}_j in the i -th irrelevant part. For example, if we consider the type I zigzag path z_i with $\ell(z_i) = 8$, and the deformation parameter X_i with $|X_i| = 3$ and $z_i[2m+4] \notin X_i$, then the i -th deformed part will change as shown in Figure 22.


 FIGURE 22. An example of the behavior of \tilde{x}'_j in the i -th deformed part

5.2. Properties of zigzag paths on deformed dimer models. In this subsection, we study the slopes of zigzag paths of the deformed dimer models. In particular, we can describe them in terms of zigzag paths of the original dimer model, and such a description plays a crucial role to discuss the relationship with the mutations of polygons.

Proposition 5.4. *Let the notation be the same as in Definition 4.1 and 4.3 (resp. 4.5). Then, $z_{i,j}$ given in (zig-3) of Definition 4.3 (resp. (zag-3) of Definition 4.5) is a type I zigzag path $z_{i,j}$ of $\nu_{\mathcal{X}}^{\text{zig}}(\Gamma)$ (resp. $\nu_{\mathcal{Y}}^{\text{zag}}(\Gamma)$) with $\ell(z_{i,j}) = \ell(z_i)$. Moreover, $z_{i,j}$ does not have a self-intersection on the universal cover, and satisfies $[z_{i,j}] = -[z_i] = -v$ and hence it is not homologically trivial.*

Proof. We consider the case of $\nu_{\mathcal{X}}^{\text{zig}}(\Gamma)$. The case of $\nu_{\mathcal{Y}}^{\text{zag}}(\Gamma)$ is similar.

First, $z_{i,j}$ is a zigzag path of $\bar{\nu}_{\mathcal{X}}^{\text{zig}}(\Gamma)$ by definition. We see that zigzag paths of $\bar{\nu}_{\mathcal{X}}^{\text{zig}}(\Gamma)$ intersecting with $\tilde{z}_{i,j}$ take the form either \tilde{y}'_k given in Observation 5.2 or \tilde{x}'_j given in Observation 5.3. In particular, these intersect with $\tilde{z}_{i,j}$ precisely once in each deformed part, and \tilde{y}'_k crosses the i -th deformed part in the direction from the i -th irrelevant part to the $(i+1)$ -th irrelevant part and \tilde{x}'_j crosses the i -th deformed part in the direction from the $(i+1)$ -th irrelevant part to the i -th irrelevant part for all i . Since other zigzag paths do not intersect with $\tilde{z}_{i,j}$, we have that $z_{i,j}$ is a type I zigzag path of $\bar{\nu}_{\mathcal{X}}^{\text{zig}}(\Gamma)$. Also, $\tilde{z}_{i,j}$ does not have a self-intersection by definition. By these properties, the edges constituting $z_{i,j}$ are not removed by the operation (zig-5). In addition, since $z_{i,j}$ contains no 2-valent nodes, the operation (zig-6) does not affect $z_{i,j}$. Therefore, we have that $z_{i,j}$ is a type I zigzag path of $\nu_{\mathcal{X}}^{\text{zig}}(\Gamma)$, and remaining assertions follow from the definition of $z_{i,j}$. \square

Proposition 5.5. *Let the notation be the same as in Definition 4.1, 4.3 and 4.5. In particular, y_1, \dots, y_t (resp. x_1, \dots, x_s) are zigzag paths of Γ intersecting with a chosen type I zigzag path z at some zigs (resp. zags) of z . Then, we have the followings.*

- (1) *For any zigzag path y_k of Γ , there exists a unique zigzag path y'_k of $\nu_{\mathcal{X}}^{\text{zig}}(\Gamma)$ such that it does not have a self-intersection on the universal cover and satisfies $[y_k] = [y'_k]$ where $k = 1, \dots, t$.*
- (2) *For any zigzag path x_j of Γ , there exists a unique zigzag path x'_j of $\nu_{\mathcal{Y}}^{\text{zag}}(\Gamma)$ such that it does not have a self-intersection on the universal cover and satisfies $[x_j] = [x'_j]$ where $j = 1, \dots, s$.*

Proof. We consider the case of $\nu_{\mathcal{X}}^{\text{zig}}(\Gamma)$, and the case of $\nu_{\mathcal{Y}}^{\text{zag}}(\Gamma)$ is similar.

We use the same notations used in Observation 5.2. In particular, we consider the zigzag path \tilde{y}'_k of $\tilde{\Gamma}'$ which coincides with \tilde{y}_k in all irrelevant parts, and behaves as the right of Figure 19 in each deformed part, thus it does not have a self-intersection. Since bypasses inserted in the operation (zig-4) do not affect the behavior of \tilde{y}'_k , we can extend \tilde{y}'_k as a zigzag path of the universal cover of $\bar{\nu}_{\mathcal{X}}^{\text{zig}}(\Gamma)$. By projecting \tilde{y}'_k onto $\bar{\nu}_{\mathcal{X}}^{\text{zig}}(\Gamma)$, we have the zigzag path y'_k of $\bar{\nu}_{\mathcal{X}}^{\text{zig}}(\Gamma)$. By the construction given in Observation 5.2, we see that $[y_k] = [y'_k]$. Since \tilde{y}'_k coincides with \tilde{y}_k in all irrelevant parts and Γ is consistent, it does not behave pathologically in irrelevant parts as it infringes the consistency condition. Furthermore, \tilde{y}'_k

intersects with zigzag paths with the forms $\tilde{z}_{i,j}$ and \tilde{x}'_j (see Observation 5.3) in some deformed parts, but they do not intersect with each other in the same direction more than once. Therefore, the edges constituting y'_k are not removed by the operation (zig-5), and hence y'_k is not changed by (zig-5). In addition, the operation (zig-6) does not change the slopes. Thus, we naturally extend this zigzag path y'_k as the one of $\nu_{\mathcal{X}}^{\text{zig}}(\Gamma)$, which is determined uniquely and satisfies $[y_k] = [y'_k]$ by the construction. \square

By the proof of Proposition 5.4 and 5.5, the zigzag paths $\tilde{z}_{i,j}$ and \tilde{y}'_k do not have a self-intersection, and do not intersect with other zigzag paths in the same direction more than once. Furthermore, the intersections between \tilde{x}'_j and $\tilde{z}_{i,j}$ or \tilde{y}'_k are not bypasses (see Observation 5.2 and 5.3). Thus, we have the following lemma.

Lemma 5.6. *Let the notation be the same as in Definition 4.1, 4.3 and 4.5. Then we have the followings.*

- (1) *The edges removed by the operation (zig-5) are a part of bypasses added in (zig-4) or edges appearing in some irrelevant parts that are intersections between pairs of zigzag paths x_1, \dots, x_s .*
- (2) *The edges removed by the operation (zag-5) are a part of bypasses added in (zag-4) or edges appearing in some irrelevant parts that are intersections between pairs of zigzag paths y_1, \dots, y_t .*

Before showing the next proposition, we introduce some notations.

Setting 5.7. Let z be a zigzag path on a consistent dimer model Γ . We recall that corner perfect matchings are ordered in the anti-clockwise direction along the vertices of Δ_Γ (see Subsection 2.2). Let P, P' be adjacent corner perfect matchings on Γ such that the difference of P and P' contains z (see Proposition 3.5). We assume that P, P' are ordered with this order, in which case $P \cap z = \text{Zig}(z)$ and $P' \cap z = \text{Zag}(z)$. Then, we set $P_z := P$ and $P'_z := (P \setminus \text{Zig}(z)) \cup \text{Zag}(z)$. By Proposition 3.6, P_z, P'_z are boundary perfect matchings corresponding to certain lattice points on the edge of Δ_Γ whose outer normal vector is $[z]$, and we see that the difference of P_z and P'_z , namely $P_z \cup P'_z \setminus P_z \cap P'_z$, forms z . Thus, by this construction, $h(P'_z, P_z) \in \mathbb{Z}^2$ is a primitive lattice element with $\langle [z], h(P'_z, P_z) \rangle = 0$.

Proposition 5.8. *Let the notation be the same as in Definition 4.1, 4.3 and 4.5. In particular, x_1, \dots, x_s (resp. y_1, \dots, y_t) are zigzag paths of Γ intersecting with a chosen type I zigzag path z at some zags (resp. zigs) of z . Let $h(P'_z, P_z)$ be a primitive lattice element as above. Then, we have the followings.*

- (1) *For any zigzag path x_j of Γ , there exists a unique zigzag path x'_j of $\nu_{\mathcal{X}}^{\text{zig}}(\Gamma)$ such that*

$$[x'_j] = [x_j] + \langle [x_j], h(P'_z, P_z) \rangle [z],$$

where $j = 1, \dots, s$.

- (2) *For any zigzag path y_k of Γ , there exists a unique zigzag path y'_k of $\nu_{\mathcal{Y}}^{\text{zag}}(\Gamma)$ such that*

$$[y'_k] = [y_k] + \langle [y_k], h(P'_z, P_z) \rangle [z],$$

where $k = 1, \dots, t$.

Proof. We consider the case of $\nu_{\mathcal{X}}^{\text{zig}}(\Gamma)$, and the case of $\nu_{\mathcal{Y}}^{\text{zag}}(\Gamma)$ is similar.

We recall that $|x_j \cap z| = |x_j \cap z_i|$ for all $i = 1, \dots, r$, and this number is denoted by m_j (see Definition 4.1). We first show that

$$m_j = \langle [x_j], h(P'_z, P_z) \rangle \quad (5.1)$$

for $j = 1, \dots, s$. Let p_{x_j} be the path of the quiver Q_Γ going along the left side of x_j (see Observation 3.7). In particular, considering p_{x_j} as the element in $H_1(\mathbb{T})$, we have that $[p_{x_j}] = [x_j]$. By our assumption, the intersections $x_j \cap z$ are contained in $\text{Zag}(z) = P' \cap z$. Thus, p_{x_j} crosses z at a zig of z . Since $P \cap z = \text{Zig}(z)$, every time p_{x_j} crosses z , the height function $h_{P, P'}$ increases by 1. Since $m_j = |x_j \cap z|$, we have the equation (5.1).

Then, we show that for each x_j there exists a zigzag path x'_j on $\overline{\nu}_{\mathcal{X}}^{\text{zig}}(\Gamma) = \overline{\nu}_{\mathcal{X}}^{\text{zig}}(\Gamma, \{z_1, \dots, z_r\})$ such that

$$[x'_j] = [x_j] + m_j [z] \quad (5.2)$$

for $j = 1, \dots, s$. We divide x_j into sub-zigzag paths $x_j^{(1)}, \dots, x_j^{(m_j)}$. By definition, $x_j^{(1)}$ intersects with z_r at a zag of z_r . We denote this zag by $z_r[2m] := x_j^{(1)} \cap z_r$, in which case the white (resp. black) node that is the end point of $z_r[2m]$ is denoted by $w_r[2m-1]$ (resp. $b_r[2m+1]$). By considering the universal cover $\tilde{\Gamma}$, we naturally define $\tilde{x}_j, \tilde{x}_j^{(1)}, \tilde{z}_r, \tilde{z}_r[2m], \tilde{w}_r[2m-1], \tilde{b}_r[2m+1]$ etc. Also, we assume that \tilde{z}_r is contained in the $(r, 0)$ -th deformed part. Then, \tilde{x}_j crosses the $(r, 0)$ -th deformed part in the direction

from the $(r+1, 0)$ -th irrelevant part to the $(r, 0)$ -th irrelevant part, in which case the entrance of the $(r, 0)$ -th deformed part is $\tilde{b}_r[2m+1]$ and the exit is $\tilde{w}_r[2m-1]$.

In what follows, we use the same notations used in Observation 5.3. In particular, we pay attention to the zigzag path \tilde{x}'_j of the universal cover $\tilde{\nu}_{\mathcal{X}}^{\text{zig}}(\Gamma)^\sim$ of $\nu_{\mathcal{X}}^{\text{zig}}(\Gamma)$, which behaves as follows:

- (A_r) If $z_r[2m] \notin X_r$, then \tilde{x}'_j goes into the $(r, 0)$ -th deformed part of $\tilde{\nu}_{\mathcal{X}}^{\text{zig}}(\Gamma)^\sim$ from $\tilde{b}_r[2m+1]$ and goes out from $\tilde{w}_r[2m-1]$ (see also Figure 20). After crossing the $(r, 0)$ -th deformed part, it goes into the $(r, 0)$ -th irrelevant part, and it behaves as the same as \tilde{x}_j in that part.
- (B_r) If $z_r[2m] \in X_r$, then \tilde{x}'_j goes into the $(r, 0)$ -th deformed part of $\tilde{\nu}_{\mathcal{X}}^{\text{zig}}(\Gamma)^\sim$ from $\tilde{b}_r[2m+1]$ and goes out from $\tilde{w}_r[2m-1+2n] = \tilde{w}_r[2m-1+\ell(z)]$ (see also Figure 21 and 22). After crossing the $(r, 0)$ -th deformed part, it goes into the $(r, 0)$ -th irrelevant part, and it behaves as the same as the shift of \tilde{x}_j , which we denote $\tilde{x}_j(1)$, in that part.

Then, \tilde{x}'_j goes into the $(r-1, 0)$ -th deformed part of $\tilde{\nu}_{\mathcal{X}}^{\text{zig}}(\Gamma)^\sim$. We let $\tilde{z}_{r-1}[2m'] := \tilde{x}_j \cap \tilde{z}_{r-1}$ and $\tilde{z}_{r-1}[2m''] := \tilde{x}_j(1) \cap \tilde{z}_{r-1}$. We note that on the dimer model Γ we have $z_{r-1}[2m'] = z_{r-1}[2m''] = x_j^{(1)} \cap z_{r-1}$ by definition.

- We assume that $z_r[2m] \in X_r$ in the above argument. Then $z_{r-1}[2m'] \notin X_{r-1}$ by the definition of X_r and X_{r-1} . (Furthermore, $x_j^{(1)} \cap z_i \notin X_i$ for any $i \neq r$.) In this case, \tilde{x}'_j crosses the $(r-1, 0)$ -th deformed part of $\tilde{\nu}_{\mathcal{X}}^{\text{zig}}(\Gamma)^\sim$ as the same as (A_r) above. Then, it behaves as the same as $\tilde{x}_j(1)$ in the $(r-1, 0)$ -th irrelevant part.
- We assume that $z_r[2m] \notin X_r$ in the above argument.
 - If $z_{r-1}[2m'] \notin X_{r-1}$, then \tilde{x}'_j crosses the $(r-1, 0)$ -th deformed part of $\tilde{\nu}_{\mathcal{X}}^{\text{zig}}(\Gamma)^\sim$ as the same as (A_r). Then, it behaves as the same as \tilde{x}_j in the $(r-1, 0)$ -th irrelevant part.
 - If $z_{r-1}[2m'] \in X_{r-1}$, then \tilde{x}'_j crosses the $(r-1, 0)$ -th deformed part of $\tilde{\nu}_{\mathcal{X}}^{\text{zig}}(\Gamma)^\sim$ as the same as (B_r). Then, it behaves as the same as $\tilde{x}_j(1)$ in the $(r-1, 0)$ -th irrelevant part.

Repeating these inductive arguments, we see that \tilde{x}'_j crosses the $(i, 0)$ -th deformed part of $\tilde{\nu}_{\mathcal{X}}^{\text{zig}}(\Gamma)^\sim$ for $i = r, r-1, \dots, 1$ with this order, and goes into $(1, 0)$ -th irrelevant part. In particular, in any case \tilde{x}'_j behaves as the same as $\tilde{x}_j(1)$ in this irrelevant part.

Then, \tilde{x}'_j goes into the $(r, -1)$ -th deformed part, in which case we consider the sub-zigzag path $x_j^{(2)}$ of Γ and the intersection between $\tilde{z}_r(-1)$ and $\tilde{x}_j^{(2)}$ on $\tilde{\Gamma}$. By the same arguments as above, we see that \tilde{x}'_j crosses the $(i, -1)$ -th deformed part of $\tilde{\nu}_{\mathcal{X}}^{\text{zig}}(\Gamma)^\sim$ for $i = r, r-1, \dots, 1$ with this order. Then, it goes into $(1, -1)$ -th irrelevant part and behaves as the same as $\tilde{x}_j(2)$ in this irrelevant part.

Repeating these arguments, we finally see that \tilde{x}'_j crosses the $(i, -m_j+1)$ -th deformed part of $\tilde{\nu}_{\mathcal{X}}^{\text{zig}}(\Gamma)^\sim$ for $i = r, r-1, \dots, 1$ with this order, and behaves as the same as $\tilde{x}_j(m_j)$ in the $(1, -m_j+1)$ -th irrelevant part. Then, \tilde{x}'_j goes into the $(r, -m_j)$ -th deformed part of $\tilde{\nu}_{\mathcal{X}}^{\text{zig}}(\Gamma)^\sim$, in which case we denote the black node that is the entrance of this deformed part by B . Since $m_j = |x_j \cap z_i|$, the projection of $\tilde{x}_j \cap \tilde{z}_i(-m_j)$ on Γ coincides with $z_i[2m]$, which is the starting edge of our arguments. Thus, B coincides with $\tilde{b}_r[2m+1]$ if they are projected onto $\tilde{\nu}_{\mathcal{X}}^{\text{zig}}(\Gamma)$, which means we could follow all edges of the zigzag path x'_j of $\tilde{\nu}_{\mathcal{X}}^{\text{zig}}(\Gamma)$. By these arguments, we see that the slope of \tilde{x}'_j changes $[z]$ in each deformed part, thus we have that $[x'_j] = [x_j] + m_j[z]$.

Finally, we apply the operations (zig-5) and (zig-6) to $\tilde{\nu}_{\mathcal{X}}^{\text{zig}}(\Gamma)$. Then, we obtain the deformed dimer model $\nu_{\mathcal{X}}^{\text{zig}}(\Gamma)$ and the zigzag path on it having the same slope as \tilde{x}'_j . This zigzag path is determined uniquely by the construction, and we use the same notation for this zigzag path by the abuse of the notation. Since (zig-5) and (zig-6) do not change the slopes of zigzag paths, we have (5.2). \square

5.3. The perfect matching polygons of deformed dimer models. Since the PM polygon of a consistent dimer model can be determined by the slopes of zigzag paths (see Proposition 3.5), we have the PM polygon of the deformed dimer model by using the description of slopes in Proposition 5.4, 5.5 and 5.8. For example, if we consider the deformed dimer models shown in Example 4.10, we have the PM polygons shown in Example 5.9 below. In Section 6, we will see that these are exactly the mutations of the PM polygon of the original dimer model.

Example 5.9. We consider the PM polygons associated to the deformed dimer models given in Example 4.10. Thus, let Γ be a consistent dimer model given in Figure 1, and $\nu_p^{\text{zig}}(\Gamma, z)$ (resp. $\nu_q^{\text{zag}}(\Gamma, z)$) be

the dimer model deformed at zig (resp. zag) of z as shown in Figure 11 (resp. Figure 12). Then, we respectively have the following PM polygons.

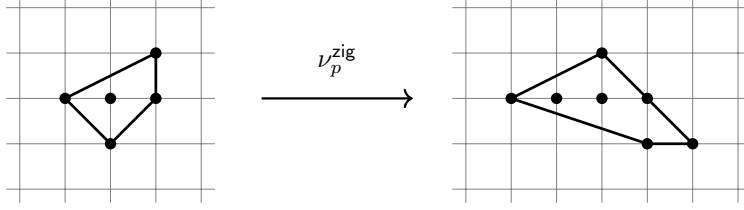


FIGURE 23. The change of the associated PM polygon via the deformation at zig

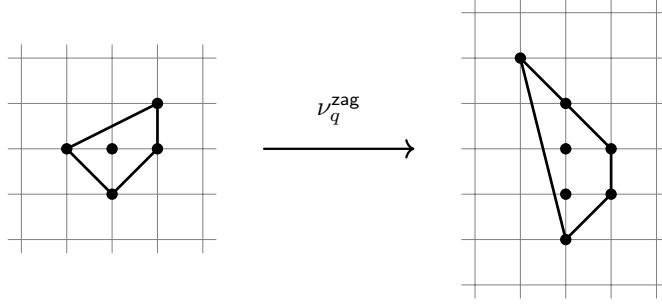


FIGURE 24. The change of the associated PM polygon via the deformation at zag

Since the slopes of zigzag paths $\nu_{\mathcal{X}}^{\text{zig}}(\Gamma)$ and $\nu_{\mathcal{Y}}^{\text{zag}}(\Gamma)$ do not depend on a choice of X_1, \dots, X_r (resp. Y_1, \dots, Y_r) by Proposition 5.4, 5.5 and 5.8, we have the following proposition. However, we remark that the deformed dimer model depends on a choice of deformation parameters, thus $\nu_{\mathcal{X}}^{\text{zig}}(\Gamma, \{z_1, \dots, z_r\}) \not\cong \nu_{\mathcal{X}'}^{\text{zig}}(\Gamma, \{z_1, \dots, z_r\})$ in general (the zag version is similar).

Proposition 5.10. *Let the notation be the same as in Definition 4.1, 4.3 and 4.5. For other zig deformation parameter $\mathcal{X}' := \{X'_1, \dots, X'_r\}$ and zag deformation parameter $\mathcal{Y}' := \{Y'_1, \dots, Y'_r\}$, we have*

$$\Delta_{\nu_{\mathcal{X}}^{\text{zig}}(\Gamma, \{z_1, \dots, z_r\})} = \Delta_{\nu_{\mathcal{X}'}^{\text{zig}}(\Gamma, \{z_1, \dots, z_r\})} \quad \text{and} \quad \Delta_{\nu_{\mathcal{Y}}^{\text{zag}}(\Gamma, \{z_1, \dots, z_r\})} = \Delta_{\nu_{\mathcal{Y}'}^{\text{zag}}(\Gamma, \{z_1, \dots, z_r\})}.$$

6. RELATIONSHIPS WITH MUTATIONS OF POLYGONS

In this section, we discuss a relationship between the deformations of consistent dimer models and the mutations of polygons. We first define the mutation for lattice polytopes of any dimension, and then we mainly discuss the case of polygons.

6.1. Preliminaries on mutations of polytopes. Following [ACGK], we introduce the notion of mutations of polytopes. Thus, let $N \cong \mathbb{Z}^d$ be a lattice of rank d , and $P \subset N_{\mathbb{R}} := N \otimes_{\mathbb{Z}} \mathbb{R}$ be a convex lattice polytope, and we assume that P contains the origin $\mathbf{0}$. We denote by $\mathcal{V}(P)$ the set of vertices of P . We say that two polytopes $P, Q \subset N_{\mathbb{R}}$ are *isomorphic* if they are transformed into each other by $\text{GL}(d, \mathbb{Z})$ -transformations, in which case we denote $P \cong Q$.

We first prepare some notions used in the definition of the mutations of polytopes.

Definition 6.1 (Mutation data). Let $w \in M := \text{Hom}_{\mathbb{Z}}(N, \mathbb{Z}) \cong \mathbb{Z}^d$ be a primitive lattice vector. The element $w \in M$ determines the linear map $\langle w, - \rangle : N_{\mathbb{R}} \rightarrow \mathbb{R}$. We set

$$h_{\max}(P, w) := \max\{\langle w, u \rangle \mid u \in P\} \quad \text{and} \quad h_{\min}(P, w) := \min\{\langle w, u \rangle \mid u \in P\},$$

which are integers because P is a lattice polytope. If the situation is clear, we simply denote these by h_{\max} and h_{\min} respectively. We define the *width* of P with respect to w as

$$\text{width}(P, w) := h_{\max}(P, w) - h_{\min}(P, w).$$

We note that if the origin $\mathbf{0}$ is contained in the strict interior P° of P , then $h_{\min} < 0$ and $h_{\max} > 0$, in which case we have $\text{width}(P, w) \geq 2$. We say that a lattice point $u \in N$ (resp. a subset $F \subset N_{\mathbb{R}}$) is at *height* m with respect to w if $\langle w, u \rangle = m$ (resp. $\langle w, u \rangle = m$ for any $u \in F$).

For each height $h \in \mathbb{Z}$, we let

$$w_h(P) := \text{conv}\{u \in P \cap N \mid \langle w, u \rangle = h\},$$

which is the (possibly empty) convex hull of all lattice points in P at height h . By definition, $w_{h_{\min}}(P)$ and $w_{h_{\max}}(P)$ are faces of P . Using these notations, we define the mutation of a polytope as follows.

Definition 6.2. Let the notation be the same as above. We assume that there exists a lattice polytope $F \subset N_{\mathbb{R}}$ such that $\langle w, u \rangle = 0$ for any $u \in F$ and for each negative height $h_{\min} \leq h < 0$ there exists a possibly empty lattice polytope $G_h \subset N_{\mathbb{R}}$ satisfying

$$\{u \in \mathcal{V}(P) \mid \langle w, u \rangle = h\} \subseteq G_h + (-h)F \subseteq w_h(P), \quad (6.1)$$

where $+$ means the Minkowski sum, and we especially define $Q + \emptyset = \emptyset$ for any polytope Q . We call F a *factor* of P with respect to w . Then, we define the (*combinatorial*) *mutation* of P given by the vector w , factor F and polytopes $\{G_h\}$ as

$$\text{mut}_w(P, F) := \text{conv} \left(\bigcup_{h=h_{\min}}^{-1} G_h \cup \bigcup_{h=0}^{h_{\max}} (w_h(P) + hF) \right).$$

We note that the mutation is independent of the choice of $\{G_h\}$ (see [ACGK, Proposition 1]). Also, a translation of the factor F does not affect the mutation, that is, for any $u \in N$ with $\langle w, u \rangle = 0$ we have that $\text{mut}_w(P, F) \cong \text{mut}_w(P, u + F)$, see [ACGK] for more details.

Remark 6.3 (The mutation for the case of $d = 2$). When $d = 2$, we choose an edge E of a lattice polygon P , and take $w \in M \cong \mathbb{Z}^2$ as a primitive inner normal vector for E . By a choice of w , we see that $w_{h_{\min}}(P) = E$ and $w_{h_{\max}}(P)$ is either a vertex or an edge of P . Then, we take a primitive lattice element $u_E \in N$ satisfying $\langle w, u_E \rangle = 0$, and define a line segment $F := \text{conv}\{\mathbf{0}, u_E\}$, which is parallel to E at height 0 and has the unit lattice length. Since u_E is uniquely defined up to sign, so is F . In this case, P admits a mutation with respect to w (equivalently we can take polytopes $\{G_h\}$ satisfying (6.1)) if and only if $|E \cap N| - 1 \geq -h_{\min}$, see [KNP, Lemma 1]. We note that the mutation does not depend on the choice of u_E (and hence F), that is, $\text{mut}_w(P, F) \cong \text{mut}_w(P, -F)$, which means they are $\text{GL}(2, \mathbb{Z})$ -equivalent.

Now, we collect fundamental properties on this mutation.

Proposition 6.4 (see [ACGK, Lemma 2 and Proposition 2]). *Let the notation be the same as above.*

- (1) *If $Q := \text{mut}_w(P, F)$, then we have that $P = \text{mut}_{(-w)}(Q, F)$.*
- (2) *P is a Fano polytope if and only if $\text{mut}_w(P, F)$ is a Fano polytope.*

Here, we recall that a convex lattice polytope $P \subset N_{\mathbb{R}}$ with $\dim P = d$ is called *Fano* if the origin is contained in the strict interior of P , and the vertices $\mathcal{V}(P)$ of P are primitive lattice points of N .

Then, we consider the mutation of a lattice polytope P in terms of the dual P^* of P in M . To do this, we first discuss the dual P^* for a polyhedron P . We consider the family of polyhedra (not necessarily convex polytopes) which are of the following form:

$$\mathcal{P}^d := \left\{ \bigcap_{v \in S} H_{v, \geq -k_v} \cap \bigcap_{v' \in T} H_{v', \geq 0} \subset N_{\mathbb{R}} \mid S, T \subset M, |S|, |T| < \infty, k_v \in \mathbb{Z}_{>0} \right\},$$

where $H_{v, \geq k} = \{u \in N_{\mathbb{R}} \mid \langle v, u \rangle \geq k\}$ for $v \in M$ and $k \in \mathbb{R}$. We note that a lattice polytope containing the origin of $N_{\mathbb{R}}$ belongs to \mathcal{P}^d but the one not containing the origin does not belong to \mathcal{P}^d since one of the supporting hyperplanes of such polytope is of the form $H_{v, \geq k}$ for some $v \in M$ and some positive integer k .

For a given $P \in \mathcal{P}^d$, we consider the dual $P^* \subset M_{\mathbb{R}}$ of P defined as

$$P^* := \{v \in M_{\mathbb{R}} \mid \langle v, u \rangle \geq -1 \text{ for all } u \in P\} \subset M_{\mathbb{R}}.$$

Then, we have the following statements.

Proposition 6.5. *Let the notation be the same as above. Then, we have that*

- (i) $P^* \in \mathcal{P}^d$ for any $P \in \mathcal{P}^d$,

(ii) $(P^*)^* = P$.

Proof. (i) Let $P \in \mathcal{P}^d$. Since P is a polyherdon, there exist a polytope Q and a polyhedral cone C such that $P = Q + C$, where $+$ denotes the Minkowski sum (see [Sch, Corollary 7.1b]). Let $Q = \text{conv}(\{\frac{1}{k_1}u_1, \dots, \frac{1}{k_p}u_p\})$ and let $C = \text{cone}(\{u'_1, \dots, u'_q\})$. Note that we can choose u_i, u'_j from N and $k_i \in \mathbb{Z}_{>0}$ because of the form of P . In what follows, we will claim that

$$P^* = \bigcap_{i=1}^p H_{u_i, \geq -k_i} \cap \bigcap_{j=1}^q H_{u'_j, \geq 0}.$$

First, we take $v \in P^*$. Then, we have that $\langle v, u \rangle \geq -1$ for any $u \in P$. Since $\frac{1}{k_i}u_i \in Q + \mathbf{0} \subset P$, where $\mathbf{0} \in C$ denotes the origin, we see that $\langle v, \frac{1}{k_i}u_i \rangle \geq -1$, i.e., $\langle v, u_i \rangle \geq -k_i$ for each i . If there is j with $\langle v, u'_j \rangle < 0$, then $\langle v, u' + ru'_j \rangle < -1$ for some $u' \in Q$ and some sufficiently large r . Moreover, we have $u' + ru'_j \in Q + C = P$. This contradicts to $v \in P^*$, thus $\langle v, u'_j \rangle \geq 0$ for each j . Therefore, $v \in \bigcap_{i=1}^p H_{u_i, \geq -k_i} \cap \bigcap_{j=1}^q H_{u'_j, \geq 0}$.

On the other hand, we take $v \in \bigcap_{i=1}^p H_{u_i, \geq -k_i} \cap \bigcap_{j=1}^q H_{u'_j, \geq 0}$. For any $u \in P$, as mentioned above, there exist $u' \in Q$ and $u'' \in C$ such that $u = u' + u''$. Let $u' = \sum_{i=1}^p \frac{r_i}{k_i}u_i$, where $r_i \geq 0$ with $\sum_{i=1}^p r_i = 1$, and let $u'' = \sum_{j=1}^q s_j u'_j$, where $s_j \geq 0$. By using these expressions together with the inequalities $\langle v, u_i \rangle \geq -k_i$ for each i and $\langle v, u'_j \rangle \geq 0$ for each j , we see that

$$\langle v, u \rangle = \langle v, u' \rangle + \langle v, u'' \rangle = \sum_{i=1}^p \frac{r_i}{k_i} \langle v, u_i \rangle + \sum_{j=1}^q s_j \langle v, u'_j \rangle \geq -\sum_{i=1}^p r_i = -1,$$

thus we have $v \in P^*$.

(ii) For any $u \in P$, we have $\langle v, u \rangle \geq -1$ for any $v \in P^*$ which means that $P \subset (P^*)^*$. On the other inclusion, we take $u \in N_{\mathbb{R}} \setminus P$. Let $P = \bigcap_{v \in S} H_{v, \geq -k_v} \cap \bigcap_{v' \in T} H_{v', \geq 0}$. Then either $\langle v, u \rangle < -k_v$ for some $v \in S$ or $\langle v', u \rangle < 0$ for some $v' \in T$ holds. In the former case, since $\langle v, u' \rangle \geq -k_v$ for any $u' \in P$, we have $\frac{1}{k_v}v \in P^*$. This means that there is $v'' := \frac{1}{k_v}v \in P^*$ such that $\langle v'', u \rangle < -1$, and hence $u \notin (P^*)^*$. Similarly, in the latter case, since $\langle rv', u' \rangle \geq 0 \geq -1$ for any $u' \in P$ and $r \geq 0$, we have $rv' \in P^*$. This implies that $u \notin (P^*)^*$ for sufficiently large r , and hence $u \notin (P^*)^*$. Therefore, we obtain that $(P^*)^* \subset P$, as required. \square

We then define the map $\varphi : M_{\mathbb{R}} \rightarrow M_{\mathbb{R}}$ as $\varphi(v) := v - v_{\min}w$ where $v_{\min} := \min\{\langle v, u \rangle \mid u \in F\}$. In particular, when $d = 2$ (see Remark 6.3), this map can be described as

$$\varphi(v) = \begin{cases} v & \text{if } \langle v, u_E \rangle \geq 0, \\ v - \langle v, u_E \rangle w & \text{if } \langle v, u_E \rangle < 0. \end{cases} \quad (6.2)$$

for $F = \text{conv}\{\mathbf{0}, u_E\}$. The next proposition is crucial to prove our main result Theorem 6.10.

Proposition 6.6. *For any $P \in \mathcal{P}^d$, we have that*

$$\varphi(P^*) = \text{mut}_w(P, F)^*.$$

Proof. Although this equality essentially follows from [ACGK, Proposition 4] and the discussions in [ACGK, p.12], we give a precise proof for the completeness.

Let $Q = \text{mut}_w(P, F)$. To show $\varphi(P^*) \subset Q^*$, we take $v \in P^*$ arbitrarily and consider $\varphi(v) = v - v_{\min}w \in \varphi(P^*)$. We will claim that $\langle v - v_{\min}w, u \rangle \geq -1$ for any $u \in Q$. It suffices to show this for each vertex $u \in \mathcal{V}(Q)$.

- For $u \in \mathcal{V}(Q)$, we assume that $\langle w, u \rangle \geq 0$. Then we can write $u = u_P + \langle w, u_P \rangle u_F$ for some $u_P \in \mathcal{V}(P)$ and $u_F \in \mathcal{V}(F)$. In particular, we have

$$\langle v - v_{\min}w, u \rangle = \langle v, u_P \rangle + \langle w, u_P \rangle (\langle v, u_F \rangle - v_{\min}) \geq \langle v, u_P \rangle \geq -1.$$

- For $u \in \mathcal{V}(Q)$, we assume that $\langle w, u \rangle < 0$. For any $u_F \in \mathcal{V}(F)$, we have $u - \langle w, u \rangle u_F \in P$. Hence, $\langle v, u - \langle w, u \rangle u_F \rangle \geq -1$. In particular, $\langle v, u \rangle \geq -1 + v_{\min} \langle w, u \rangle$. Thus, we see that

$$\langle v - v_{\min}w, u \rangle = \langle v, u \rangle - v_{\min} \langle w, u \rangle \geq -1.$$

To show $Q^* \subset \varphi(P^*)$, we will claim that for any $v \in Q^*$ there is $v' \in P^*$ such that $v = \varphi(v')$. Let Δ_F be the normal fan of F in $M_{\mathbb{R}}$ and let $\sigma \in \Delta_F$ be a maximal cone in Δ_F . The discussions in [ACGK, p.12] say that there exists $M_{\sigma} \in \text{GL}_d(\mathbb{Z})$ such that the map φ is equal to M_{σ} , i.e., $\varphi(v) = vM_{\sigma}$. Thus, we conclude that $\varphi(v') = v$ for $v' = vM_{\sigma}^{-1}$. \square

Example 6.7. We consider the polygon P given in the left of the following figure, and this coincides with the PM polygon of the dimer model given in Figure 1 (see also Figure 5). We assume that the double circle stands for the origin $\mathbf{0}$. We consider the edge E whose primitive inner normal vector is $w = (1, 1)$, in which case $h_{\min} = -1$ and $h_{\max} = 2$. We take $u_E = (1, -1) \in N$ which satisfies $\langle w, u_E \rangle = 0$, and consider the line segment $F = \text{conv}\{\mathbf{0}, u_E\}$. Then, we have the mutation $\text{mut}_w(P, F)$ of the polygon P as shown in Figure 25. This mutated polygon $\text{mut}_w(P, F)$ is the same as the PM polygon of $\nu_p^{\text{zig}}(\Gamma, z)$ given in Example 5.9. Also, we can see that if we take the line segment $-F = \text{conv}\{\mathbf{0}, -u_E\}$, the mutated polygon $\text{mut}_w(P, -F)$ coincides with the PM polygon of $\nu_q^{\text{zag}}(\Gamma, z)$ given in Example 5.9. Therefore, the PM polygon of $\nu_p^{\text{zig}}(\Gamma, z)$ and that of $\nu_q^{\text{zag}}(\Gamma, z)$ are isomorphic (see Remark 6.3). In the next subsection, we will show this phenomenon for general situations.

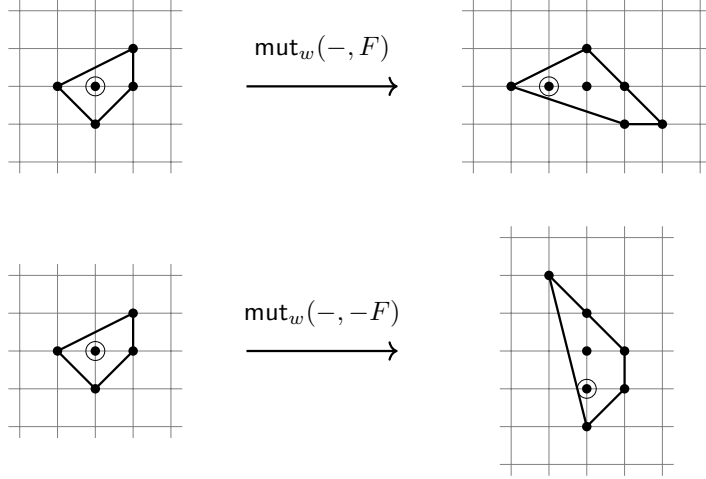


FIGURE 25. An example of the mutation of P

6.2. Mutations of the PM polygon are induced by deformations. In this subsection, we show that the mutation of the PM polygon of a consistent dimer model coincides with the PM polygon of the deformed dimer model (see Theorem 6.10).

We first recall that for any lattice polygon P there exists a reduced consistent dimer model Γ giving P as the PM polygon of Γ by Theorem 2.5. Then, we observe the relationship between the deformation data (see Definition 4.1) and the mutation data (see Definition 6.1).

Setting 6.8. Let Γ be a reduced consistent dimer model, and Δ_Γ be the PM polygon of Γ . We take a type I zigzag path z of Γ with $v := [z] \in \mathbb{Z}^2$. Then, by Proposition 3.5 there is the edge E of Δ_Γ whose outer normal vector is v . Since Δ_Γ is determined up to translation, there is ambiguity concerning the position of the origin. Thus, we fix the origin $\mathbf{0}$ for Δ_Γ so that $\mathbf{0} \in \Delta_\Gamma$. Let $w := -v$, and consider

$$h_{\max} = h_{\max}(\Delta_\Gamma, w) := \max\{\langle w, u \rangle \mid u \in \Delta_\Gamma\} \quad \text{and} \quad h_{\min} = h_{\min}(\Delta_\Gamma, w) := \min\{\langle w, u \rangle \mid u \in \Delta_\Gamma\}.$$

Now, we let $r := -h_{\min}$ and assume that $r \leq |\mathcal{Z}_v^I(\Gamma)|$. Since the length of the line segments of E is $|E \cap N| - 1$ and this is equal to $|\mathcal{Z}_v(\Gamma)|$ by Proposition 3.5, we have that

$$-h_{\min} = r \leq |\mathcal{Z}_v^I(\Gamma)| \leq |\mathcal{Z}_v(\Gamma)| = |E \cap N| - 1,$$

thus Δ_Γ admits the mutation with respect to w (see Remark 6.3). Let $\ell(z) := 2n$. Then, by Lemma 3.9 we have that

$$\begin{aligned} n = \ell(z)/2 &= |\mathbf{P} \cap z| + \langle h(\mathbf{P}, \mathbf{P}_i), w \rangle = |\mathbf{P} \cap z| + \langle h(\mathbf{P}, \mathbf{P}_0) - h(\mathbf{P}_i, \mathbf{P}_0), w \rangle \\ &= |\mathbf{P} \cap z| + \langle h(\mathbf{P}, \mathbf{P}_0), w \rangle - \langle h(\mathbf{P}_i, \mathbf{P}_0), w \rangle \end{aligned}$$

where \mathbf{P} is a perfect matching on Γ , \mathbf{P}_0 is the reference perfect matching, and $\mathbf{P}_i \in \text{PM}_{\max}(z)$. Since $h(\mathbf{P}_i, \mathbf{P}_0)$ is a lattice point on E by Lemma 3.8, we have $\langle h(\mathbf{P}_i, \mathbf{P}_0), w \rangle = h_{\min}$. If $\mathbf{P} \in \text{PM}_{\min}(z)$, then $|\mathbf{P} \cap z| = 0$ by Lemma 3.12 and this means $\langle h(\mathbf{P}, \mathbf{P}_0), w \rangle = h_{\max}$. Thus, we have that $n = h_{\max} - h_{\min} = \text{width}(\Delta_\Gamma, w)$.

Collectively, we consider the mutation data and the deformation data which respectively correspond each other as in Table 1.

Mutation data	Deformation data
w	$-v$
h_{\min}	$-r$
h_{\max}	h
$\text{width}(\Delta_\Gamma, w)$	n

TABLE 1. The comparison between the mutation data and the deformation data

Using these integers r, h , we take type I zigzag paths z_1, \dots, z_r and the zig (resp. zag) deformation parameter \mathcal{X} (resp. \mathcal{Y}) with respect to z_1, \dots, z_r as in Definition 4.1. We then have the deformed consistent dimer models $\nu_{\mathcal{X}}^{\text{zig}}(\Gamma) = \nu_{\mathcal{X}}^{\text{zig}}(\Gamma, \{z_1, \dots, z_r\})$ and $\nu_{\mathcal{Y}}^{\text{zag}}(\Gamma) = \nu_{\mathcal{Y}}^{\text{zag}}(\Gamma, \{z_1, \dots, z_r\})$.

We determine the origin of the PM polygons $\Delta_{\nu_{\mathcal{X}}^{\text{zig}}(\Gamma)}$ and $\Delta_{\nu_{\mathcal{Y}}^{\text{zag}}(\Gamma)}$ as follows. First, there are zigzag paths y'_1, \dots, y'_t on $\nu_{\mathcal{X}}^{\text{zig}}(\Gamma)$ whose slope respectively corresponds to that of zigzag paths y_1, \dots, y_t on Γ by Proposition 5.5. Then, we put $\Delta_{\nu_{\mathcal{X}}^{\text{zig}}(\Gamma)}$ on Δ_Γ so that the edges corresponding to y'_1, \dots, y'_t respectively coincide with the ones of Δ_Γ corresponding to y_1, \dots, y_t . We determine the origin for $\Delta_{\nu_{\mathcal{X}}^{\text{zig}}(\Gamma)}$ so that it is the same position as the one for Δ_Γ . Considering the zigzag paths on $\nu_{\mathcal{Y}}^{\text{zag}}(\Gamma)$ obtained from the zigzag paths x_1, \dots, x_s on Γ , we can also determine the origin for $\Delta_{\nu_{\mathcal{Y}}^{\text{zag}}(\Gamma)}$.

Remark 6.9. In Setting 6.8, we assumed that $r \leq |\mathcal{Z}_v^I(\Gamma)|$ for defining the deformation data. As we mentioned in Remark 4.2, even if there does not exist enough type I zigzag paths, we sometimes make a type II zigzag path type I without changing the PM polygon by using the mutation of dimer models (see Appendix A). Moreover, it is known that for a given lattice polygon P there exists an isoradial dimer model giving P as the PM polygon by [Gul], in which case all zigzag paths are type I (see Definition 3.4), and hence $|\mathcal{Z}_v^I(\Gamma)| = |\mathcal{Z}_v(\Gamma)|$. Thus, if $-h_{\min} \leq |E \cap N| - 1$ we can find a certain isoradial dimer model Γ satisfying $-h_{\min} = r \leq |\mathcal{Z}_v^I(\Gamma)| = |E \cap N| - 1$.

For the edge E of Δ_Γ given in Setting 6.8, we take a primitive lattice element $u_E \in N$ such that $\langle w, u_E \rangle = 0$. Here, there are two choices of u_E and we fix u_E as follows. We recall the primitive lattice element $h(P'_z, P_z)$ given in Settings 5.7, which satisfies $\langle [z], h(P'_z, P_z) \rangle = 0$. Thus, we set $u_E := h(P'_z, P_z)$, in which case we have that $\langle w, u_E \rangle = \langle -[z], u_E \rangle = 0$. Then, we set the line segment $F := \text{conv}\{\mathbf{0}, u_E\}$. Under these settings, we have our main theorem as follows.

Theorem 6.10. *Let the notation be the same as in Definition 4.1, 4.3, 4.5, and Setting 6.8 (see also Table 1). Then, we have that*

$$\text{mut}_w(\Delta_\Gamma, F) = \Delta_{\nu_{\mathcal{X}}^{\text{zig}}(\Gamma, \{z_1, \dots, z_r\})},$$

$$\text{mut}_w(\Delta_\Gamma, -F) = \Delta_{\nu_{\mathcal{Y}}^{\text{zag}}(\Gamma, \{z_1, \dots, z_r\})}.$$

Proof. We prove the first equation, and the other one follows from a similar argument.

First, we show that

$$\varphi(\Delta_\Gamma^*) = \Delta_{\nu_{\mathcal{X}}^{\text{zig}}(\Gamma, \{z_1, \dots, z_r\})}^*$$

where φ is the map given in (6.2).

Let $E_1 := E, E_2, \dots, E_m$ be edges of Δ_Γ , and we assume that these are ordered cyclically in the anti-clockwise direction. As we mentioned in Setting 6.8, we suppose that $\mathbf{0} \in \Delta_\Gamma$. Let $w_1 := w, w_2, \dots, w_m$ be inner normal vectors corresponding to E_1, \dots, E_m respectively (see Figure 26). Also, we let $v_i = -w_i$ for $i = 1, \dots, m$, which is the outer normal vectors corresponding to E_i . We then consider $u \in \Delta_\Gamma$ such that $\langle w_1, u \rangle = h_{\max}(\Delta_\Gamma, w_1) = h$, that is, we consider $w_{h_{\max}}(\Delta_\Gamma)$ which is either a vertex or an edge of Δ_Γ . If $w_{h_{\max}}(\Delta_\Gamma)$ is an edge, we easily see that it is parallel to E , in which case we may write $E_a := w_{h_{\max}}(\Delta_\Gamma)$ for some $1 < a < m$. If $w_{h_{\max}}(\Delta_\Gamma)$ is a vertex, we set the edges intersecting at $w_{h_{\max}}(\Delta_\Gamma)$ as E_{a-1}, E_{a+1} and set $E_a = \emptyset$ where $1 < a < m$. Here, we recall that by Proposition 3.5, for each $E_i \neq \emptyset$ there exist zigzag paths on Γ such that the slopes coincide with v_i , and the set of such zigzag paths is denoted by $\mathcal{Z}_{v_i} = \mathcal{Z}_{v_i}(\Gamma)$.

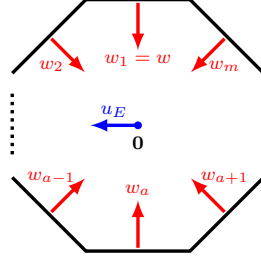


FIGURE 26. The PM polygon Δ_Γ and its inner normal vectors (the case where the origin is contained in the strict interior of Δ_Γ).

First, we consider the edge E_1 and zigzag paths in $\mathcal{Z}_{v_1} = \mathcal{Z}_{(-w)}$. By definition, we have that $\langle -v_1, u_E \rangle = 0$ and $\{z_1, \dots, z_r\} \subseteq \mathcal{Z}_{(-w)}^I \subseteq \mathcal{Z}_{(-w)}$. If $|\mathcal{Z}_{(-w)}| > r$, then there exists a zigzag path in $\mathcal{Z}_{(-w)}$ that is not in $\{z_1, \dots, z_r\}$. If $E_a \neq \emptyset$, we have zigzag paths in \mathcal{Z}_{v_a} . Since E_1 and E_a are parallel, v_1 and v_a are linearly dependent, and hence $\langle v_a, u_E \rangle = 0$. Then, we see that zigzag paths in \mathcal{Z}_{v_a} do not intersect with a type I zigzag path z satisfying $[z] = v_1$ in the universal cover (see Lemma 3.15).

Next, we consider the edges E_2, \dots, E_{a-1} of Δ_Γ and zigzag paths in $\mathcal{Z}_1 := \mathcal{Z}_{v_2} \cup \dots \cup \mathcal{Z}_{v_{a-1}}$. We see that v_i with $i = 2, \dots, a-1$ satisfies $\langle -v_i, u_E \rangle < 0$ by a choice of the edges E_2, \dots, E_{a-1} . By the same argument as in the proof of Proposition 4.12, we see that the zigzag paths in \mathcal{Z}_1 intersect with a type I zigzag path z satisfying $[z] = v_1$ precisely once in the universal cover (see Lemma 3.15), and especially they intersect with z in $\text{Zag}(z)$. Thus, we have that $\mathcal{Z}_1 = \{x_1, \dots, x_s\}$, and for each $i = 2, \dots, a-1$ the vector v_i satisfies $v_i = [x_j]$ for some $j = 1, \dots, s$.

Then, we consider the edges E_{a+1}, \dots, E_m of Δ_Γ and zigzag paths in $\mathcal{Z}_2 := \mathcal{Z}_{v_{a+1}} \cup \dots \cup \mathcal{Z}_{v_m}$. We see that v_i with $i = a+1, \dots, m$ satisfies $\langle -v_i, u_E \rangle > 0$ by a choice of the edges E_{a+1}, \dots, E_m . By a similar argument as above, we see that the zigzag paths in \mathcal{Z}_2 intersect with a type I zigzag path z satisfying $[z] = v_1$ precisely once in the universal cover, and especially they intersect with z in $\text{Zig}(z)$. Thus, we have that $\mathcal{Z}_2 = \{y_1, \dots, y_t\}$, and for each $i = a+1, \dots, m$ the vector v_i satisfies $v_i = [y_k]$ for some $k = 1, \dots, t$.

Collectively, we see that a zigzag path of Γ takes one of the following forms:

- z_1, \dots, z_r ,
- $z'_1, \dots, z'_{r'}$ contained in $\mathcal{Z}_{(-w)} \setminus \{z_1, \dots, z_r\}$ for $w = -v_1$ with $\langle w, u_E \rangle = 0$ if $|\mathcal{Z}_{(-w)}| > r$,
- $z''_1, \dots, z''_{r''}$ contained in \mathcal{Z}_w for $w = -v_1$ with $\langle w, u_E \rangle = 0$ if $E_a \neq \emptyset$,
- x_j where $j = 1, \dots, s$, in which case it satisfies $\langle -[x_j], u_E \rangle < 0$,
- y_k where $k = 1, \dots, t$, in which case it satisfies $\langle -[y_k], u_E \rangle > 0$.

The slopes of these zigzag paths give the supporting hyperplanes of Δ_Γ by Proposition 3.5. Precisely, if Δ_Γ contains the origin $\mathbf{0}$ as an interior lattice point, then

$$H_{-\zeta, \geq -k_\zeta} = \{u \in N_{\mathbb{R}} \mid \langle -\zeta, u \rangle \geq -k_\zeta\}$$

is the supporting hyperplane of Δ_Γ for any zigzag path ζ of Γ and a certain positive integer k_ζ . If the origin $\mathbf{0}$ lies on the boundary of Δ_Γ , k_ζ is replaced by 0 for the zigzag paths corresponding to the edges that contain $\mathbf{0}$. By Proposition 6.5 and its proof, Δ_Γ^* can be denoted by $\Delta_\Gamma^* = Q + C$ where Q is a polygon and C is a polyhedral cone. Since the set of the slopes of zigzag paths of Γ coincides with $\{v_1, \dots, v_m\}$ if we identify the same slopes, we see that the set $\{u_1, \dots, u_p, u'_1, \dots, u'_q\}$, which generates Q and C in the proof of Proposition 6.5, is given by $\{w_1, \dots, w_m\}$ in our situation. In what follows, we assume that $\mathbf{0}$ is contained in the strict interior of Δ_Γ , in which case $\Delta_\Gamma^* = Q$ and $Q = \text{conv}(\{\frac{1}{k_1}w_1, \dots, \frac{1}{k_m}w_m\})$ for some positive integer k_i giving the supporting hyperplane $H_{w_i, \geq -k_i}$ of Δ_Γ where $i = 1, \dots, m$. We remark that $\frac{1}{k_a}w_a$ appears in the above generating set if $E_a \neq \emptyset$. Since $\langle w_i, u_E \rangle \geq 0$ for $i = 1, a, a+1, \dots, m$ and $\langle w_i, u_E \rangle < 0$ for $i = 2, \dots, a-1$, we see that

$$\varphi(\Delta_\Gamma^*) = \text{conv}(\{\frac{1}{k_1}w_1, \frac{1}{k_2}w'_2, \dots, \frac{1}{k_{a-1}}w'_{a-1}, \frac{1}{k_a}w_a \text{ (if } E_a \neq \emptyset), \frac{1}{k_{a+1}}w_{a+1}, \dots, \frac{1}{k_m}w_m\}) \quad (6.3)$$

where $w'_i := w_i - \langle w_i, u_E \rangle w$ for $i = 2, \dots, a-1$. We also note that when $E_a = \emptyset$, we can take the positive integer k_a so that the line $\{u \in N_{\mathbb{R}} \mid \langle v_1, u \rangle = -k_a\}$, which is parallel to E_1 , passes through the vertex of Δ_Γ that is the intersection of E_{a-1} and E_{a+1} . By the choice of k_a , we have that $\langle \frac{1}{k_a}v_1, u \rangle \geq -1$ for any $u \in \Delta_\Gamma$, thus $\frac{1}{k_a}v_1 = \frac{1}{k_a}(-w_1) \in \Delta_\Gamma^*$ and hence $\frac{1}{k_a}v_1 = \frac{1}{k_a}(-w_1) \in \varphi(\Delta_\Gamma^*)$.

We then consider the deformed dimer model $\nu_{\mathcal{X}}^{\text{zig}}(\Gamma) = \nu_{\mathcal{X}}^{\text{zig}}(\Gamma, \{z_1, \dots, z_r\})$. By Observation 5.1, the lift of a zigzag path with the form z'_i or z''_i on the universal cover is contained in some irrelevant part, and hence it does not change even if we apply the deformation. Also, by Proposition 5.8, we have the zigzag paths x'_1, \dots, x'_s on $\nu_{\mathcal{X}}^{\text{zig}}(\Gamma)$ satisfying

$$-[x'_j] = -[x_j] - \langle [x_j], h(\mathbf{P}'_z, \mathbf{P}_z) \rangle [z] = w_i - \langle w_i, u_E \rangle w$$

for $j = 1, \dots, s$ and some $i = 2, \dots, a-1$. Furthermore, by Proposition 5.5, we have the zigzag paths y'_1, \dots, y'_t on $\nu_{\mathcal{X}}^{\text{zig}}(\Gamma)$ satisfying

$$-[y'_k] = -[y_k] = w_i$$

for $k = 1, \dots, t$ and some $i = a+1, \dots, m$. Thus, we see that the zigzag paths x_j, y_k vary as they satisfy the condition (6.2) when we apply the deformation $\nu_{\mathcal{X}}^{\text{zig}}$ to Γ . In addition, we have the zigzag path with the form $z_{i,j}$ defined in (zig-3). Thus, the zigzag paths on the consistent dimer model $\nu_{\mathcal{X}}^{\text{zig}}(\Gamma)$ are

$$\{z'_i\}_{1 \leq i \leq r'} \text{ (if } |\mathcal{Z}_{(-w)}| > r), \{z''_i\}_{1 \leq i \leq r''} \text{ (if } E_a \neq \emptyset), \{x'_j\}_{1 \leq j \leq s}, \{y'_k\}_{1 \leq k \leq t}, \text{ and } \{z_{i,j}\}_{\substack{1 \leq i \leq r \\ 1 \leq j \leq p_i}}$$

By the description of their slopes and Proposition 3.5, we see that the inner normal vectors of $\Delta_{\nu_{\mathcal{X}}^{\text{zig}}(\Gamma)}$ are

$$\{w_1, w'_2, \dots, w'_{a-1}, w_a = -w_1, w_{a+1}, \dots, w_m\},$$

and these vectors give the supporting hyperplanes of $\Delta_{\nu_{\mathcal{X}}^{\text{zig}}(\Gamma)}$ just like Δ_{Γ} as above. Here, w_1 appears in the above set if $|\mathcal{Z}_{(-w_1)}| = |\mathcal{Z}_{v_1}| > r$, but we always have that $\frac{1}{k_1}w_1 \in \Delta_{\nu_{\mathcal{X}}^{\text{zig}}(\Gamma)}^*$ by the same argument as we used for showing $\frac{1}{k_a}(-w_1) \in \Delta_{\Gamma}^*$ above. Whereas w_a certainly appears since $[z_{i,j}] = -[z_i] = -w_1 = w_a$ (see Lemma 5.4). Thus, we have that

$$\Delta_{\nu_{\mathcal{X}}^{\text{zig}}(\Gamma)}^* = \text{conv}\left(\left\{\frac{1}{k_1}w_1, \frac{1}{k_2}w'_2, \dots, \frac{1}{k_{a-1}}w'_{a-1}, \frac{1}{k_a}w_a, \frac{1}{k_{a+1}}w_{a+1}, \dots, \frac{1}{k_m}w_m\right\}\right).$$

By the description (6.3) and the fact that $\frac{1}{k_1}w_1$ and $\frac{1}{k_a}w_a = \frac{1}{k_a}(-w_1)$ are contained in both $\varphi(\Delta_{\Gamma}^*)$ and $\Delta_{\nu_{\mathcal{X}}^{\text{zig}}(\Gamma)}^*$, we see that $\varphi(\Delta_{\Gamma}^*) = \Delta_{\nu_{\mathcal{X}}^{\text{zig}}(\Gamma)}^*$.

The case where the origin $\mathbf{0}$ lies on the boundary of Δ_{Γ} can be proved by a similar argument if we consider the hyperplane $\{u \in N_{\mathbb{R}} \mid \langle -[\zeta], u \rangle \geq 0\}$ instead of $\{u \in N_{\mathbb{R}} \mid \langle -[\zeta], u \rangle \geq -k_{\zeta}\}$ for the zigzag paths corresponding to the edges that contain $\mathbf{0}$, in which case $-[\zeta]$ will be a generator of a polyhedral cone C .

By Proposition 6.5(2) and 6.6, we conclude that $\text{mut}_w(\Delta_{\Gamma}, F) = \Delta_{\nu_{\mathcal{X}}^{\text{zig}}(\Gamma)}$. \square

Since $\text{mut}_w(\Delta_{\Gamma}, F) \cong \text{mut}_w(\Delta_{\Gamma}, -F)$ (see Remark 6.3), we immediately have the following.

Corollary 6.11. *Let the notation be the same as in Definition 4.1, 4.3 and 4.5. Then, we have that*

$$\Delta_{\nu_{\mathcal{X}}^{\text{zig}}(\Gamma, \{z_1, \dots, z_r\})} \cong \Delta_{\nu_{\mathcal{Y}}^{\text{zag}}(\Gamma, \{z_1, \dots, z_r\})},$$

that is, they are $\text{GL}(2, \mathbb{Z})$ -equivalent.

We then show that the deformations at zig and at zag are mutually inverse operations on the level of the associated PM polygon.

Setting 6.12. Let $\nu_{\mathcal{X}}^{\text{zig}}(\Gamma, \{z_1, \dots, z_r\})$ be the reduced consistent dimer model defined in Definition 4.3. We consider the following deformation data for $\nu_{\mathcal{X}}^{\text{zig}}(\Gamma, \{z_1, \dots, z_r\})$. We consider a type I zigzag path $z_{i,j}$ which satisfies $[z_{i,j}] = -v =: w$ (see Proposition 5.4). Since $\{z_{i,j}\}_{\substack{1 \leq i \leq r \\ 1 \leq j \leq p_i}}$ are the subset of type I zigzag

paths, we have that $|\mathcal{Z}_{\nu_{\mathcal{X}}^{\text{zig}}(\Gamma)}^I| \geq \sum_{i=1}^r p_i = h$. Then, we take a subset $\{z'_1, \dots, z'_h\}$ of type I zigzag paths of $\nu_{\mathcal{X}}^{\text{zig}}(\Gamma)$, and do the same procedure as in Definition 4.1(4)–(7), and we especially have the zag deformation parameter $\mathcal{Y}' = \{Y'_1, \dots, Y'_h\}$ of the weight $\mathbf{q}' = (q'_1, \dots, q'_h)$ with $\sum_{i=1}^h q'_i = r$. We can do the same arguments for the case of $\nu_{\mathcal{Y}}^{\text{zag}}(\Gamma, \{z_1, \dots, z_r\})$. In particular, we take a subset $\{z''_1, \dots, z''_h\}$ of type I zigzag paths on $\nu_{\mathcal{Y}}^{\text{zag}}(\Gamma)$ and have the zig deformation parameter $\mathcal{X}' = \{X'_1, \dots, X'_h\}$ of the weight $\mathbf{p}' = (p'_1, \dots, p'_h)$ with $\sum_{i=1}^h p'_i = r$.

Corollary 6.13. *Let the notation be the same as Setting 6.12. Then, we have that*

$$\Delta_{\nu_{\mathcal{Y}'}^{\text{zag}}(\nu_{\mathcal{X}}^{\text{zig}}(\Gamma, \{z_i\}_{i=1}^r), \{z'_\ell\}_{\ell=1}^h)} = \Delta_{\Gamma} \quad \text{and} \quad \Delta_{\nu_{\mathcal{X}'}^{\text{zig}}(\nu_{\mathcal{Y}}^{\text{zag}}(\Gamma, \{z_i\}_{i=1}^r), \{z''_\ell\}_{\ell=1}^h)} = \Delta_{\Gamma}.$$

Proof. This follows from Proposition 6.4(1) and Theorem 6.10. \square

As we mentioned in Section 1, the mutation of a Fano polygon is important from the viewpoint of mirror symmetry and the classification of Fano manifolds. To observe the mutations of Fano polygons by using the deformations of dimer models, we assume that the polygons Δ_Γ , $\Delta_{\nu_{\mathcal{X}}^{\text{zig}}(\Gamma, \{z_1, \dots, z_r\})}$ and $\Delta_{\nu_{\mathcal{Y}}^{\text{zag}}(\Gamma, \{z_1, \dots, z_r\})}$ contain the origin in their strict interiors. Then, we have the following corollary.

Corollary 6.14. *Let the notation be the same as above. Then, we see that Δ_Γ is Fano if and only if $\Delta_{\nu_{\mathcal{X}}^{\text{zig}}(\Gamma, \{z_1, \dots, z_r\})}$ (resp. $\Delta_{\nu_{\mathcal{Y}}^{\text{zag}}(\Gamma, \{z_1, \dots, z_r\})}$) is Fano.*

Proof. This follows from Proposition 6.4(2) and Theorem 6.10. \square

APPENDIX A. MUTATIONS OF DIMER MODELS

In this section, we introduce the other operation called the *mutation of dimer models*. From a viewpoint of physics, dimer models and their mutations correspond to quiver gauge theories and Seiberg duality. The mutation of dimer models can be defined for each quadrangle face of a dimer model, and the operation called *spider move* (see e.g., [GK, Boc3]), which is the inverse operation shown in Figure 27, is the main ingredient for defining the mutation.

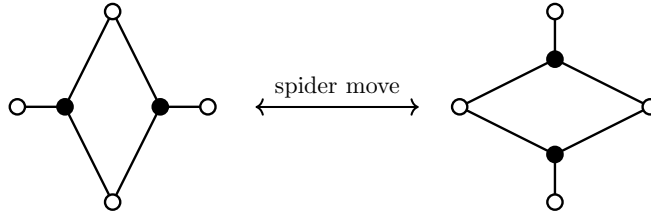


FIGURE 27.

We note that there are two types of the spider move (and hence the mutation) depending on the color of the two interior nodes. Thus, by replacing black nodes by white ones and vice versa, we define the other type. We now describe the black one.

Definition A.1 (The mutation of dimer models). Let Γ be a dimer model. We pick a quadrangle face $f \in \Gamma_2$. Then, the *mutation* of Γ at f , denoted by $\mu_f(\Gamma)$, is the operation consisting of the following procedures:

- (I) Consider black nodes appearing on the boundary of f . If there exist black nodes that are not 3-valent, we apply the split moves to those nodes and make them 3-valent as shown in Figure 28.
- (II) Then, we apply the spider move to f (see Figure 27).
- (III) If the resulting dimer model contains 2-valent nodes, we remove them by applying the join moves.

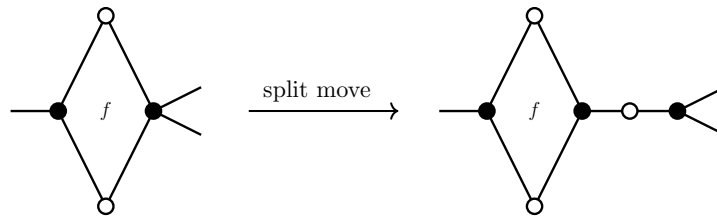


FIGURE 28.

Applying the mutation at a quadrangle face, we obtain the new dimer model from a given one, although it sometimes induces the isomorphic one. We also remark that the mutation is an inverse operation, that is, $\mu_f(\mu_f(\Gamma)) = \Gamma$ holds. We say that dimer models Γ and Γ' are *mutation equivalent* if they are transformed into each other by repeating the mutation of dimer models. Moreover, we also see that the join, split and spider moves do not change the slopes of zigzag paths and preserve conditions in Definition 3.3, thus we have the following.

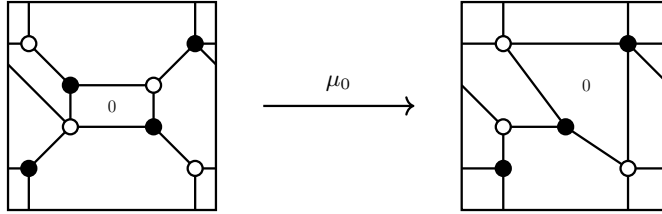
Proposition A.2. *The mutation of dimer models turns consistent dimer models into consistent dimer models associated with the same lattice polygon.*

In addition, it has been conjectured that all consistent dimer models associated with the same lattice polygon are mutation equivalent, but it is still open in general (see [Boc3, pp396–397]). We note that partial answers were given in several papers, see e.g., [Boc2, GK, HS, Nak1].

Remark A.3. The mutation of dimer models is also defined as the dual of the *mutation of a quiver with potential* (= QP) in the sense of [DWZ] (see e.g., [Boc2, subsection 7.2], [Nak1, Section 4]). Although we can consider the mutation of a QP for any vertex of the quiver having no loops and 2-cycles, the resulting QP is not necessarily the dual of a dimer model. To make the resulting one the dual of a dimer model, we need the assumption that the mutated vertex has two incoming (equivalently, two outgoing) arrows, which is equivalent to the face of a dimer model corresponding to such a vertex is quadrangle.

In the theory of deformations of dimer models, type I zigzag paths are important. We can use the mutations for making a type II zigzag path type I as in the example below.

Example A.4. We consider the following dimer model Γ (the left one). Since the face 0 is a quadrangle, we can apply the mutation and have the dimer model $\mu_0(\Gamma)$ as follows.



We can see that the zigzag path on Γ whose slope is $(-1, 1)$ or $(1, -1)$ is type II. On the other hand, we see that $\mu_0(\Gamma)$ is isoradial, and hence all zigzag paths are type I.

APPENDIX B. LARGE EXAMPLES

As we mentioned in Section 4, we sometimes skip the operations (zig-4) and (zig-5) (resp. (zag-4) and (zag-5)) when we define the deformation $\nu_{\mathcal{X}}^{\text{zig}}(\Gamma, \{z_1, \dots, z_r\})$ (resp. $\nu_{\mathcal{Y}}^{\text{zag}}(\Gamma, \{z_1, \dots, z_r\})$) of a consistent dimer model Γ . However, as the following example shows, (zig-4) and (zig-5) (resp. (zag-4) and (zag-5)) are indispensable to define the deformations that are compatible with the mutations of polygons as shown in Theorem 6.10. For example, we often encounter such a situation when we consider a consistent dimer model whose PM polygon is relatively large.

Example B.1. We consider the lattice polygon P shown in the left of Figure 29. In particular, we assume that the double circle stands for the origin $\mathbf{0}$. We consider the edge E whose primitive inner normal vector is $w = (0, -1)$, in which case $h_{\min} = -3$ and $h_{\max} = 1$. We take $u_E = (-1, 0)$ which satisfies $\langle w, u_E \rangle = 0$, and consider the line segment $F = \text{conv}\{\mathbf{0}, u_E\}$. Then, we have the mutation $\text{mut}_w(P, F)$ of the polygon P as shown in the right of Figure 29.

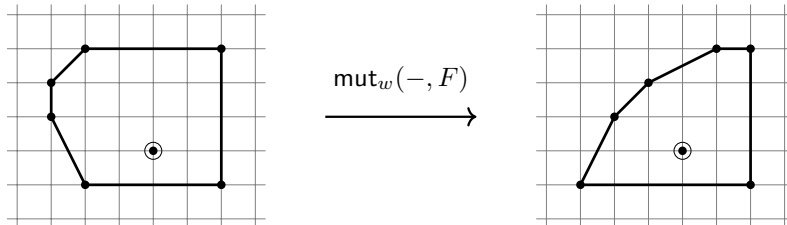
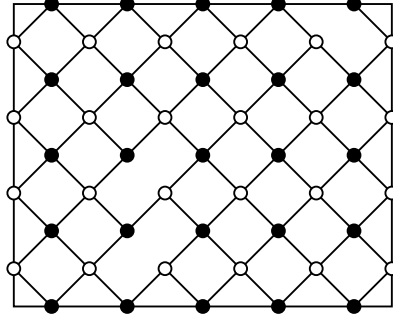
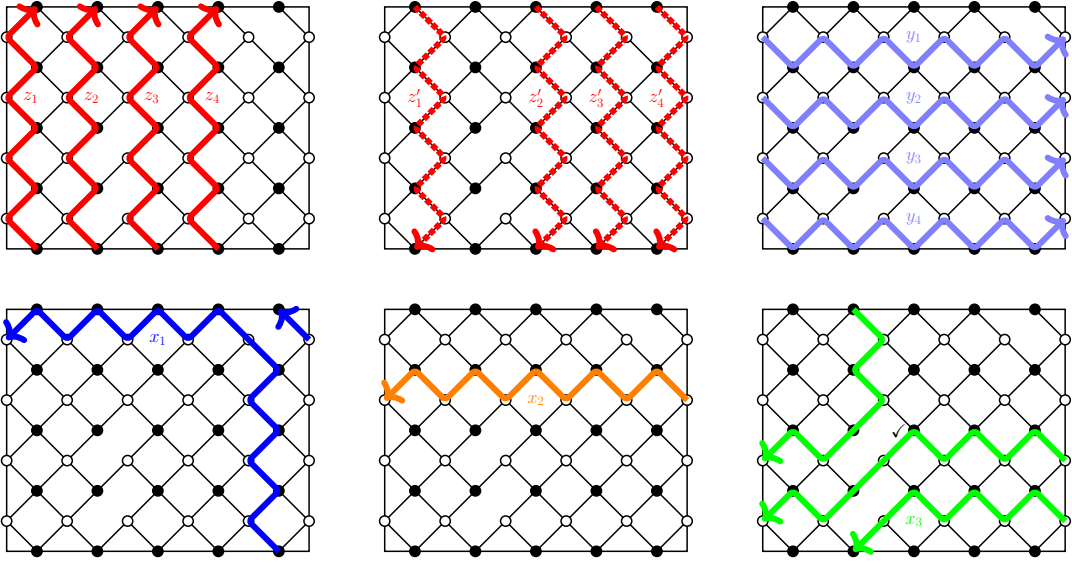


FIGURE 29. The lattice polygons P and $\text{mut}_w(P, F)$ for $w = (0, -1)$ and $F = \text{conv}\{\mathbf{0}, (-1, 0)\}$

We then consider the dimer model Γ shown in Figure 30. The zigzag paths on this dimer model Γ are Figure 31. Thus, we can check that Γ is consistent and the PM polygon Δ_Γ coincides with P by Proposition 3.5.


 FIGURE 30. A consistent dimer model Γ whose PM polygon coincides with P

 FIGURE 31. The list of zigzag paths of Γ

Then, we consider the deformation of Γ that induces $\text{mut}_w(P, F)$ as the PM polygon (see Theorem 6.10). To do this, we first fix the deformation data (see Definition 4.1) as follows. First, the zigzag path z_i on Γ is type I with $\ell(z_i) = 8$, and its slope is $[z_i] = (0, 1) = -w$ for $i = 1, \dots, 4$. Let $r := -h_{\min} = 3$ and $h := h_{\max} = 1$ (see Table 1). In particular, these satisfy $r = 3 < |\mathcal{Z}_{(-w)}^I(\Gamma)| = 4$ and $r + h = \ell(z_i)/2 = 4$.

We take the set of type I zigzag paths $\{z_1, z_2, z_3\}$, and consider the deformation $\nu_{\mathcal{X}}^{\text{zig}}(\Gamma, \{z_1, z_2, z_3\})$ of Γ at zig of $\{z_1, z_2, z_3\}$ with respect to \mathcal{X} , where \mathcal{X} is the zig deformation parameter defined as follows. To define \mathcal{X} , we focus on x_1, x_2, x_3 shown in Figure 31, which are the zigzag paths intersected with z_i at some zags of z_i . They satisfy $m_1 := |x_1 \cap z_1| = 1$, $m_2 := |x_2 \cap z_2| = 1$, and $m_3 := |x_3 \cap z_3| = 2$ for any i , thus we consider the set of sub-zigzag paths $\{x_1 = x_1^{(1)}, x_2 = x_2^{(1)}, x_3^{(1)}, x_3^{(2)}\}$. Here, we fix an intersection of z_3 and x_3 marked by \checkmark in Figure 31 as the starting edge of $x_3^{(1)}$. We then set the zig deformation parameter $\mathcal{X} := \{X_1, X_2, X_3\}$ with respect to $\{z_1, z_2, z_3\}$, where $X_1 = \{x_1 \cap z_1 = x_1^{(1)} \cap z_1\}$, $X_2 = \{x_2 \cap z_2 = x_2^{(1)} \cap z_2\}$ and $X_3 = \{x_3^{(1)} \cap z_3, x_3^{(2)} \cap z_3\}$, in which case the weight of \mathcal{X} is $\mathbf{p} = (1, 1, 2)$.

Using these deformation data, we apply the operations (zig-1)–(zig-3) to Γ . Then, we have the dimer model shown in the left of Figure 32. Here, we remark that we easily see that the slopes of zigzag paths on this dimer model do not one-to-one correspond to the primitive side segments of $\text{mut}_w(P, F)$, thus we can not obtain Theorem 6.10 without the operations (zig-4) and (zig-5), which is different from the case of Definition 4.8. Thus, we apply (zig-4), that is, we insert some bypasses. Then, we have the dimer model $\bar{\nu}_{\mathcal{X}}^{\text{zig}}(\Gamma) = \bar{\nu}_{\mathcal{X}}^{\text{zig}}(\Gamma, \{z_1, z_2, z_3\})$ as shown in the right of Figure 32. By Proposition 4.12, this dimer model is non-degenerate, but it is not consistent. Indeed, we can see that some nodes appearing on the zigzag path x_3' shown in Figure 33 are not properly ordered (see Definition 3.3(4)).

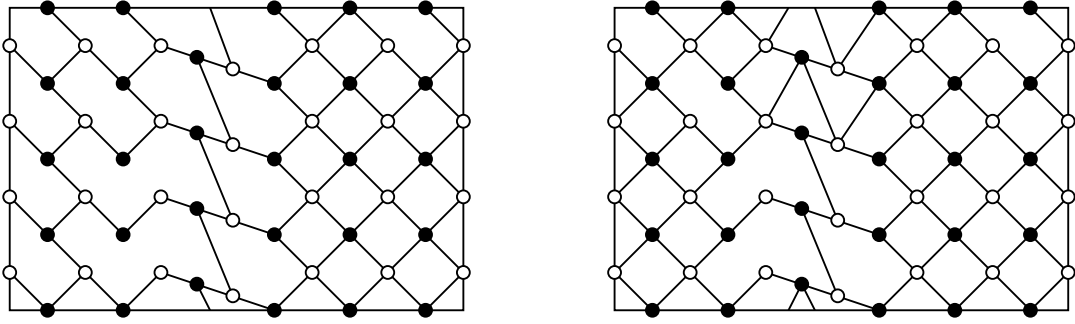


FIGURE 32. The dimer model obtained by applying (zig-1)–(zig-3) to Γ (left), and the dimer model $\overline{\nu}_{\mathcal{X}}^{\text{zig}}(\Gamma, \{z_1, z_2, z_3\})$ obtained by applying (zig-1)–(zig-4) to Γ (right)

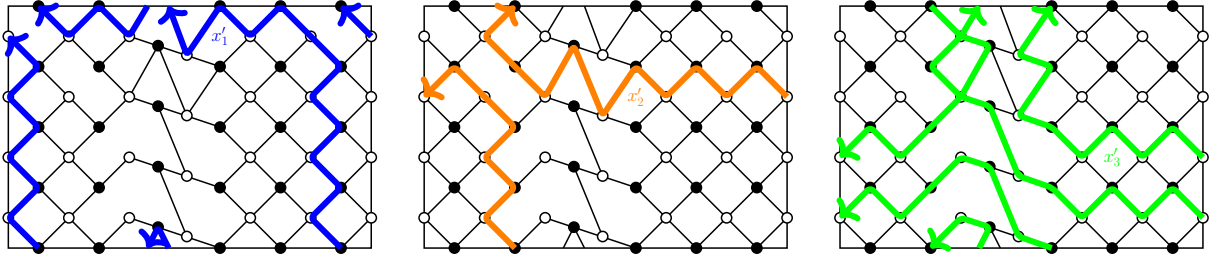


FIGURE 33. The zigzag paths x'_1, x'_2, x'_3 of $\overline{\nu}_{\mathcal{X}}^{\text{zig}}(\Gamma, \{z_1, z_2, z_3\})$

By Lemma 5.6, some edges constituting the zigzag paths x'_1, x'_2, x'_3 shown in Figure 33 might be removed by the operation (zig-5). Thus, paying attention to these zigzag paths, we apply (zig-5) to $\overline{\nu}_{\mathcal{X}}^{\text{zig}}(\Gamma)$ and make it consistent. Namely, if we remove pairs of edges (1)–(5) shown in the type A (left) of Figure 34, which are the intersections of pairs of zigzag paths on the universal cover that intersect with each other in the same direction more than once, from $\overline{\nu}_{\mathcal{X}}^{\text{zig}}(\Gamma)$ with this order. Then, we have the dimer model shown in the left of Figure 35, and applying (zig-6) we finally have the dimer model $\nu_{\mathcal{X}}^{\text{zig}}(\Gamma, \{z_1, z_2, z_3\})$ shown in the right of Figure 35.

Whereas there are other ways to remove edges. For example, if we remove pairs of edges (1)–(5) shown in the type B (right) of Figure 34, then we have another dimer model shown in the left of Figure 36, and applying (zig-6) we have the dimer model $\nu_{\mathcal{X}}^{\text{zig}}(\Gamma, \{z_1, z_2, z_3\})$ shown in the right of Figure 36.

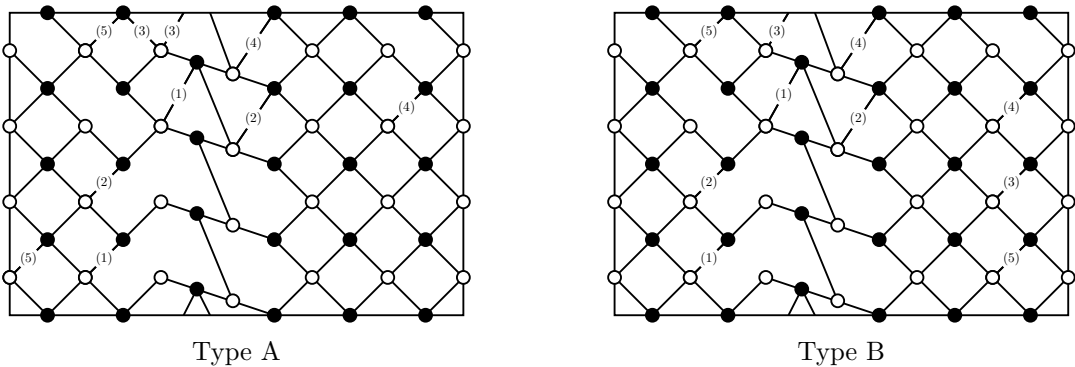


FIGURE 34. The two ways to remove edges from $\overline{\nu}_{\mathcal{X}}^{\text{zig}}(\Gamma, \{z_1, z_2, z_3\})$ by (zig-5)

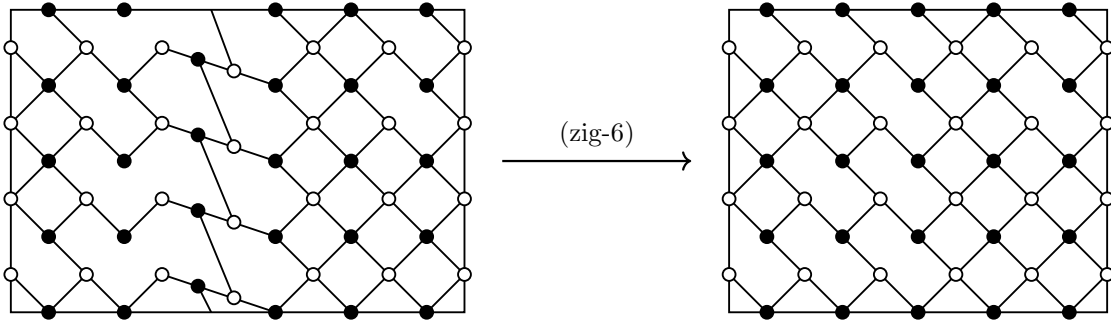


FIGURE 35. The dimer model $\nu_{\mathcal{X}}^{\text{zig}}(\Gamma, \{z_1, z_2, z_3\})$ obtained from the type A of Figure 34

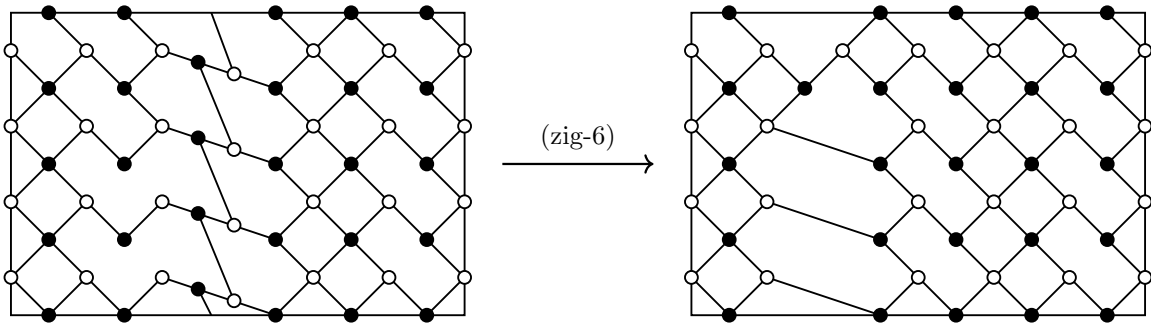


FIGURE 36. The dimer model $\nu_{\mathcal{X}}^{\text{zig}}(\Gamma, \{z_1, z_2, z_3\})$ obtained from the type B of Figure 34

Let Γ_A (resp. Γ_B) be the deformed dimer model shown in the right of Figure 35 (resp. Figure 36). We can check that Γ_A and Γ_B are not isomorphic, but they are mutation equivalent. Indeed, by applying the mutations of Γ_B at the faces $1, \dots, 10$ with this order (see Figure 37), we can recover Γ_A . Here, we recall that the mutation of a dimer model can be defined at a quadrangle face. Although some faces indexed by $\{1, \dots, 10\}$ are not quadrangle, such faces will be a quadrangle in the process of these series of mutations.

The PM polygon of the dimer models Γ_A and Γ_B are the same (see Proposition A.2), and it coincides with the lattice polygon shown in the right of Figure 29 by Theorem 6.10.

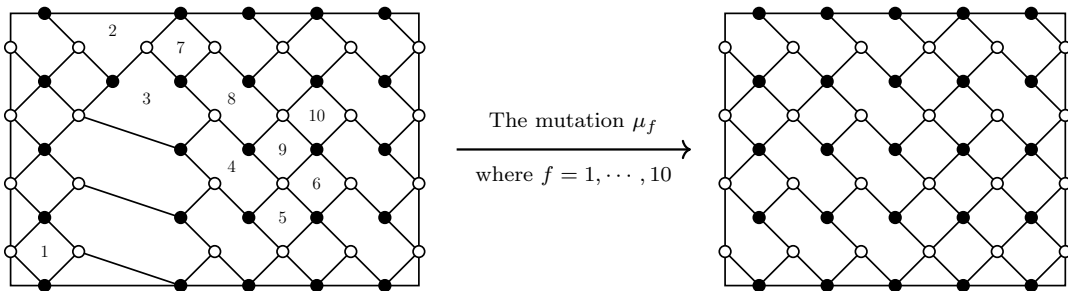


FIGURE 37. The mutations of Γ_B (left) at the faces $1, \dots, 10$ induce Γ_A (right)

APPENDIX C. REMARKS ON DEFORMATIONS OF HEXAGONAL AND SQUARE DIMER MODELS

As we mentioned in Remark 4.9, we can skip the operations (zig-4) and (zig-5) (resp. (zag-4) and (zag-5)) for the case of hexagonal and square dimer models as we will see below. Here, we say that a dimer model Γ is *hexagonal* (resp. *square*) if Γ is homotopy equivalent to a dimer model whose faces are all regular hexagon (resp. square) dimer model. We note that hexagonal and square dimer models are isoradial. These dimer models have been studied in several papers, especially we have the followings.

Proposition C.1 (see e.g., [IN, Nak2, UY]). *Let Γ be a consistent dimer model. Then, we have the followings.*

- (1) Γ is a hexagonal dimer model if and only if the PM polygon Δ_Γ is a triangle.
- (2) If Γ is a square dimer model, then the PM polygon Δ_Γ is a parallelogram.

For these nice classes of dimer models, we may skip the operations (zig-4) and (zig-5) (or (zag-4) and (zag-5)) when we apply the deformation.

Proposition C.2. *Let the notation be the same as in Definition 4.1, 4.3, and 4.5. In addition, we assume that a dimer model Γ is hexagonal or square, in which case Γ is isoradial. Then, the deformation $\nu_{\mathcal{X}}^{\text{zig}}(\Gamma, \{z_1, \dots, z_r\})$ is defined by the operations (zig-1)–(zig-3) and (zig-6). Similarly, the deformation $\nu_{\mathcal{Y}}^{\text{zag}}(\Gamma, \{z_1, \dots, z_r\})$ is defined by the operations (zag-1)–(zag-3) and (zag-6).*

Proof. We prove the case of the deformation at zig, and the case of the deformation at zag is similar.

The zigzag paths z_1, \dots, z_r have the same slope and such a slope is the outer normal vector of an edge of the PM polygon Δ_Γ by Proposition 3.5.

- (1) We assume that Γ is a hexagonal dimer model. Then, Δ_Γ is a triangle by Proposition C.1(1). Let e_1, e_2, e_3 be edges of Δ_Γ which are ordered cyclically in the anti-clockwise direction. We may assume that the slopes of z_1, \dots, z_r are the outer normal vector of e_1 . We then consider the zigzag paths x_1, \dots, x_s (resp. y_1, \dots, y_t) intersected with z_i at zags (resp. zigs) of z_i . Since Γ is isoradial, it is properly ordered. Thus, by Proposition 3.5 we see that $[x_1] = \dots = [x_s]$ (resp. $[y_1] = \dots = [y_t]$), and $[x_j]$ (resp. $[y_k]$) is the outer normal vector of e_2 (resp. e_3).
- (2) We assume that Γ is a square dimer model. Then, Δ_Γ is a parallelogram by Proposition C.1(2). Let e_1, e_2, e_3, e_4 be edges of Δ_Γ which are ordered cyclically in the anti-clockwise direction. In particular, $\{e_1, e_3\}, \{e_2, e_4\}$ are pairs of edges that are parallel. We may assume that the slopes of z_1, \dots, z_r are the outer normal vector of e_1 , in which case the zigzag paths having the slope $-[z_i]$ correspond to e_3 . Then, in a similar way as above, we have the zigzag paths x_1, \dots, x_s (resp. y_1, \dots, y_t) such that $[x_j]$ (resp. $[y_k]$) is the outer normal vector of e_2 (resp. e_4).

In both cases, we see that any pair of zigzag paths in x_1, \dots, x_s (resp. y_1, \dots, y_t) does not have the intersection on the universal cover by Lemma 3.15 because Γ is isoradial.

Then, we consider $\bar{\nu}_{\mathcal{X}}^{\text{zig}}(\Gamma, \{z_1, \dots, z_r\})$ for the case of $r \neq 1$ (see Definition 4.8 for the case of $r = 1$). By Lemma 5.6 and the fact that there is no intersection between x_1, \dots, x_s , we see that the edges removed by (zig-5) are bypasses added in (zig-4). Furthermore, by Observation 5.2 and 5.3 a zigzag path passing through a bypass takes the form \tilde{x}'_j . Since the slopes of x_1, \dots, x_s are all the same in our situation, those of x'_1, \dots, x'_s are all the same (see Proposition 5.8). Thus, any bypass on the universal cover of $\bar{\nu}_{\mathcal{X}}^{\text{zig}}(\Gamma, \{z_1, \dots, z_r\})$ is either

- (i) a self-intersection of a zigzag path \tilde{x}'_j , or
- (ii) the intersection of a pair of zigzag paths $\tilde{x}'_j, \tilde{x}'_{j'}$, with $[x'_j] = [x'_{j'}]$.

We also see that an edge which is either (i) or (ii) is certainly a bypass, because of Observation 5.3 and the fact that such an intersection can not appear in the irrelevant part. Moreover, if a bypass is the intersection of zigzag paths \tilde{x}'_j and $\tilde{x}'_{j'}$, then they have another intersection because $[x_j] = [x_{j'}]$, and such an intersection is also a bypass. Thus, if there exists a bypass that can not be removed by (zig-5), then it prevents the consistency condition. Therefore, we can remove all bypasses added in (zig-4) by using (zig-5), and hence we may skip these operations. \square

Acknowledgement. The authors thank Alexander Kasprzyk for valuable lectures and discussions on mutation of Fano polygons. The first author is supported by JSPS Grant-in-Aid for Young Scientists (B) 17K14177. The second author is supported by World Premier International Research Center Initiative (WPI initiative), MEXT, Japan, and JSPS Grant-in-Aid for Young Scientists (B) 17K14159.

REFERENCES

[Akhtar et al.] M. Akhtar, T. Coates, A. Corti, L. Heuberger, A. M. Kasprzyk, A. Oneto, A. Petracci, T. Prince and K. Tveiten, *Mirror symmetry and the classification of orbifold del Pezzo surfaces*, Proc. Amer. Math. Soc. **144**(2) (2016), 513–527.
 [ACGK] M. Akhtar, T. Coates, S. Galkin and A. M. Kasprzyk, *Minkowski polynomials and mutations*, SIGMA Symmetry Integrability Geom. Methods Appl. **8** (2012), 094, 17pages.
 [BIU] C. Beil, A. Ishii, and K. Ueda, *Cancellativization of dimer models*, arXiv:1301.5410.
 [Boc1] R. Bocklandt, *Consistency conditions for dimer models*, Glasgow Math. J., **54** (2012), 429–447.
 [Boc2] R. Bocklandt, *Generating toric noncommutative crepant resolutions*, J. Algebra, **364** (2012), 119–147.

- [Boc3] R. Bocklandt, *A dimer ABC*, Bull. Lond. Math. Soc. **48** (2016), no. 3, 387–451.
- [Bro] N. Broomhead, *Dimer model and Calabi-Yau algebras*, Mem. Amer. Math. Soc., **215** no. 1011, (2012).
- [Coates et al.] T. Coates, A. Corti, S. Galkin, V. Golyshev, and A. M. Kasprzyk, *Mirror symmetry and Fano manifolds*, In European Congress of Mathematics, pages 285–300. Eur. Math. Soc., Zurich, 2013.
- [DWZ] H. Derksen, J. Weyman and A. Zelevinsky, *Quivers with potentials and their representations. I. Mutations*, Selecta Math. (N.S.) **14** (2008), no. 1, 59–119.
- [Duf] R. J. Duffin, *Potential theory on a rhombic lattice*, J. Combinatorial Theory **5** (1968), 258–272.
- [GU] S. Galkin and A. Usnich, *Mutations of potentials*, Preprint IPMU 10–0100, 2010.
- [GK] A. B. Goncharov and R. Kenyon, *Dimers and cluster integrable systems*, Ann. Sci. Éc. Norm. Supér. (4) **46** (2013), no. 5, 747–813.
- [Gul] D. R. Gulotta, *Properly ordered dimers, R-charges, and an efficient inverse algorithm*, J. High Energy Phys. (2008), no. 10, 014, 31pp.
- [HS] A. Hanany and R.-K. Seong, *Brane Tilings and Reflexive Polygons*, Fortschr. Phys. **60** (2012), no. 6, 695–803.
- [Ilt] N. O. Ilten, *Mutations of Laurent polynomials and flat families with toric fibers*, SIGMA Symmetry Integrability Geom. Methods Appl. **8** (2012), 047, 7 pages.
- [IU1] A. Ishii and K. Ueda, *A note on consistency conditions on dimer models*, Higher dimensional algebraic varieties, RIMS Kôkyûroku Bessatsu, **B24**, Res. Inst. Math. Sci. (RIMS), Kyoto, (2011), 143–164.
- [IU2] A. Ishii and K. Ueda, *Dimer models and the special McKay correspondence*, Geom. Topol. **19** (2015) 3405–3466.
- [IN] O. Iyama and Y. Nakajima, *On steady non-commutative crepant resolutions*, J. Noncommut. Geom. **12** (2018), no. 2, 457–471.
- [KNP] A. Kasprzyk, B. Nill, and T. Prince, *Minimality and mutation-equivalence of polygons*, Forum of Mathematics, Sigma (2017), Vol. 5, e18, 48 pages.
- [Kenn] K. D. Kennaway, *Brane tilings*, Internat. J. Modern Phys. A, **22** (2007), no. 18, 2977–3038.
- [Keny] R. Kenyon, *An introduction to the dimer model*, School and Conference on Probability Theory, ICTP Lect. Notes, XVII, Abdus Salam Int. Cent. Theoret. Phys., Trieste, (2004), 267–304.
- [KS] R. Kenyon and J. M. Schlenker, *Rhombic embeddings of planar quadgraphs*, Trans. Amer. Math. Soc., **357** (2005), no. 9, 3443–3458.
- [Mer] C. Mercat, *Discrete Riemann surfaces and the Ising model*, Comm. Math. Phys. **218** (2001), no. 1, 177–216.
- [Nak1] Y. Nakajima, *Mutations of splitting maximal modifying modules: The case of reflexive polygons*, Int. Math. Res. Not. IMRN, **23** (2019), no. 2, 470–550.
- [Nak2] Y. Nakajima, *Semi-steady non-commutative crepant resolutions via regular dimer models*, to appear in Algebraic Combinatorics, arXiv:1608.05162.
- [Sch] A. Schrijver, *Theory of Linear and Integer Programming*, John Wiley & Sons, 1986.
- [UY] K. Ueda and M. Yamazaki, *A note on dimer models and McKay quivers*, Comm. Math. Phys. **301** (2011), no. 3, 723–747.

(A Higashitani) DEPARTMENT OF MATHEMATICS, KYOTO SANGYO UNIVERSITY, MOTOYAMA, KAMIGAMO, KITA-KU, KYOTO, JAPAN, 603-8555

E-mail address: ahigashi@cc.kyoto-su.ac.jp

(Y. Nakajima) KAVLI INSTITUTE FOR THE PHYSICS AND MATHEMATICS OF THE UNIVERSE (WPI), UTIAS, THE UNIVERSITY OF TOKYO, KASHIWA, CHIBA 277-8583, JAPAN

E-mail address: yusuke.nakajima@ipmu.jp